


1-1-2016

Insights Into De Novo Fes-Cluster Biogenesis Via The Eukaryotic Fes-Cluster (isc) Pathway In Vitro

Stephen Paul Dzul
Wayne State University,

Follow this and additional works at: https://digitalcommons.wayne.edu/oa_dissertations

 Part of the [Biochemistry Commons](#), and the [Molecular Biology Commons](#)

Recommended Citation

Dzul, Stephen Paul, "Insights Into De Novo Fes-Cluster Biogenesis Via The Eukaryotic Fes-Cluster (isc) Pathway In Vitro" (2016).
Wayne State University Dissertations. 1528.
https://digitalcommons.wayne.edu/oa_dissertations/1528

This Open Access Dissertation is brought to you for free and open access by DigitalCommons@WayneState. It has been accepted for inclusion in Wayne State University Dissertations by an authorized administrator of DigitalCommons@WayneState.

**INSIGHTS INTO *DE NOVO* FE-S CLUSTER BIOGENESIS VIA THE
EUKARYOTIC FE-S CLUSTER PATHWAY (ISC) *IN VITRO***

by

STEPHEN DZUL

DISSERTATION

Submitted to the School of Medicine

of Wayne State University

Detroit, Michigan

in partial fulfillment of the requirements

for the degree of

DOCTOR OF PHILOSOPHY

2016

MAJOR: BIOCHEMISTRY AND
MOLECULAR BIOLOGY

Approved By:

Advisor Date

DEDICATION

This work is dedicated to my loving grandparents, Irene and Paul Dzul. Their incredible lives have been and will continue to be an inspiration to me. Both Irene and Paul Dzul passed away during the completion of this work and they are dearly missed.

ACKNOWLEDGEMENTS

I would like to acknowledge the help I received from many people during the course of graduate school. Firstly, I need to thank parents, Andrew and Christina Dzul, for their unwavering support and encouragement. Thank you to the Wayne State University MD/PhD program for keeping their faith in me and continued commitment over these past 6 years and beyond. I need to give my deepest thanks to my advisor, Dr. Timothy Stemmler, for his continued help and support throughout graduate school. Thank you to Dr. Andrew Dancis and his laboratory for providing almost all of the plasmid constructs that I needed to get my project up and running quickly. Thank you to Dr. Brian Edwards, Dr. David Evans, and Dr. Bharati Mitra for serving on my dissertation committee. Thank you to our lab manager, Lindsey Thompson, for keeping the lab organized and supplied. Thank you to Dr. Shyamalee Kandegadara for her guidance. Lastly, I need to thank all past and present group members of the Stemmler lab who worked with me on a daily basis over these years, in particular Dr. Andria Rodrigues, who taught me how to do almost everything in the lab during my first year. This space is too small to acknowledge all the people who have helped me over these 4 years, but thank you to everyone involved.

TABLE OF CONTENTS

DEDICATION	ii
ACKNOWLEDGEMENTS	iii
TABLE OF CONTENTS	iv
LIST OF TABLES	x
LIST OF FIGURES	xi
CHAPTER 1: INTRODUCTION TO GENERAL FE-S CLUSTER BIOGENESIS PATHWAYS	1
1.0 Prelude	1
1.1 Introduction	2
1.2 Fe-S Cluster Structure	2
1.3 General Fe-S Cluster Biogenesis Pathways	5
1.3.1 Iron Sulfur Cluster (ISC) Pathway	5
1.3.2 Cytosolic Iron-Sulfur Assembly (CIA) Pathway	8
1.3.3 Sulfur Assimilation (SUF) Pathway	9
1.4 Fe-S Cluster Biogenesis Regulation	12
1.5 Fe-S Cluster Function	15
1.6 Fe-S Clusters in Human Disease	16
1.6.1 Friedreich's Ataxia	17
1.6.2 ISCU Myopathy	17
1.6.3 GLRX5 Sideroblastic Anemia	18
1.6.4 Additional Diseases Related to Dysfunctional FeS-Cluster Biogenesis	19
CHAPTER 2: DEVELOPMENT AND VALIDATION OF OPTIMAL METHOD FOR APO-ISU1 TO FES-ISU1 TRANSFORMATION <i>IN VITRO</i>	20

2.0 Prelude	20
2.1 Introduction	20
2.2 Methods	22
2.2.1 Protein Expression and Isolation	22
2.2.2 Original Conditions for FeS-Isu1 Formation	22
2.2.3 Optimal Conditions for FeS-Isu1 Formation	23
2.3 Results	24
2.3.1 Original FeS-Isu1 Formation Method Unable to Identify Persulfide-Accepting Cysteine of Isu1	24
2.3.2 Secondary Species Forms During FeS-Isu1 Formation Using Original Conditions	26
2.3.3 Optimization of FeS-Isu1 Formation Method	28
2.4 Discussion	32
2.4.1 Active-site Cysteines Essential for FeS-Cluster Coordination on Isu1	32
2.4.2 Identifying FeS-Mineral Secondary Species During FeS-Isu1 Formation	33
2.4.3 Behavior of FeS-Isu1 Formation Under Optimal Conditions is Consistent With FeS-Cluster Formation	33
CHAPTER 3: <i>IN VITRO</i> CHARACTERIZATION OF A NOVEL ISU HOMOLOGUE FROM <i>DROSOPHILA MELANOGASTER</i> FOR <i>DE NOVO</i> FE-S CLUSTER FORMATION.	35
3.0 Prelude	35
3.1 Abstract	36
3.2 Introduction	38
3.3 Methods	39
3.3.1 Protein Expression and Purification.	39
3.3.2 Secondary Structure Characterization of yIsu1 and flscU	41
3.3.3 Fe-Binding Analysis to flscU	42

3.3.4 X-ray Absorption Spectroscopy (XAS) Studies of Fe Bound to flscU _____	43
3.3.5 Fe-S Cluster Formation Reaction _____	45
3.3.6 Complementation of Yeast ISC by flscU _____	47
3.3.7 Cellular Iron-Uptake _____	47
3.4 Results _____	48
3.4.1 Molecular Characteristics of Recombinant flscU _____	48
3.4.2 Biophysical Characterization of flscU _____	51
3.4.3 Transformation of apo-flscU to FeS-flscU <i>in vitro</i> _____	60
3.4.4 Cross-Reactivity of flscU with yeast Nfs1-Isd11 and Yfh1 _____	65
3.4.5 <i>In vivo</i> replacement of yIsu1 with flscU _____	67
3.5 Discussion _____	69
3.6 Acknowledgements _____	74
CHAPTER 4: ISU1'S INTERACTION WITH NFS1 INHIBITS FES-ISU1 FORMATION IN VITRO _____	75
4.0 Prelude _____	75
4.1 Abstract _____	75
4.2 Introduction _____	76
4.3 Materials and Methods _____	79
4.3.1 Expression and Purification of SD, SDU, and SDUF Complexes _____	79
4.3.2 Characterization of SDUF Complex Stability _____	80
4.3.3 Identification of SD, SDU, SDUF Complex Protein Stoichiometries _____	81
4.3.4 Determination of SDUF Fold Stability _____	81
4.3.5 FeS-Isu1 Formation Reaction Assay with Complexed and Exogenous Isu1 _____	82
4.3.6 Probing Complex Formation Between Yeast Nfs1-Isd11, flscU, and Yfh1 _____	84
4.3.7 Measurement of Acid-Labile Sulfide Content _____	84

4.3.8 Estimation of Fe-Binding via Quantitation of FeS-Mineralization _____	85
4.3.9 Visible Absorption Spectroscopy _____	86
4.4 Results and Discussion _____	86
4.4.1 Successful Isolation of SDU, SDUF Complexes _____	86
4.4.2 Physical Characteristics of Recombinant SDU and SDUF Complexes _____	88
4.4.3 Nfs1-Isd11, Isu1, and Yfh1 Complexation Does Not Significantly Effect Protein Fold Stability _____	90
4.4.4 Exogenous Isu1 Required for Formation of FeS-Isu1 _____	93
4.4.5 Fe-S Cluster Formation using flscU with yeast Nfs1-Isd11 and Yfh1 _____	93
4.4.6 High Cysteine Desulfurase Activity Identified in SDUF _____	96
4.4.7 SDU and SDUF Complexes Retain Ability to Bind Mononuclear Fe ²⁺ _____	99
4.4.8 Frataxin Binding Increases PLP-cofactor Binding in SDUF _____	102
4.4.9 Proposed Model for SDUF Function <i>in vitro</i> _____	104
4.4.10 Insights into Mechanism for Fe-S Cluster Assembly <i>in vivo</i> _____	104
CHAPTER 5: <i>IN VITRO</i> EFFECTS OF FRATAXIN ON <i>DE NOVO</i> FE-S CLUSTER FORMATION _____	107
5.0 Prelude _____	107
5.1 Introduction _____	107
5.2 Methods _____	108
5.2.1 Protein Expression and Isolation _____	108
5.2.2 Effect of Frataxin on FeS-Isu1 Formation _____	110
5.2.3 Pull-Down Assay For Measuring Dfh-flscU Binding _____	111
5.3 Results _____	112
5.3.1 Effect of Frataxin is Concentration Dependent Under Physiologic Salt Levels _	112
5.3.2 Testing Dfh as Fe-Donor for FeS-flscU Formation _____	114
5.3.3 Both Dfh and Yfh1 Stimulate FeS-flscU Formation Using Yeast Nfs1-Isd11 ____	117

5.3.4 Dfh-flscU Binding Not Significantly Affected by Fe ²⁺	117
5.4 Discussion	120
5.4.1 Frataxin's Inhibition of Fe-S Cluster Formation Related to Protein Instability <i>in vitro</i>	120
5.4.2 Frataxin as an Allosteric Activator of Nfs1	120
5.4.3 The FeS-Isu1 Formation Method Unable to Assess Fe-Delivery by Dfh to flscU	121
5.4.4 Dfh-flscU Binding is Not Significantly Affected by Iron	121
5.4.5 Frataxin as Allosteric Activator of Nfs1 <i>in vivo</i>	122
CHAPTER 6: CONCLUSIONS AND FUTURE DIRECTIONS	123
6.0 Prelude	123
6.1 Introduction	123
6.2 Summary of Results	124
6.2.1 Optimal Method for Forming FeS-Isu1 <i>in vitro</i>	124
6.2.2 Characterization of Isu1 Ortholog from <i>D. melanogaster</i> , flscU	125
6.2.3 Isolation and Characterization of Nfs1-Isd11-Isu1-Yfh1 ("SDUF") Complex	125
6.2.4 Frataxin Functions as an Allosteric Activator of Cysteine Desulfurase <i>in vitro</i>	126
6.3 Correlations to ISC Function <i>in vivo</i>	126
6.3.1 Regulation of Iron Critical for Efficient Fe-S Cluster Formation <i>in vivo</i>	126
6.3.2 Nfs1-Isu1 Binding Studies Suggests Model for ISC Function <i>in vivo</i>	127
6.3.3 Frataxin Can Activate Cysteine Desulfurase Enzyme Nfs1 <i>in vivo</i>	127
6.4 Future Directions	128
6.4.1 Structural Characterization of <i>apo</i> vs FeS-Isu1	128
6.4.2 Investigation of Direct Sulfur Transfer from Nfs1 to Isu1	129
6.4.3 Functional Assays Incorporating Downstream ISC	129
6.4.4 Additional Characterization of SDUF	130

6.4.5 Expanding ISC Studies to Other Organisms	131
REFERENCES	132
ABSTRACT	172
AUTOBIOGRAPHICAL STATEMENT	174

LIST OF TABLES

Table 3.1: Fe-binding to flscU average simulation results including values for dissociation constants (K_{D1} and K_{D2}).....	54
Table 3.2: Best-fit simulation Fe XAS parameters for Fe-flscU, FeS-flscU and Yah1.....	59
Table 4.1: Best-fit model parameters for fits 1, 2, and 3 of SDUF melt profile including melting temperature (T_m), heat of melting (ΔH), and scaling factor (A_w).....	92

LIST OF FIGURES

Figure 1.1: Structure for the 3 most common forms of Fe-S Cluster _____	4
Figure 1.2: Diagram depicting the main Fe-S cluster transfer steps in the ISC, SUF, and CIA systems _____	11
Figure 1.3: Illustration of suf and isc operons, which describe an important regulatory mechanism for SUF and ISC in bacteria _____	14
Figure 2.1: FeS-Isu1 formation for various Isu1 mutants _____	25
Figure 2.2: Non-specific increase light-scattering observed using original FeS-Isu1 formation method suggests precipitation of reaction materials _____	27
Figure 2.3: Isu1, Nfs-Isd11, DTT, Cysteine, and Fe are required for FeS-Isu1 formation under optimal conditions _____	30
Figure 2.4: FeS-Isu1 formation for varying <i>apo</i> -Isu1 concentrations using the original FeS-Isu1 formation method compared to the optimal method _____	31
Figure 3.1: Sequence alignment between Isu1 from <i>Saccharomyces cerevisiae</i> (yIsu1) and <i>Drosophila melanogaster</i> (flscU) _____	49
Figure 3.2: Representative SDS-PAGE gel and circular dichroism spectra comparing recombinant <i>D. melanogaster</i> IscU (flscU) to <i>S. cerevisiae</i> Isu1 (yIsu1) _____	50
Figure 3.3: Fe-Binding Competition Assay with MagFura and Fura-FF ligands upon titration of Fe(II) in the presence of 8 μ M flscU _____	53
Figure 3.4: X-ray Absorption Near-Edge Spectra (XANES) for Fe-flscU, FeS-flscU, and FeS-Yah1 _____	57
Figure 3.5: Extended X-ray Absorption Fine Structure (EXAFS) and Fourier transforms (FT) of flscU and Yah1 _____	58
Figure 3.6: Increase in light scattering observed during FeS-Isu1 formation reaction _____	62
Figure 3.7: Circular dichroism and visible absorption spectra comparing FeS-flscU and FeS-yIsu1 _____	64
Figure 3.8: Change in Circular Dichroism signal at 560nm for 50 μ M flscU monomer and 10 μ M Nfs1-Isd11 monomer under varying Fe(II) concentrations and FeS-flscU formation via 50 μ M <i>apo</i> -flscU in the presence of 10 μ M Nfs1-Isd11, 10 μ M Nfs1-Isd11 and 10 μ M Yfh1, and 10 μ M Nfs1-Isd11, 10 μ M yIsu1, and 10 μ M Yfh1 _____	66
Figure 3.9: <i>In vivo</i> rescue of strain lacking yIsu1 by expression of flscU _____	68

Figure 3.10: Model for competing FeS-Isu and FeS mineralization pathways _____	73
Figure 4.1: Separation of SDUF into SD, U, and F components using standard Ni-column purification method _____	87
Figure 4.2: Comparison of recombinant SD, SDU, and SDUF complexes as isolated _____	89
Figure 4.3: Differential Scanning Calorimetric melt profile for SDUF _____	91
Figure 4.4: Functional studies of SD, SDU, and SDUF with complexed and exogenous Isu1 and stoichiometric amounts of Nfs1-Isd11, flscU, and Yfh1 _____	95
Figure 4.5: FeS-flscU formation and methylene blue acid-labile sulfide content with excess flscU and SD, SDU, and SDUF _____	98
Figure 4.6: FeS mineral production under various FeS-flscU formation conditions suggests complexed Isu1 retains Fe-binding capacity _____	101
Figure 4.7: Visible absorption spectra of 10 μ M SD, SDU, and SDUF complexes demonstrating increased PLP-feature for SDUF _____	103
Figure 4.8: Model for SDUF-mediated FeS-Isu1 formation via uncomplexed <i>apo</i> -Isu1 in the disordered conformation _____	106
Figure 5.1: FeS-flscU transformation over time under differing Yfh1 concentrations with 150mM and 500mM NaCl _____	113
Figure 5.2: Effects of 75 μ M <i>apo</i> - (blue) vs <i>holo</i> - (red) Dfh compared to no frataxin (black) on FeS-flscU formation _____	115
Figure 5.3: FeS-Isu1 transformation with no frataxin, 10 μ M Yfh1, and 10 μ M Dfh in 500mM NaCl solution _____	116
Figure 5.4: SDS-PAGE of various protein mixtures from Ni-column pull down assay measuring His6-flscU binding to untagged Dfh _____	119

CHAPTER 1: INTRODUCTION TO GENERAL FE-S CLUSTER BIOGENESIS PATHWAYS

1.0 Prelude

Iron sulfur (Fe-S) clusters are essential cofactors found in a variety of proteins throughout all forms of life. Proteins that bind Fe-S clusters are termed “Fe-S proteins” and they have been identified in many fundamental biochemical pathways. Despite their importance, I remember that when I first started working in Dr. Tim Stemmler’s research lab in October 2012, I had never heard of an “Fe-S cluster”. After several years of working in this field, however, I finally appreciate the significance of this essential and ubiquitous cofactor. During my first year researching Fe-S cluster synthesis, I was astonished to learn that key enzymes from my introductory biology courses such as DNA polymerase III, aconitase, and succinate dehydrogenase all utilize Fe-S clusters. In fact, Fe-S clusters are so fundamental to life that there are relatively few human diseases related to Fe-S cluster formation because dysfunctional Fe-S cluster biogenesis is usually incompatible with life. Despite the huge variety of proteins requiring Fe-S clusters, there are a limited number of pathway in eukaryotes that accommodates all cellular Fe-S proteins. The major pathway is called the “Iron Sulfur Cluster” pathway, or “ISC”, and it is localized to the mitochondria in eukaryotes. The ISC pathway is the focus of my dissertation.

My original project focused on identifying mechanistic details of a key ISC protein from *Saccharomyces cerevisiae* involved in Fe-S cluster formation, Isu1. Over the 4 years I worked in the lab, the aims and scope of my project would change dramatically. In fact, my research proposal from Spring 2013 barely resembles the project I would ultimately pursue. In order to understand the various aspects of my work, however, you must first be familiar with the background of the field. This first chapter describes the current status of

the field. This chapter is adapted from a review article I co-authored on the topic; and the material included in this chapter from that review were written entirely by myself. Material from this review article that is not relevant to Fe-S cluster biogenesis has been excluded.

The reference for this article is:

Barupala, D. P.; Dzul, S. P.; Riggs-Gelasco, P. J.; Stemmler, T. L. *Archives of biochemistry and biophysics* 2016, 592, 60.

1.1 Introduction

After heme, Iron-sulfur (Fe-S) clusters are the second major form of complex iron cofactors found in biology. Due to the high abundance of iron and sulfur on the earth's surface, and the easy association of these atoms under anaerobic conditions, Fe-S clusters likely developed early in evolution before the earth's transition to an aerobic atmosphere. Consequently, these cofactors are ubiquitous in all organisms and play a role in almost every biological pathway. Here we provide an overview of the structure, formation, and function of Fe-S cluster cofactors.

1.2 Fe-S Cluster Structure

In many ways, Fe-S clusters are simpler than heme. While heme is a mixture of organic (protoporphyrin) and inorganic (iron) components, Fe-S clusters are strictly inorganic. Iron atoms in biological Fe-S clusters interact directly with protein residues, with sulfur atoms bridging the neighboring iron atoms. Fe-S clusters exist in a variety of configurations depending on their respective number of iron and sulfur atoms. The three most common forms (2Fe-2S, 3Fe-4S and 4Fe-4S) are illustrated in 1.1. More complex Fe-S clusters have also been observed, including the 7Fe-8S and 8Fe-8S clusters identified in ferredoxins from *Desulfovibrio africanus*.¹

The Fe atoms within the Fe-S cluster can exist in either ferric or ferrous forms and cycling between these redox states allows the transfer of electrons for redox reactions. The tendency of the oxidized Fe-S cluster to gain an electron is termed the “reduction potential”. By convention, this potential is expressed in comparison to a reference standard hydrogen electrode, which is assigned a potential of 0 V. Depending on Fe-S cluster type, interactions with neighboring amino acids, and solvent accessibility, a single Fe-S cluster can carry up to two electrons with a reduction potential spanning ~ 1000 mV.² This remarkable range of accessible reduction potentials can largely explain the biological utility of the Fe-S cluster.

Fe-S clusters do not exist freely but are intimately connected to their apoprotein partner. Free iron forms an insoluble complex when bound to sulfide, so the protein plays a critical role in solubilizing the Fe-S unit. Fe-S proteins usually bind their corresponding Fe-S cofactor via ionic interactions between cysteine thiols and iron in the Fe-S cofactor. In some cases, Fe-S clusters are alternatively ligated via histidine residues. Subsets of 2Fe2S clusters, such as those found in Rieske proteins (see section 3.5), are coordinated by two cysteine and two histidines (Cys₂His₂)³ and a common coordination theme of proteins involved in Fe-S cluster biogenesis is Cys₃His₁ coordination.⁴

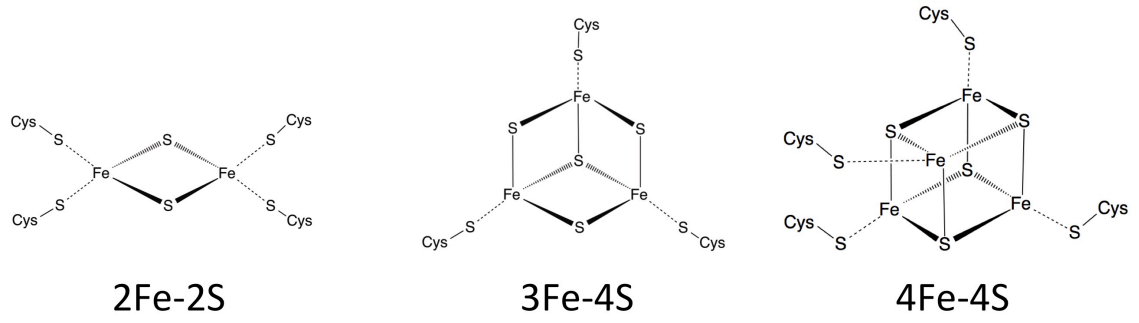


Figure 1.1: Structure for the 3 most common forms of Fe-S Cluster: 2Fe-2S, 3Fe-4S, and 4Fe-4S.

1.3 General Fe-S Cluster Biogenesis Pathways

Production of Fe-S clusters must be highly regulated to prevent unwanted reactions of both free iron and sulfur. Similar to heme-proteins, Fe-S proteins are synthesized in their *apo*-state and obtain their Fe-S cluster cofactor from a dedicated Fe-S cluster formation pathway. At present, there are three known general pathways for Fe-S cluster formation: the iron sulfur cluster (ISC), cytosolic iron sulfur assembly (CIA), and sulfur assimilation (SUF) pathways. These three pathways provide Fe-S clusters for the majority of Fe-S proteins in almost all organisms. While dedicated Fe-S cluster forming pathways can exist for individual Fe-S proteins, such as the nitrogen fixation (Nif) pathway that provides an Fe-S cluster for the nitrogenase enzyme in nitrogen-fixing bacteria,⁵ this introduction will focus only on the general Fe-S cluster production pathways.

1.3.1 Iron Sulfur Cluster (ISC) Pathway

The most robust and best-characterized pathway for Fe-S cluster biosynthesis is the iron sulfur cluster (ISC) pathway. A simplified description of this pathway is provided in Figure 1.2. The ISC pathway, present in bacteria and in the mitochondria of eukaryotes, provides general housekeeping Fe-S clusters to a large number of Fe-S proteins. In eukaryotes, this pathway provides Fe-S clusters for several key mitochondrial Fe-S proteins. ISC was initially identified in the *Azotobacter vinelandii* and *Escherichia coli* bacterial species, where ISC genes are arranged in the *isc* operon. Additional early work in eukaryotes (in *Saccharomyces cerevisiae* and human proteins) revealed a highly homologous system localized to the mitochondria. In addition to providing for mitochondrial Fe-S proteins, the ISC system provides a component to the cytosolic and

nuclear Fe-S cluster formation pathways, thus ISC is essential for the maturation of all cellular Fe-S proteins in eukaryotes.⁶⁻⁷

ISC serves as a template for understanding general Fe-S cluster production. In human ISC, *de novo* 2Fe-2S synthesis occurs on the dedicated scaffold protein ISCU.⁸ Sulfur for this reaction is provided by ISC's dedicated cysteine desulfurase enzyme NFS1 via a persulfide intermediate that gets transferred to ISCU⁹ upon formation of an ISCU-NFS1 complex. In eukaryotes, NFS1 has a dedicated protein co-factor ISD11 that is essential for NFS1 function.¹⁰ Electrons for NFS1 persulfide release are provided by the 2Fe-2S cluster containing ferredoxin FDX, which in turn gets reduced by the ferredoxin reductase FDXR that uses NADPH as its final electron source.¹¹⁻¹² FDX also interacts with ISCU, providing 2 reducing equivalents for assimilation of two 2Fe-2S clusters on an ISCU dimer to form a single 4Fe-4S cluster⁸. An additional Fe-binding protein Frataxin interacts with the NFS1-ISCU complex and regulates NFS1 activity.¹³ Additionally, there are other scaffold proteins (ISCA¹⁴ and NFU1¹⁵) that interact with ISC proteins and these are believed to be required for the maturation of a specific subset of Fe-S proteins.

Despite intense study, the physiologic source of iron for ISC remains a subject of debate. Several potential iron donors have been investigated and iron delivery to ISCU has been demonstrated from several potential sources *in vitro* within a variety of systems. The protein frataxin^{16,17} interacts with the ISCU-NFS1 complex and could be the source of iron for the pathway.¹⁷ In bacteria, two additional members of the *isc* operon have been investigated as potential iron donors, IscX and IscA. The small acidic protein IscX binds iron and regulates cysteine desulfurase activity in a manner very similar to frataxin.¹⁸ The alternative scaffold IscA is also an interesting candidate because of its tight ($K_D \sim 10^{19}$)

binding affinity for mononuclear iron¹⁹ and its capability of delivering iron to IscU.²⁰⁻²¹ An additional interesting hypothesis is that iron may come from a glutathione-glutaredoxin complex²². The lack of conclusive evidence for a specific iron source suggests that *in vivo*, there could be multiple iron sources or that the mode of iron delivery may be atypical.

A detailed mechanism for Fe-S cluster delivery from ISCU to downstream targets is currently under investigation. The Fe-S cluster bound to ISCU is transferred to the glutaredoxin GLRX5.²³⁻²⁴ Efficient transfer from ISCU to GLRX5 requires involvement of the ATPase SSQ1, which binds to both ISCU and GLRX5.²⁵ Binding of SSQ1 to ISCU, along with the interaction of a DnaJ-like co-chaperone JAC1,²⁶ destabilizes the Fe-S cluster on ISCU facilitating its transfer from ISCU to GLRX5.²⁷ GLRX5 is considered the end of the ISC pathway because it is the last common Fe-S cluster carrier for all mitochondrial Fe-S proteins. GLRX5 continues the cluster transfer process, however, and it is able to interact with a variety of downstream Fe-S proteins.²⁸⁻³⁰ The specific recipient depends on the ultimate destination of the Fe-S cluster. For example, 4Fe-4S cluster conversion and delivery is facilitated by GLRX5's interaction with two other Fe-S proteins, ISCA and IBA57.³¹

Despite being mostly localized to mitochondria,³² ISC is required for maturation of all cellular Fe-S proteins.⁷ The mechanism by which cytosolic Fe-S proteins depend on mitochondrial ISC is actively being investigated. Because Fe-S clusters are not able to cross the inner mitochondrial membrane,³³ this mechanism likely involves the transport of an Fe-S cluster precursor out of the mitochondria and into the cytosol. Recent work has identified an unknown compound produced by mitochondrial NFS1 (named 'X-S') that may provide reduced sulfur for cytosolic Fe-S cluster formation.³⁴

1.3.2 Cytosolic Iron-Sulfur Assembly (CIA) Pathway

Recent studies have revealed the involvement of another essential and highly conserved Fe-S biosynthetic pathway that is present within the cytosol and nucleus of eukaryotes. This pathway is called cytosolic iron-sulfur assembly (CIA).³⁵ This pathway has been identified in many eukaryotic systems and is essential in almost all cases.³⁶ CIA is unique among Fe-S maturation pathways in that it does not obtain reduced sulfur via a dedicated cysteine desulfurase. A simplified description of the CIA pathway is provided in Figure 1.2. Instead of an NFS1 analog, CIA relies on mitochondrial export of a sulfur-containing compound, 'X-S', via the mitochondrial export protein ABCB7³⁷ and the intermembrane space protein ALR.³⁸ The identity of X-S is currently unknown, but may be glutathione-complexed to an Fe-S cluster.³⁶ In human CIA, the primary scaffold for *de novo* Fe-S assembly is a tetrameric complex formed between CFD1 and NBP35, which binds a bridging 4Fe-4S cluster between the CFD1 and NBP35 subunits.³⁹ Reducing equivalents for this reaction are provided by an Fe-S containing protein CIAPIN1 (similar to FDX in ISC), which in turn gets reduced by the diflavin reductase NDOR1 (similar to FDXR in ISC), utilizing reducing equivalents from NADPH.⁴⁰⁻⁴¹

The 4Fe-4S clusters from the NBP35-CFD1 complex get transferred to another Fe-S protein IOP1, which binds two 4Fe-4S clusters per monomer.⁴²⁻⁴³ IOP1, in turn, delivers its Fe-S clusters to a multi-component complex called the CIA targeting complex, which consists of at least three proteins CIA1, CIA2B, and MMS19.⁴⁴ The CIA targeting complex is able to interact with a variety of recipient Fe-S proteins, likely an indication of its function in downstream Fe-S cluster delivery.

1.3.3 Sulfur Assimilation (SUF) Pathway

Of the three Fe-S general cluster formation pathways, the sulfur assimilation (SUF) pathway is probably the most ancient. SUF predominantly exists in prokaryotes, however it is found in specific locations in eukarya, including the chloroplasts in some plants⁴⁵ and the apicoplasts in some plasmodium species,⁴⁶ and recently proteins homologous to bacterial SUF were discovered in the cytosol of a blastocystis species.⁴⁷ At present, SUF has been best characterized in the Gram-negative bacteria *Escherichia coli* and *Erwynia chrysanthemi* where its genes are organized into the *suf* operon (Figure 1.3).

The SUF pathway is similar to ISC in many ways. Like in ISC, SUF provides general Fe-S cluster formation to accommodate a variety of Fe-S proteins. In fact, SUF and ISC seem to be redundant in Gram-negative bacteria, as the removal of the entire *isc* or *suf* operon results in no deleterious effects. Simultaneous *suf/isc* operon deletion, however, is lethal.⁴⁸ While ISC and SUF follow the same general mechanism for Fe-S cluster formation (Figure 1.2), SUF seems to be favored under conditions of oxidative stress and iron limitation⁴⁹ and the SUF proteins are correspondingly more stable under adverse conditions *in vitro*.⁵⁰ In *E. coli*, the SUF pathway centers around two heteromeric complexes called SufBC and SufSE.

The primary scaffold SufB requires a binding partner SufC for activity, forming the SufBC complex in a SufB₂C₂ arrangement. The SufBC complex can form a 4Fe-4S cluster on SufB that can be transferred to recipient proteins.⁵¹ The exact role of SufC in this process is unknown, but it has ATPase activity that is essential for Fe-S cluster formation on SufB.⁵² SufB, on its own is relatively unstable and prone to spontaneous oligomerization. There is also a paralogue of SufB, named SufD that is able to replace a SufB in the SufBC complex, resulting in the SufBCD complex.⁵³ However, SufBC is likely the most active form.⁵⁴ The SUF

cysteine desulfurase SufS functions in a similar manner to NFS1, accepting sulfur from cysteine via a persulfide intermediate. SufS has an essential binding partner SufE, which is required for activity, forming the SufSE complex.⁵⁵ While it may seem SufE is similar to ISD11 from eukaryotic ISC, SufE functions differently from ISD11 in that it accepts the persulfide from SufS and allows the SufS enzyme to complete its turnover.⁵⁶

Details of SUF's downstream cluster delivery are not as well established as in the ISC pathway. The 4Fe-4S cluster formed by SufBC can be transferred to the A-type carrier protein SufA *in vitro*,^{51,54} but SufBC also may be able to transfer directly to recipient apo-proteins. *In vivo*, SufA is functionally redundant with the ISCA bacterial homologue⁵⁷ and possibly acts as an intermediate carrier of the 4Fe-4S cluster from SufB, passing it off to downstream apoproteins.⁵⁸⁻⁵⁹ Another protein involved in this process (ErpA) has redundant function with SufA but is necessary for the development of active Fe-S proteins.⁶⁰

Several important details of the SUF pathway remain to be identified. As in ISC, the *in vivo* source of iron is unknown. Also of interest is SufD's incorporation in the SufBCD complex, which allows SufB to accept iron *in vivo*⁵² and facilitates binding of a FADH₂ cofactor.⁵³ This cofactor may be able to reduce ferric iron, facilitating potential Fe³⁺ sources such as ferritins or ferric citrate.⁶¹ While SufA can deliver mononuclear iron to SufBC *in vitro*,²⁰ it is currently believed to function downstream of *de novo* Fe-S formation (Figure 1.2). The source of electrons for SufS turnover and for Fe-S formation remains in question.⁶²

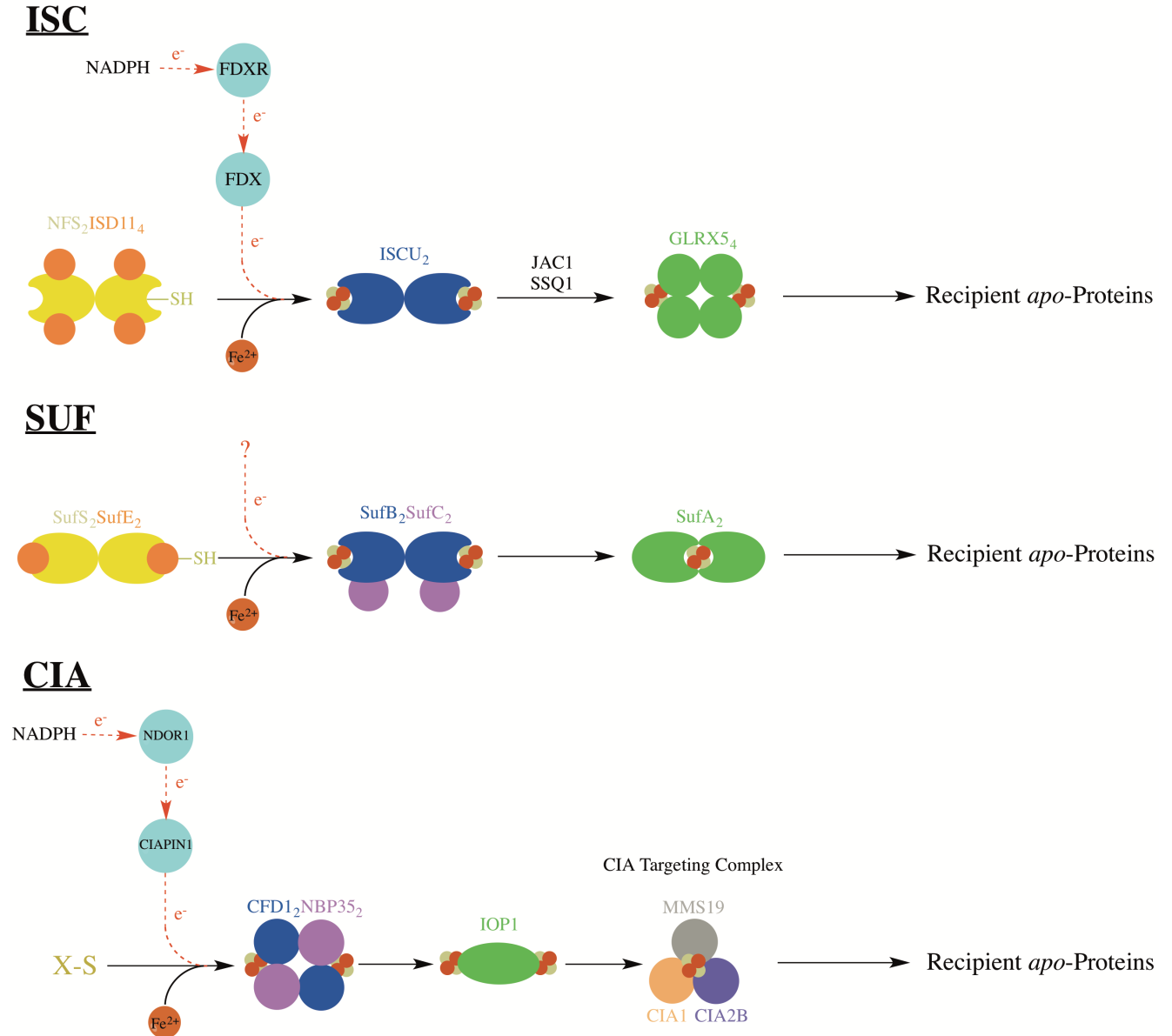


Figure 1.2: Diagram depicting the main Fe-S cluster transfer steps in the ISC, SUF, and CIA systems. Protein names used are from the human system for ISC and CIA, and from the bacterial system for SUF.

1.4 Fe-S Cluster Biogenesis Regulation

The best-developed model for Fe-S biogenesis pathway regulation comes from work done in Gram-negative bacterial systems, where both the ISC and SUF pathways are present. This work reveals a fascinating interplay between ISC and SUF, where the necessary ISC and SUF genes are organized into their respective *isc* and *suf* operons (Figure 1.3). While this introduction has focused on eukaryotic systems, regulatory mechanisms in bacteria may provide insight into how this regulation occurs in eukaryotes. At the center of *E. coli* Fe-S cluster biogenesis regulation is a DNA-binding protein IscR, the first member of the *isc* operon, which directly regulates both the ISC and SUF systems.

Under non-stressed conditions, ISC is favored over SUF for general housekeeping of Fe-S cluster biosynthesis.⁶³ The transcriptional regulator IscR can bind a 2Fe-2S cluster (forming *holo*-IscR), obtaining its Fe-S cluster from the same ISC machinery utilized by other Fe-S proteins.⁶⁴ In the *holo* configuration, IscR binds to the *isc* promoter and prevents binding of RNA polymerase.⁶⁵ Thus, *holo*-IscR acts as a feedback regulator, inhibiting transcription of the entire *isc* operon when ISC activity is sufficient.⁶⁶ IscR is a relatively poor substrate for ISC-mediated Fe-S cluster loading⁶⁷ and *holo*-IscR can only form after the ISC proteins have exhausted their interactions with other *apo*-Fe-S proteins. In addition to being a weak ISC substrate, IscR does not bind its Fe-S cluster tightly and effectively acts as a sensor of cellular iron and oxygen conditions.⁶⁸ Under high-oxygen or low-iron conditions, *holo*-IscR quickly reverts to *apo*-IscR. Therefore under typical aerobic conditions, high oxygen levels cause *holo*-IscR to revert to *apo*-IscR. *Apo*-IscR dissociates from the *isc* promoter and *isc* is uninhibited.

In the *apo* configuration, IscR does not bind to the *isc* promoter but instead favors binding to the *suf* promoter, activating transcription of SUF genes⁶⁹. Appropriate interaction of *apo*-IscR with the *suf* promoter involves two additional transcription factors: the ferric uptake regulator (Fur) and the peroxide responsive regulator (OxyR). *Suf* expression is constitutively repressed by Fur, which binds Fe²⁺ under non-stressed conditions when iron levels are sufficient and oxidative stress is low. With its Fe²⁺ cofactor, Fur binds to the *suf* promoter at the same site as *apo*-IscR, inhibiting *suf* expression⁷⁰. When the cell faces iron deficiency, Fur loses its iron cofactor, dissociates from the *suf* promoter, thus triggering transcription of *suf*. The cell's preference for SUF over ISC in the presence of oxidative stress also reveals the involvement of another transcription factor (OxyR), as oxidized OxyR recruits RNA polymerase to the *suf* promoter.

There are additional regulatory mechanisms for cluster bioassembly beyond the level of gene expression. The small non-coding RNA RyhB, for example, is encoded just upstream of the SUF promoter and can bind to the *iscRSUA* mRNA to prevent its translation⁷¹. RyhB expression, however, is constitutively repressed by Fur-Fe²⁺, so RyhB effectively inhibits ISC when conditions favor SUF⁷².

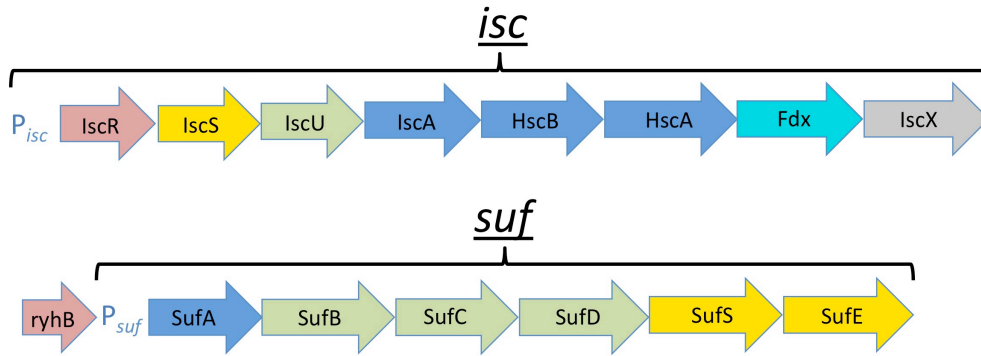


Figure 1.3: Illustration of *suf* and *isc* operons, which describe an important regulatory mechanism for SUF and ISC in bacteria. Operons depicted are from the *E. coli* model system. Steps are colored based on on the encoded protein's function as follows: red (regulatory), yellow (sulfur delivery), green (primary scaffold), blue (downstream Fe-S cluster delivery), gray (unknown).

1.5 Fe-S Cluster Function

Fe-S clusters are versatile biological cofactors found in the most fundamental biochemical pathways, including aconitase and succinate dehydrogenase of the citric acid cycle and respiratory complexes I-III of the electron transport chain.³² Nuclear Fe-S proteins also have a unique role in DNA damage recognition and repair. Several forms of DNA polymerase, helicase, glycosylase, and primase all contain Fe-S clusters.³⁶ Considering their remarkable range of functions, a thorough summary of various Fe-S proteins is well beyond the limited scope of this introduction. New Fe-S proteins continue to be discovered but in many cases, the role of the Fe-S cluster within the Fe-S protein remains unknown, even if the cluster's presence is essential for proper protein function.

Fe-S clusters can be found in the active site of many essential enzymes and usually are involved directly in catalysis. Being stable in a variety of redox states, Fe-S clusters are best known for their role as electron carriers. Fe-S clusters can carry usually one, but sometimes two electrons and are, subsequently, stable in various reduced states. 2Fe-2S clusters, for example, can exist in oxidized ($\text{Fe}^{3+}/\text{Fe}^{3+}$) or reduced ($\text{Fe}^{3+}/\text{Fe}^{2+}$) forms while 4Fe-4S clusters are stable in oxidized ($\text{Fe}^{3+}/\text{Fe}^{3+}/\text{Fe}^{3+}/\text{Fe}^{2+}$), intermediate ($\text{Fe}^{3+}/\text{Fe}^{3+}/\text{Fe}^{2+}/\text{Fe}^{2+}$), and reduced ($\text{Fe}^{3+}/\text{Fe}^{2+}/\text{Fe}^{2+}/\text{Fe}^{2+}$) forms.⁷³ The reduction potential of an Fe-S cluster is often modulated by interactions with nearest neighbor protein residues and by access to solvent, allowing for a large range of biological functions. Ferredoxins are considered the archetypical Fe-S cluster electron carriers and were the earliest Fe-S proteins to be functionally characterized.⁷⁴ Ferredoxins are involved in many essential biochemical pathways, transferring electrons for cellular respiration,

photosynthesis, and nitrogen fixation.⁷⁵ A ferredoxin is even involved in the ISC iron sulfur cluster biogenesis pathway, as discussed previously (see section 3.3.1).⁷⁶

But Fe-S cluster-mediated electron transfer is not limited to ferredoxins. In fact, one of the most fundamental electron transfer processes, the electron transport chain (ETC), utilizes numerous Fe-S clusters. Respiratory complexes I, II, and III of the ETC all contain Fe-S clusters. Respiratory complex I uses a network of 8 Fe-S clusters for step-wise electron transfer.⁷⁷ Similarly, complex II contains an Fe-S protein component called SDHB with a 2Fe-2S, 3Fe-4S, and 4Fe-4S cluster⁷⁸. Lastly, complex III utilizes a unique Fe-S cluster called a “Rieske center”.⁷⁹ The Rieske center is a 2Fe-2S cluster where one of the iron atoms is coordinated by histidines instead of cysteines, resulting in a Cys₂His₂ coordination.⁸⁰

Fe-S clusters can also be involved in non-redox reactions. The 4Fe-4S cluster in aconitase, for example, catalyzes a hydration-dehydration reaction, ligating directly to the citrate substrate.⁸¹ In some cases, Fe-S clusters appear to only serve a structural function and not participate in chemistry directly, as is the case in endonuclease III.⁸²

1.6 Fe-S Clusters in Human Disease

Unlike in Gram-negative bacteria, where ISC/SUF redundancy allows for removal of an entire pathway, in humans the absence or mutation of a single component is often incompatible with life. In select cases there are human diseases that have been linked to defective Fe-S cluster biogenesis pathways. Below we describe several diseases directly linked to dysfunctional Fe-S cluster formation.

1.6.1 Friedreich’s Ataxia

With an incidence of 1 in 50,000,⁸³⁻⁸⁴ and a carrier prevalence of 1 in 100 in certain populations,⁸⁵ *Friedreich’s ataxia* (FRDA) is by far the most prevalent disease linked to

defective Fe-S cluster formation. FRDA is an autosomal recessive genetic disease caused by a GAA-trinucleotide repeat expansion in an intron of the frataxin gene, a protein involved in the ISC pathway.⁸⁶ This trinucleotide repeat expansion leads to under-expression of the frataxin gene and subsequently, low levels of frataxin.⁸⁷ These insufficient frataxin levels are responsible for the pathophysiology of FRDA, but the precise role of frataxin is still unknown.⁸⁸ Frataxin may deliver iron to the ISC pathway,⁸⁹ be an allosteric activator of the ISCU-NFS1 complex,¹³ or may have a combination of roles. FRDA tissues demonstrate increased mitochondrial iron deposits⁹⁰ which leads to increased oxidative stress and cell death in metabolically active tissues such as cardiomyocytes and neurons of the dorsal root ganglia. FRDA presents early in adolescence with progressive ataxia, or difficulty coordinating movement, sensory loss, weakness, and dysarthria. FRDA patients are usually wheelchair bound in their teens with a significantly reduced quality of life and life expectancy.⁹¹ Median age of survival is 35 years with cardiac dysfunction usually being the cause of death.⁹²

1.6.2 ISCU Myopathy

ISCU myopathy (IM) is an additional condition related to a defect in Fe-S cluster biogenesis. It is the 2nd most common disorder linked to defective Fe-S cluster synthesis but is much less common than FRDA with only 25 known cases. To date, all patients identified with IM have come from families of Swedish ancestry.³² Similar to FRDA, the IM phenotype is inherited in an autosomal recessive pattern. IM is caused by a splicing defect during ISCU post-transcriptional processing that leads to defective ISCU protein.⁹³⁻⁹⁴ Loss of ISCU leads to lower ISC activity and a resulting deficiency of essential Fe-S proteins, including succinate dehydrogenase and aconitase of the citric acid cycle.⁹⁵ Symptoms are

exacerbated in cells that are metabolically active, such as the myocytes of skeletal muscle during exercise, and patients with IM experience exercise intolerance.⁹⁶ Prolonged activity can lead to tachycardia, tachypnea, and muscle pain.⁹⁷ Unlike FRDA, IM is not progressive and most cases have a normal life expectancy.

1.6.3 GLRX5 Sideroblastic Anemia

GLRX5 Sideroblastic Anemia (GSA), a disease caused by mutated GLRX5, has only been identified in a single patient to date. While GSA is exceedingly rare, this particular case study has revealed a unique mechanism linking Fe-S cluster production to general iron homeostasis.⁹⁸⁻⁹⁹ GLRX5, involved in the last step of the ISC pathway, directs Fe-S cluster delivery from ISCU to downstream targets. One target is the iron-responsive protein IRP1, an Fe-S protein activated when its Fe-S cluster is absent.⁹⁸ Defective GLRX5, therefore, leads to constitutively active IRP1. IRP1 regulates several proteins involved in iron homeostasis,¹⁰⁰ including those involved in heme production. In particular, *apo*-IRP1 inhibits expression of the initial enzyme in heme synthesis, aminolevulinate synthase (ALAS2). Defective GLRX5, therefore, leads to insufficient heme and impaired erythropoiesis, resulting in anemia. Iron that would be directed towards heme production accumulates in the mitochondria of erythroblasts, creating the characteristic ringed-sideroblasts.⁶²

1.6.4 Additional Diseases Related to Dysfunctional Fe-S cluster Biogenesis

Succinate Dehydrogenase (SDH) subunit B, the Fe-S cluster containing protein of the succinate dehydrogenase complex, is a known tumor suppressor. Succinate, the substrate for SDH, stabilizes hypoxia-inducible factor (HIF), which regulates key processes in cell division and blood vessel growth under hypoxic conditions. Mutations in SDHB or in fact

any of the other main subunits of SDH (SDHA, SDHC, and SDHD) cause susceptibility to tumor formations known as paragangliomas or pheochromocytomas in a disorder called *Hereditary Paraganglioma-Pheochromocytoma*,¹⁰¹ stemming from the accumulation of succinate and stabilization of HIF. SDHAF2, an assembly protein that flavinates SDH, is also implicated in paragangliomas. Recently, two additional Fe-S assembly proteins, SDHAF1 and SDHAF3, were found to stabilize Fe-S cluster assembly in SDH.¹⁰² The later two proteins have LYR-motifs (Leu-Tyr-Arg) common to proteins involved in Fe-S cluster assembly. SDHAF1 deficiency is known to cause leukoencephalopathy.¹⁰³

Lastly, mutations in either NFU1 or BOLA3, two different genes involved in Fe-S cluster biogenesis, leads to *multiple mitochondrial dysfunction syndrome*, a condition characterized by defects in Complexes I, II, and III and pyruvate/ α -ketoglutarate dehydrogenases. NFU1 is thought to be an alternative to ISCU as a scaffold for Fe-S assembly. Both BOLA3 and NFU1 appear to be involved in lipoate synthesis, possibly related to a role in assembling Fe-S clusters in lipoic acid synthase (LIAS), thus providing an explanation for the reduced PDH and α -KGDH activities characteristic of this syndrome. The impaired energy production results in lactic acidosis, encephalopathy¹⁰⁴ and early death.

CHAPTER 2: DEVELOPMENT AND VALIDATION OF OPTIMAL METHOD FOR *APO-ISU1* TO *FES-ISU1* TRANSFORMATION *IN VITRO*

2.0 Prelude

One of the earliest goals of my project was to measure the ‘activity’ of Isu1. This required a detailed understanding of the method that had been developed to assess Isu1 activity.¹⁰⁵ This method, which I will call the “FeS-Isu1 formation method”, would become the focus of my dissertation and will be used extensively throughout this work. This chapter is probably the most important chapter in my dissertation, as it describes how I needed to change the aims of my research from what was originally outlined in my dissertation proposal. In this section, I describe my original project on the characterization of the Isu1 Fe-S cluster coordination site and explain why the primary method I was relying on for these studies, the FeS-Isu1 formation method, was not suitable for this application. Next, I describe how the method was modified to maximize Fe-S cluster yield and describe steps taken to validate these new conditions. I need to give credit and thanks to former graduate student Dr. Andria Rodrigues, who provided many valuable insights and experiences during my first two years on these topics. I did all the writing and experiments in this section.

2.1 Introduction

Fe-S clusters are essential cofactors found throughout biology. Proteins that bind Fe-S clusters are termed “FeS-proteins” and these proteins are found in many of the most fundamental biochemical pathways. In eukaryotes, there is a single mitochondrial pathway that is essential for the formation of most cellular Fe-S clusters.¹⁰⁶ This pathway, called the “Fe-S cluster Pathway” or “ISC”, is a focus of my lab’s research. The model organism my

project uses for this work is the yeast *Saccharomyces cerevesiae* species. In yeast, *de novo* mitochondrial Fe-S cluster formation occurs on the scaffold protein “Isu1”.^{105, 107} Reduced sulfur is provided via a persulfide intermediate from the cysteine desulfurase enzyme “Nfs1”,¹⁰⁸ with the protein cofactor “Isd11” essential for Nfs1 activity.¹⁰⁹ Reducing equivalents for Nfs1 activity are provided by the ferredoxin “Yah1”.¹¹⁰ Another protein, frataxin, is believed to be involved in this process as an allosteric regulator of Nfs1¹¹¹⁻¹¹³ and/or in Fe(II) delivery to Isu1.¹¹⁴⁻¹¹⁶

Among the earliest goals for researchers studying ISC was to reproduce the Fe-S cluster forming ability of the pathway *in vitro* using isolated proteins. *Agar et al.*¹⁰⁵ were the first to successfully produce an Fe-S cluster on *apo*-Isu1, creating “FeS-Isu1”, *in vitro* in the bacterial system, and this work was adapted into eukaryotic ISC by the Lill¹¹⁷ and Barondeau¹¹⁸ research groups. Originally, the major goal of this project was to characterize the Fe-S cluster coordination site of the scaffold protein Isu1 utilizing this method. Specifically, we set out to identify the cysteine residue that accepts the persulfide intermediate from Nfs1. Previous students Andria Rodrigues, John Rotondo, and myself had synthesized Isu1 mutant plasmid constructs where the active-site cysteine residues (at positions 69, 96, and 139 in yeast) were substituted for inert alanines. We hypothesized that the Isu1 species with this cysteine residue absent would be uniquely unable to perform *de novo* Fe-S cluster formation. The results obtained using this strategy, however, were the opposite of similar studies reported using human ISC proteins.¹⁵ This led to questions regarding the methodology and further investigation suggested that this method was not strictly measuring Fe-S cluster formation on Isu1.

This chapter describes the original conditions that were used for FeS-Isu1 formation and unexpected behavior that was observed under these conditions. Data provided in the results section will demonstrate why these original conditions did not provide suitable results for the desired application. Modifications that were made to the FeS-Isu1 reaction conditions to generate the “optimal conditions” for FeS-Isu1 formation are also described and validated.

2.2 Methods

2.2.1 Protein Expression and Isolation

Expression and purification of wild-type Isu1 and Nfs1-Isd11 was done as described in chapter 3. The C69A, C96A, and C139A Isu1 mutants were synthesized via site-directed mutagenesis using the Quikchange Lightning kit (Agilent). 21 basepair primers were ordered from GENEWIZ with a single nucleotide mismatch at the location corresponding to the appropriate Cys→Ala mutation. Mutant Cys→Ala plasmids synthesized and amplified via PCR were sent to GENEWIZ for Sanger sequencing to confirm successful mutation propagation. Transformation, expression, and isolation for Cys→Ala Isu1 mutants were identical to that done for wild-type Isu1, as described in chapter 3.

2.2.2 Original Conditions for FeS-Isu1 Formation

This section describes the original conditions that were used for FeS-Isu1 formation. Results sections 2.2.1 and 2.2.2 include more information regarding why these conditions were flawed for assessing FeS-Isu1 formation. The original protocol for converting *apo*-Isu1 to FeS-Isu1 was taken from *Tsai. et al.*¹¹⁸ This method was intended for enzymatic analysis, treating the Isu1 scaffold as an enzyme for Fe-S cluster production. As such, the original protocol utilized excess substrate under the following solution conditions: 10μM

Nfs1-Isd11, 50 μ M Isu1, 200 μ M Fe, and 5mM DTT. The buffer used was 20mM HEPES, 150mM NaCl, 5mM BME at pH=7.5 at room temperature. Reactions were made to a 1-mL volume to accommodate a 1-cm cuvette. FeS-Isu1 transformation was monitored by measuring visible absorption at 427nm using a Cary 50 Bio UV-visible spectrometer every 20 seconds for 1 hour at room temperature. After initiating the reaction with addition of cysteine to a concentration of 250 μ M, reactions were immediately sealed in the cuvette within the glovebox and transferred to the spectrometer for analysis.

2.2.3 Optimal Conditions for FeS-Isu1 Formation

This section describes the optimal conditions that I identified for FeS-Isu1 formation. The results section 2.3.3 explains why these conditions have been identified as optimal. These conditions are as follows: 10 μ M Nfs1-Isd11, 50 μ M Isu1, 75 μ M Fe, and 5mM DTT in 20mM HEPES, 500mM NaCl, 5mM BME buffer at pH=7.5 at room temperature. The procedure is, otherwise, identical to that of the original method with reactions being initiated by addition of cysteine to a concentration of 500 μ M. These optimal conditions ultimately were similar to the methods described by *Tsai et al.*,¹¹⁸ but with 1/4th the Fe concentration and twice the *apo*-Isu1 concentration. The optimal method also uses circular dichroism (CD) spectroscopy in place of visible absorption spectroscopy. CD data was collected using a Jasco J-1500 spectropolarimeter with 1cm cuvette collecting data every 20 seconds at 560nm for 50 minutes at room temperature.

2.3 Results

2.3.1 Original FeS-Isu1 Formation Method Unable to Identify Persulfide-Accepting Cysteine of Isu1

FeS-Isu1 formation using the C69A, C96A, and C139A Isu1 mutants under the original FeS-Isu1 conditions revealed all Isu1 species had reduced ability to form Fe-S clusters (Figure 2.1). While the reduction in FeS-Isu1 formation was appreciable, there remained a significant increase in absorbance at 427nm, corresponding to Fe-S cluster formation, in all Isu1 species. Our hypothesis was that the Isu1 mutant species lacking the persulfide-accepting cysteine residue would be uniquely unable to transform into FeS-Isu1. Thus, the original FeS-Isu1 method had failed to identify a unique persulfide accepting cysteine in Isu1. Alternative methods for these studies were considered, such as utilizing the “hot” S₃₅ cysteine technique,¹¹³ but never pursued.

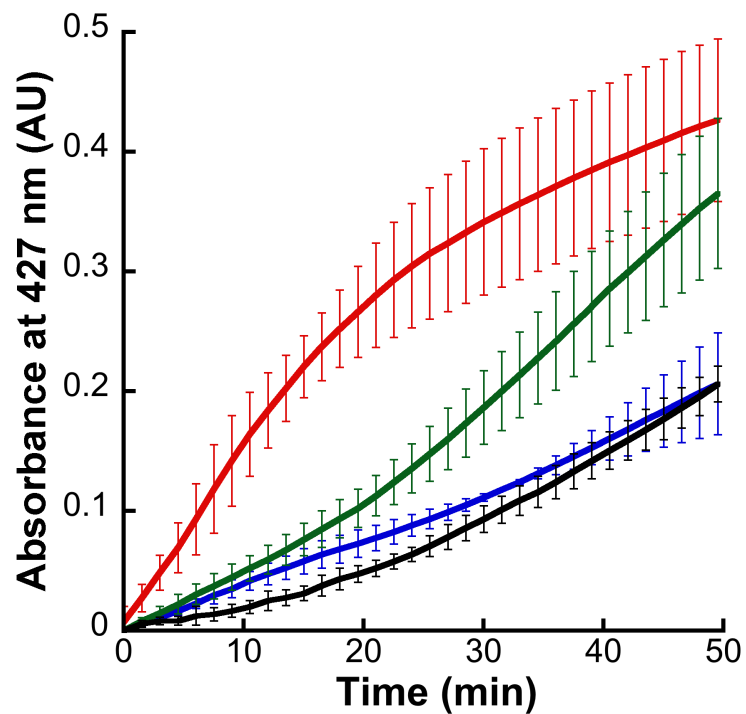


Figure 2.1: FeS-Isu1 formation for various Isu1 mutants. Wild type (red), C69A (blue), C96A (green), and C139A (black). Note all Cys₂His₁Ala₁-Isu1 mutants maintain some Fe-S cluster forming ability.

2.3.2 Secondary Species Forms During FeS-Isu1 Formation Using Original Conditions

Observations made using the original FeS-Isu1 formation method suggested that a secondary reaction was occurring. One observation made under the original conditions was that the increased absorbance observed during FeS-Isu1 formation was not specific to the chromophore associated with an Fe-S cluster at 427nm. This observation was not made with chemical delivery of sulfur to Isu1 (via Na₂S) indicating distinct differences in the cluster formation reaction mechanisms under protein driven events.¹²⁰ Instead, there was a uniform increase in absorption present at all wavelengths (Figure 2.2). The upward shift in the absorption spectra was consistent with an increase in light-scattering, possibly due to a precipitation of some reaction materials. After consultation and literature review, it was deduced that this species is most likely an insoluble or semi-soluble FeS-mineral not associated to protein.¹¹¹ A similar species was mentioned briefly in the literature as a byproduct of FeS-Isu1 formation,¹⁰⁵ but had not been adequately explained. It was possible that FeS-Isu1 formation and FeS mineralization were occurring simultaneously, but attempts to separate FeS-mineral from the reaction mixture were unsuccessful.

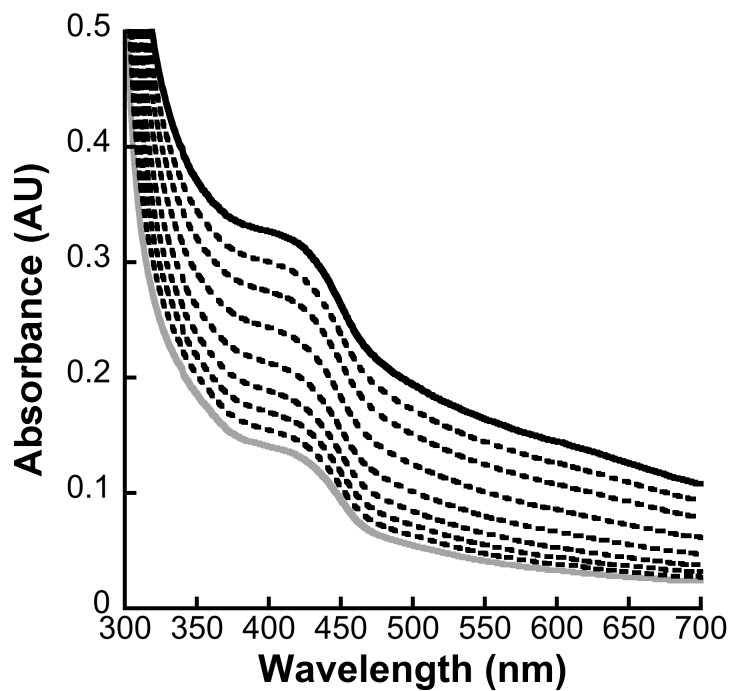


Figure 2.2: Non-specific increase light-scattering observed using original FeS-Isu1 formation method suggests precipitation of reaction materials. Entire absorption spectrum shifts up from time = 0 (gray) to time =40 minutes (black solid). Intermediate spectra are provided (black dashed) in 5 minute intervals.

2.3.3 Optimization of FeS-Isu1 Formation Method

After identifying problems with the FeS-Isu1 formation method, we investigated modifications to the protocol in order to maximize yield of FeS-Isu1, minimize FeS-mineral production, and afterwards rigorously validate the new method. Visible absorption was replaced with circular dichroism (CD) spectroscopy because CD is insensitive to formation of the FeS-mineral species and 2Fe2S-clusters have a characteristic CD signal between 300-700nm¹²¹ (see Chapter 3). Addition of excess exogenous *apo*-Isu1 to limiting Nfs1-Isd11 results in successful FeS-Isu1 formation. Analysis of the FeS-Isu1 product via CD produces a spectra similar to that found for the 2Fe2S-protein Yah1¹¹⁰ (Chapter 3) and the human wild type FeS-ISCU¹¹¹ found in the literature. To assess if the product is truly an Fe-S cluster, necessary components were systematically excluded one by one from the FeS-Isu1 formation reaction (Figure 2.3). *apo*-Isu1, Nfs1-Isd11, DTT, cysteine, and Fe²⁺ are all necessary to observe this signal, consistent with the presumed necessary components for Fe-S cluster formation.³ One important note is that FeS-Isu1 formation can occur at a reduced rate in the absence of DTT if the amount of cysteine is increased 10-fold (to 5mM), matching the original DTT concentration (data not shown). The CD signal observed depends directly on the starting concentration of *apo*-Isu1, which was not the case using the original conditions (Figure 2.4).

After performing successful FeS-Isu1 formation, this reaction was further studied to identify additional changes that would increase the yield of Fe-S clusters and reduce side reactions. In addition to the use of circular dichroism, two other important changes were made. First, the Fe concentration was reduced to 75µM. By varying the amount of Fe(II) in the reaction, it was observed that excess Fe(II) unexpectedly inhibits FeS-Isu1 formation

using the Isu1 ortholog from *Drosophila melanogaster* (Chapter 3). This effect is possibly due to the FeS-mineral side-reaction competing for reduced sulfur with Fe-Isu1. Under sub-stoichiometric Fe levels, the effect from this side-reaction is kept minimal. Second, the salt concentration of the experimental buffer was increased to 500mM NaCl. Unexpectedly, salt has a dramatic effect on the role of frataxin in this reaction (see Chapter 5) and frataxin stimulation requires 500mM NaCl conditions. Using the described optimal conditions, the non-specific increase in absorbance during FeS-Isu1 formation is minimal, suggesting reduced FeS mineralization is occurring compared to the original method (Chapter 3).

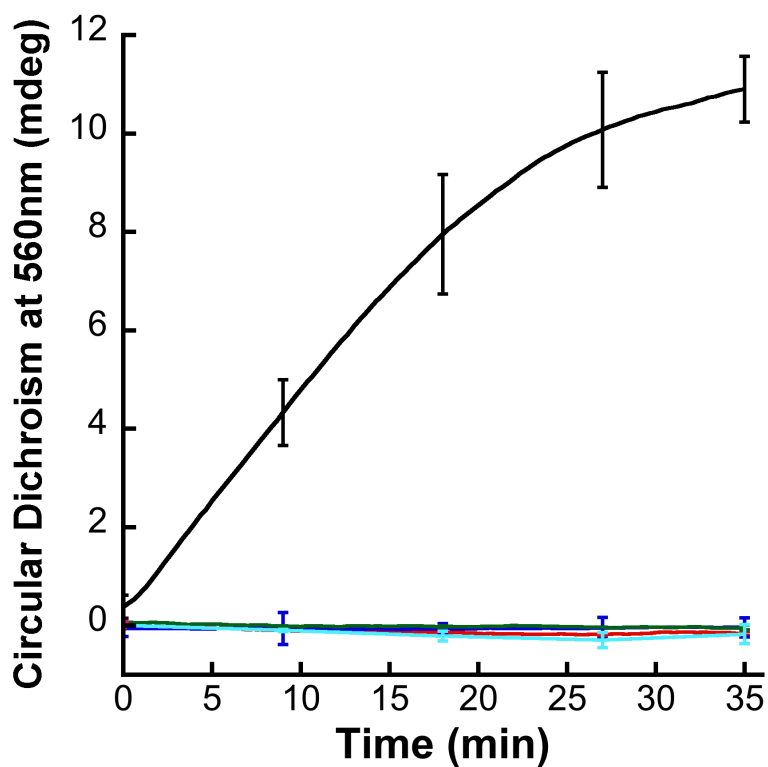


Figure 2.3: Isu1, Nfs-Isd11, DTT, Cysteine, and Fe are required for FeS-Isu1 formation under optimal conditions. 50 μ M Isu1, 10 μ M Nfs1-Isd11, 5mM DTT, 75 μ M Fe, 500 μ M cysteine (black), Fe excluded (pink), cysteine excluded (red), Nfs1-Isd11 excluded (green), Isu1 excluded (blue), and DTT excluded (cyan).

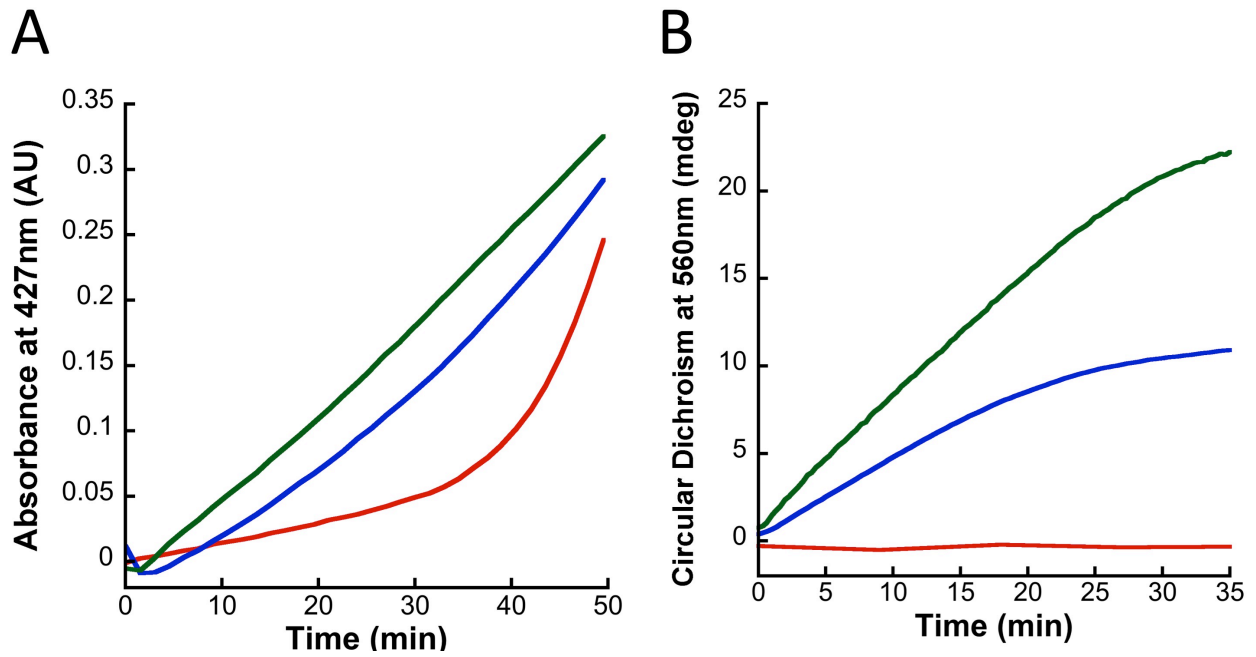


Figure 2.4: FeS-Isu1 formation for varying apo-Isu1 concentrations using the original FeS-Isu1 formation method (A) compared to the optimal method (B). No Isu1 (red), 1xIsu1 (blue), 2xIsu1 (green). Under optimal conditions, the Fe-S cluster signal depends directly on the concentration of *apo*-Isu1.

2.4 Discussion

2.4.1 Active-site Cysteines Essential for Fe-S cluster Coordination on Isu1

After further literature review, it was recognized that in addition to accepting persulfide, cysteine residues of Isu1 have a critical role in Fe-S cluster coordination.¹²² Therefore, the finding that all Cys→Ala Isu1 had retained Fe-S cluster forming ability using the original FeS-Isu1 formation method were difficult to reconcile with established basic understandings for how ISC functions. These results called into question the original FeS-Isu1 formation method and this led to further investigation for a protocol to more accurately monitor Fe-S cluster assembly. Furthermore, *Bridwell-Rabb et al.* performed similar experiments with the human Isu1 ortholog and found the opposite result that all Cys→Ala Isu1 mutants were completely unable to form FeS-Isu1.¹¹⁹ This work did, however, identify a unique persulfide-accepting cysteine using a method involving radioactive S³⁵-labeled cysteine and not FeS-Isu1 formation.¹¹⁹

The original hypothesis for a uniquely inactive Cys→Ala Isu1 mutant may have been misguided. It is unlikely that any of the Cys→Ala Isu1 mutants can produce stable Fe-S clusters, because in addition to accepting persulfide, cysteine is a critical component for coordination of the Fe in the Fe-S cluster.¹²² While most FeS-proteins utilize 4 cysteine residues for cofactor coordination,¹²³ Isu1 utilizes 3 cysteines and 1 histidine.¹²⁴ This Cys₃His₁ coordination results in a less-stable cluster that facilitates Fe-S cluster delivery.¹²⁴ In the Cys→Ala Isu1 mutants, however, there are only be 2 cysteine residues and 1 histidine and this likely is not sufficient for Fe-S cluster coordination. Therefore, all of the Cys→Ala Isu1 mutants probably should have been inactive, but it was conversely observed

they all had retained activity. This contradictory finding led to questions about the validity of the original FeS-Isu1 formation method that was used.

2.4.2 Identifying FeS-Mineral Secondary Species During FeS-Isu1 Formation

The most likely explanation for the unexpected behavior of the FeS-Isu1 formation method was the presence of a FeS-mineralization side-reaction. This FeS-mineral is likely an insoluble or semi-soluble Fe-S species that is not associated to protein.¹²⁵ This was deduced after making several observations on the original method for FeS-Isu1 formation. First, the increase in absorbance was not specific to the Fe-S cluster chromophore at 427nm (Figure 2.2), but was almost identical at any wavelength, consistent with a light-scattering phenomenon.¹²⁶ Second, the FeS-Isu1 absorption signal observed did not seem to depend directly on the starting concentration of *apo*-Isu1 (Figure 2.3). It was very irregular to find that the yield of FeS-protein produced was not directly proportional to the amount of *apo*-protein added. In fact, Isu1 could be completely excluded and a significant amount of apparent FeS-Isu1 formation was still observed by the original method. Formation of the FeS-mineral also could explain why all Cys→Ala Isu1 mutants had retained Fe-S cluster forming ability. A similar FeS-mineral byproduct, termed “High Molecular Weight Species”, was identified in *Fox et al.* while studying human ISC.¹²⁵

2.4.3 Behavior of FeS-Isu1 Formation Under Optimal Conditions is Consistent With Fe-S cluster Formation

Under the described optimal conditions, the behavior of the FeS-Isu1 formation reaction is consistent with *de novo* Fe-S cluster formation on the scaffold Isu1. The requirement for DTT, cysteine, *apo*-Isu1, Nfs1-Isd11, and Fe²⁺ reagents in FeS-Isu1 formation is consistent with reports from human,¹¹⁸ yeast,¹²⁷ and bacterial¹⁰⁵ ISC. This was

not the case using the original method, where *apo*-Isu1 could be excluded and a significant Fe-S cluster signal would still develop (Figure 2.3). One notable exception to these required reagents is frataxin, which has been previously reported is necessary for FeS-Isu1 formation when using sodium sulfide in place of Nfs1-Isd11 and cysteine.¹¹⁵ The product from the FeS-Isu1 reaction, obtained using the Isu1 ortholog from *Drosophila melanogaster*, will be further characterized in Chapter 3.

2.4.4 Significance of Competing FeS-Mineralization During FeS-Isu1 Formation

There are significant implications for the identification of FeS-mineralization during *in vitro* FeS-Isu1 formation reactions. In various literature articles that utilize visible absorption spectroscopy, it has been reported that FeS-Isu1 formation demonstrates a 'bi-phasic' pattern. This bi-phasic pattern has been interpreted differently among different researchers. Some researchers believe the second phase is associated with FeS-Isu1 formation,¹¹⁷ while others believe FeS-Isu1 formation occurred during the first phase.¹²⁸ To our knowledge, no-one has been able to explain what creates this bi-phasic pattern. These results suggest that this bi-phasic pattern is the result of simultaneous FeS-Isu1 formation and FeS-mineralization pathways, where the first phase is FeS-Isu1 formation followed by the second phase of FeS-mineralization. To support this, circular dichroism studies of FeS-Isu1 formation identify mono-phasic behavior that begins immediately upon addition of cysteine (Figure 2.3). Also note that FeS-mineralization in the absence of Isu1 (see Chapters 3 and 4) produces a dramatic increase in absorption following a ~10 minute lag period. Second, there have been reports that excess Fe²⁺ inhibits FeS-Isu1 formation for unknown reasons.²³ This work suggests a model that can explain this behavior where free Fe²⁺ competes for reduced sulfur with Fe-Isu1 (see Chapter 4).

CHAPTER 3: *IN VITRO* CHARACTERIZATION OF A NOVEL ISU HOMOLOGUE FROM *DROSOPHILA MELANOGASTER* FOR *DE NOVO* FE-S CLUSTER FORMATION.

3.0 Prelude

While investigating the FeS-Isu1 formation method described in Chapter 2, I began to utilize the fly Isu1 ortholog, “flscU”, as it had demonstrated favorable stability over its yeast counterpart. Former graduate students Dr. Kalyan Kondapalli and Dr. Swati Rawat had previously characterized this protein, but none of their results had ever been published. In particular, Chapter 3 of Dr. Rawat’s dissertation contained several flscU experiments that could serve as a springboard for my own studies. As I was struggling with my own project, characterization of flscU seemed like a logical alternative. During the course of this work, I visited Dr. Andrew Dancis’s laboratory at the University of Pennsylvania to conduct flscU complementation studies with yeast *in vivo* with the help of Dr. Agostinho Rocha. This chapter contains a manuscript in preparation for submission to the journal *Biochemistry*. Except for the *in vivo* component of the paper, the entire rest of the paper was written by me. This article has been a collaborative effort between the following co-authors:

Stephen P. Dzul[‡], *Agostinho G Rocha*[#], *Swati Rawat*[‡], *Ashoka Kandegadara*[‡], *April Kusowski*[‡],
Andrew Dancis[#], *Timothy L. Stemmler*^{‡*}

Wayne State University, Biochemistry and Molecular Biology[‡], *University of Pennsylvania,*
Department of Hematology[#]

3.1 Abstract

Fe-S clusters are iron-containing cofactors utilized by numerous proteins within several biological pathways essential to life. In eukaryotes, the primary pathway for Fe-S cluster production is the iron-sulfur cluster (ISC) pathway. The ISC pathway, localized primarily within the mitochondria, has been extensively characterized within *Saccharomyces cerevisiae*. In yeast, *de novo* Fe-S cluster formation is accomplished through coordinated assembly of the substrates iron and sulfur on the primary scaffold assembly protein "Isu1". The sulfur used for cluster assembly is provided by the cysteine desulfurase "Nfs1", a protein that works in union with its accessory protein "Isd11". Frataxin "Yfh1" helps direct cluster assembly by serving as a modulator of Nfs1 activity, by assisting in the delivery of Fe(II) to Isu1, or more likely through a combination of roles. *In vitro* studies on the yeast ISC system have been limited, however, due to the inherent instability of recombinant Isu1, a molecule prone to degradation and aggregation *in vitro*. To circumvent Isu stability issues, a recent report replaced yeast Isu1 with a homolog from the thermophilic fungus *Chaetomium thermophilum*, facilitating novel experimentation of the pathway. There are concerns, however, regarding the validity of replacing yeast Isu1 with different Isu1 orthologs. Given the unique utility of proteins within the fly model system, we were interested in pursuing a similar strategy by replacing yeast Isu1 with the fly ortholog in order to stabilize our *in vitro* ISC assembly system and assist us in elucidating molecular details of the yeast ISC pathway.

Our lab previously observed that recombinant frataxin from *Drosophila melanogaster* has remarkable stability compared to Yfh1. Here we have provided the first characterization of *D. melanogaster* Isu1 (flscU) and demonstrated its ability to function

within the yeast ISC machinery both *in vivo* and *in vitro*. Interestingly, flscU demonstrates increased stability compared to yeast Isu1, and increased yield when expressed recombinantly in bacteria. As expected based on their high sequence conservation, recombinant flscU has similar physical properties to yeast Isu1, functioning as a stable dimer with similar Fe(II) affinity and ability to form two 2Fe-2S clusters per dimer. Upon inspection, flscU and yeast ISC proteins are compatible *in vitro*; addition of Yfh1 to Nfs1-Isd11 increases the rate of Fe-S cluster formation on flscU to a similar extent as observed with yeast Isu1. Finally, flscU expressed in mitochondria of a yeast strain lacking Isu1 (and its paralog Isu2) is able to completely reverse the deletion phenotypes. These results demonstrate flscU can functionally replace yeast Isu1 and it can serve as a powerful tool for exploring molecular details within the yeast ISC pathway, both *in vivo* and *in vitro*.

3.2 Introduction

Fe-S cluster cofactors are ubiquitous in biology and play integral roles in nearly every biochemical pathway. In recent years, several human diseases have been linked to dysfunctional Fe-S cluster metabolism, including Friedreich's ataxia¹²⁹⁻¹³⁰ and IscU myopathy.¹³¹⁻¹³² Research at the molecular level into the Fe-S cluster production pathway is paramount to understanding disease pathology within these and related disorders. Since both free iron and sulfur are toxic in abundance, production of Fe-S clusters must occur within cells in a tightly regulated manner. In eukaryotes, the core pathway for Fe-S cluster production is the iron-sulfur cluster (ISC) pathway. This pathway is localized primarily within the mitochondria¹³³ and is essential for the formation of all cellular Fe-S clusters.¹³⁴ *In vivo* yeast ISC studies have provided molecular and genetic insight into how this pathway functions. In *Saccharomyces cerevisiae*, *de novo* mitochondrial Fe-S cluster formation occurs on the scaffold protein "Isu1", which provides the architecture for cofactor assembly.¹³⁵⁻¹³⁶ The cysteine desulfurase "Nfs1", when in combination with its accessory protein partner "Isd11", provides sulfur for cluster assembly.¹³⁷⁻¹³⁸ The ferredoxin "Yah1" provides reducing equivalents to direct and stabilize cofactor assembly and to reduce sulfur and perhaps iron cofactors.¹³⁹ Frataxin "Yfh1", an allosteric regulator of ISC,¹⁴⁰⁻¹⁴¹ helps facilitate Fe delivery to Isu1 by possibly mediating iron binding onto Isu1¹⁴²⁻¹⁴³ or by serving in a yet uncharacterized manner. These proteins work in a coordinated manner to assemble Fe-S cluster intermediates onto Isu1, however the molecular details of this process are still poorly understood.

Investigative studies of the *S. cerevisiae* ISC pathway *in vitro* have provided some insights into mitochondrial Fe-S cluster assembly.¹³⁴ These studies, however, have been

hampered due to the instability of recombinant Isu1, which has relatively low solubility and is prone to spontaneous aggregation.¹³⁹ Recently, *Webert et al* circumvented this limitation within their yeast characterizational studies by replacing *S. cerevisiae* Isu1 with the thermophilic ortholog from *Chaetomium thermophilum*.¹³⁹ While Isu1 ortholog replacement facilitated novel experimentation in this system, there is a potential concern regarding incomplete complementation between the *S. cerevisiae* and *C. thermophilum* ISC molecular partners. A recent study demonstrating that frataxin, a central component of ISC, functions differently in the yeast and bacterial systems¹⁴⁴ highlights these concerns. Previous characterizational studies on the frataxin ortholog from *Drosophila melanogaster*, “Dfh”, found that this protein behaves highly similarly to Yfh1, however it had enhanced stability.¹⁴³ In this current article, we characterize an Isu1 ortholog from *D. melanogaster* “flscU” and compare it to the *S. cerevisiae* Isu1 ortholog, “yIsu1” with regards to its biophysical properties and functionality related to cluster assembly. We demonstrate that flscU is functionally active in mediating Fe-S cluster assembly and is able to interact with yeast ISC proteins both *in vitro* and *in vivo*. Our data support the Webert results of the *C. thermophilum* ISC characterizational studies and provide an additional, and highly stable Isu ortholog, which can be used to further investigate the yeast ISC system.

3.3 Methods

3.3.1 Protein Expression and Purification.

S. cerevisiae Isu1 (yIsu1), Nfs1-Isd11, Yfh1, Yah1, Nfs1-Isd11-yIsu1-Yfh1 complex, and *D. melanogaster* Isu (flscU) were expressed in *E. coli* and purified in the following manner. Plasmid constructs were synthesized for each respective protein as follows: flscU and yIsu1 vectors were prepared in pET151/D-TOPO (ThermoFisher), Nfs1-Isd11 in

pST39¹⁴⁵ (Addgene), Yfh1 in pCOLAduet (Novagen), and Yah1 in pET21b (Novagen). Cells with the pET151/D-TOPO, pST39, and pET21b plasmids were grown in 100 µg/mL ampicillin; cells with pCOLAduet were grown in 50 µg/mL kanamycin. All constructs contained a 6xHis-tag on either the C- (Yfh1, yIsu1, Nfs1, Yah1) or N- (flscU) terminus. Plasmids were transformed into competent cells via heat-shock at 42°C for 30 seconds. Optimal growth conditions were identified for each respective protein. Individual proteins (yIsu1, Yfh1, and the Nfs1-Isd11-Isu1-Yfh1 complex) were expressed in BL21-RIL competent cells¹⁴⁶ (Agilent), Nfs1-Isd11 and flscU was expressed in BL21-DE3 cells (Agilent), and Yah1 was expressed in C41 cells (Lucigen). Cells with yIsu1, Yfh1, Yah1, and Nfs1-Isd11-yIsu1-Yfh1 plasmids were grown to an optical density (OD) ~0.6, induced with 0.8 mM IPTG, and incubated for 3 hours at 37°C. Nfs1-Isd11 expressing cells were induced at OD ~0.4 and incubated for 18 hours at 18°C. PLP was added, to a final concentration of 10µM, to Nfs1-Isd11 and Nfs1-Isd11-yIsu1-Yfh1 cells at the time of induction. The protein flscU was expressed using an auto-induction protocol¹⁴⁷ utilizing inoculation into ZYP-5052 rich media at 27°C for 24 hours. After harvesting, cells were lysed using an Emulsiflex-C3 homogenizer (AVESTIN). Lysis buffer for yIsu1, flscU, Yfh1, Nfs1-Isd11, and Yah1 included 50mM Sodium Phosphate (NaPi), 300mM NaCl, and 20mM imidazole. The lysis buffer for Nfs1-Isd11-yIsu1-Yfh1 complex purification was 20mM HEPES, 150mM NaCl, and 20mM imidazole. Lysate was centrifuged at 21 krpm for 45 minutes. The soluble fraction was decanted and filtered before being run through a Ni-column. The Ni-column was then washed with 5 column volumes of 50mM imidazole buffer to remove bacterial proteins. The His-tagged target protein was eluted with 5x column volumes of 200mM imidazole buffer. After elution from the Ni-column, the protein was concentrated to ~2 mL

via a 10 kDa cutoff membrane Amicon centricon and run on a gel filtration column where buffer was switched to the final experimental buffer. The experimental buffer was 20mM HEPES at pH=7.5 with differing amounts of salt depending on protein species. For Nfs1-Isd11-Isu1-Yfh1 this was 50mM NaCl, for Nfs1-Isd11, Yfh1, Yah1 this was 150mM NaCl, and for yIsu1 and flscU this was 300mM NaCl. The proteins flscU, yIsu1, Yah1, and Yfh1 were run on a S75 size exclusion column, while Nfs1-Isd11-Isu1-Yfh1 and Nfs1-Isd11 were run on a S200 size exclusion column. Purified fractions were pooled and concentrated via Amicon centrifugation. Protein concentration was determined using a Direct-detect IR spectrometer¹⁴⁸ (Millipore) and protein purity was assessed via SDS-PAGE. Typical protein purities were ~95%. Concentrated pure protein solutions were flash-frozen in liquid N₂ and stored at -80°C until immediately prior to experimentation.

3.3.2 Secondary Structure Characterization of yIsu1 and flscU

Circular dichroism (CD) spectroscopy was used to determine and compare the general folding parameters of both yIsu1 and flscU. Protein secondary structures were determined using CD spectroscopy by focusing within the far UV-region (185-260 nm). Homogeneous protein samples were diluted to 10 μ M and switched into a 1mM NaPi buffer via Amicon centrifugation in order to allow far-UV transparency. Data were collected using a 1-mm pathlength CD cuvette on a Jasco J-1500 spectrometer. Spectra were analyzed using the Spectra Manager CDPro software system¹⁴⁹ (Jasco). Simulations of the spectra were calculated using the SP37 reference set¹⁵⁰ and CONTIN method.¹⁵¹ Spectra provided in Figure 3.2B are the average of 6 scans. This process was done in triplicate to ensure reproducibility.

3.3.3 Fe-Binding Analysis to flscU

While the Fe-binding characteristics of yIsu1 have previously been reported,¹⁴² metal binding competition analysis was used to characterize the Fe-binding properties of flscU. Fe-binding to flscU was assessed using two secondary methods involving the competition of limiting amounts of iron between flscU and each of the two Fe-binding ligands, Mag-Fura-2 and Fura-FF (Molecular Probes). Experiments were done in triplicate to confirm reproducibility and to identify uncertainty intervals from this method.

Fe-binding competition between flscU and the Mag-Fura-2 ligand was performed using a protocol recently outlined for yIsu1.¹⁵² Under anaerobic conditions at room temperature, a 10mM Fe(II) solution was added in 0.5 μ L increments to a 1mL solution with 8 μ M flscU and 8 μ M Mag-Fura-2. All samples were in 20mM HEPES and 150mM NaCl buffer at pH=7.5. A UV-visible absorption spectrum was collected for each Fe(II) consecutive concentration, again under anaerobic conditions, and spectral intensities at 366nm are indicative of uncomplexed (*apo*) Mag-Fura-2 ligand were used for binding characterization determination.¹⁵² Controls was performed by anaerobically adding the Fe(II) solution to 8 μ M Mag-Fura-2 or to 8 μ M flscU, independently.

Using an analogous method to what was described with Mag-Fura-2, competition for Fe-binding to flscU was also tested using the Fe-binding fluorophore Fura-FF. In principle, Fe-competition between flscU and Fura-FF is the same as competition between flscU and Mag-Fura-2. A key difference with Fura-FF, however, is that Fura-FF is a fluorophore that complexes calcium (Ca-Fura-FF). Addition of Fe causes the calcium to dissociate from Fura-FF and bind Fe(II). The fluorescence of Fe-Fura-FF complex is about twenty times lower than that seen in the Ca-Fura-FF complex and, as a result, the total fluorescence decreases

as more Fe(II) is added to the solution. Therefore, instead of measuring the UV-visible absorption, the fluorescence excitation spectrum between 250nm-450nm is collected after each incremental titration of Fe(II) while keeping the emission wavelength at 510nm. For binding parameter determination, excitation at only 350nm considered. The experimental conditions and data analysis procedure are, otherwise, identical to that described for Mag-Fura-2.

Fe-binding parameters for Mag-Fura-2 and Fura-FF were determined using best-fit simulations with the Dyna-Fit software module¹⁵³ for a 1- or 2-binding site model. These simulations serve as controls for the binding affinity and stoichiometry of each chelator. Best-fit dissociation constants are identified using a fixed concentration and extinction coefficients for Mag-Fura-2/Fura-FF when added with the solution of the flscU protein.

3.3.4 X-ray Absorption Spectroscopy (XAS) Studies of Fe Bound to flscU

XAS was used to study the local coordination environment around the Fe-center in flscU. A solution of ferrous ammonium sulfate was added directly to flscU under sulfur free (Fe-flscU) and sulfur available (FeS-flscU) conditions. Both XAS samples were prepared anaerobically within a Coy glove box using protein, along with iron and sulfur solutions initially degassed on a Schlenk line before use. XAS samples were prepared in 20mM HEPES buffer (pH 7.5), 150mM NaCl, 5mM β -mercaptanol (BME) and 30% glycerol. Multiple independent duplicate samples were prepared under the following conditions: A) Fe-flscU was prepared by incubating flscU with 0.9 equivalents of ferrous iron and B) FeS-flscU was prepared by following Fe-S cluster assembly conditions outlined below. Samples were given 3 hours to equilibrate at 10°C before being loaded into Lucite sample cells wrapped with Kapton tape. Loaded samples were immediately flash frozen in liquid

nitrogen, removed from the glove box and stored in liquid nitrogen until XAS data collection was performed.

XAS data were collected at the Stanford Synchrotron Radiation Laboratory (SSRL) on beamline 7-3. Beamline 7-3 is equipped with a rhodium-coated silicon mirror and a Si[220] double crystal set monochromator; rejection of harmonics was achieved by detuning the monochromator to 30%. Samples were maintained at 10K using an Oxford Instrument continuous-flow liquid helium cryostat. Protein fluorescence excitation spectra were collected using a 30-element Ge solid-state Canberra array detector. XAS spectra were measured using 5eV steps in the pre-edge region (6,900 – 7,094 eV), 0.25eV steps in the edge region (7,095-7,135 eV) and 0.05 Å⁻¹ increments in the extended X-ray absorption fine structure (EXAFS) region (to k = 13 Å⁻¹), integrating from 1 to 20 seconds in a k³ weighted manner for a total scan length of approximately 40 minutes. X-ray energies were calibrated by collecting an iron foil absorption spectrum simultaneously with collection of the protein data. Each fluorescence channel of each scan was examined for spectral anomalies prior to averaging and spectra were closely monitored for photoreduction. Protein data represent the average of 7-8 scans.

XAS data were processed using the Macintosh OS X version of the EXAFSPAK program suite,¹⁵⁴ integrated with Feff version 7.2 for theoretical model generation. Data reduction and processing followed previously established protocols.¹⁴² X-ray absorption near-edge spectroscopy (XANES) analyses were performed using XAS data near the Fe K-edge (7,100-7,160 eV) for both Fe-flscU and FeS-flscU. The first derivative of the protein XANES spectra was compared to values obtained for aqueous Fe(II) and Fe(III) standard solutions to approximate the Fe oxidation state of metal in the all protein samples. EDG_FIT

software was used to analyze the pre-edge region in all protein samples. A spline function was fit over the pre-edge region (7,109-7,117 eV) and Gaussian models were applied to accommodate features observed that deviated from the spline. Best-fit models were integrated to approximate the normalized pre-edge feature area.

EXAFS fitting analysis was performed on raw/unfiltered data following a previously established strategy.¹⁵⁵ EXAFS data were fit using both single- and multiple-scattering theoretical model amplitude and phase functions for Fe-O/N, Fe-S, Fe-Fe and Fe-C interactions. During spectral simulations, metal-ligand coordination numbers were fixed at half-integer values and only the absorber-scatterer bond length (R) and Debye-Waller factor (σ^2) were allowed to freely vary. Criteria for judging the best-fit simulation utilized both the lowest mean square deviation between data and fit (F'), corrected for the number of degrees of freedom, and a reasonable Debye-Waller factor.¹⁵⁶⁻

157

3.3.5 Fe-S Cluster Formation Reaction

Fe-S cluster loaded yIsu1 (FeS-yIsu1) and cluster loaded flscU (FeS-flscU) were prepared from purified *apo-yIsu1* and *apo-flscU*. The procedure for measuring this transformation has been modified from what has been previously reported both by our lab¹⁴² and from the original method.¹³⁵ All solutions were prepared and mixed within an anaerobic glovebox (Coy). In order to achieve optimal yield of FeS-Isu, Nfs1-Isd11 or the Nfs1-Isd11-Isu1-Yfh1 complex were added in a lesser amount (10 μ M) than Isu1 (50 μ M). This is essential as, under stoichiometric conditions of Nfs1-Isd11 and Isu1, FeS-Isu formation is reduced or absent.¹⁵⁸ Yfh1, when present, was added to a 10 μ M concentration where stimulation was observed to be maximal. A limiting amount of Fe(II) ammonium

sulfate (75 μ M) was added to prevent adverse FeS-mineralization.¹⁵⁸ L-cysteine was added in 5-fold excess to a concentration of 500 μ M. The reaction buffer contained 20mM HEPES (pH = 7.5), 500mM NaCl, 5mM BME, and 5mM dithiothreitol (DTT). Reaction formation was monitored both by visible absorption and circular dichroism (CD). Visible spectra were collected with a Shimadzu UV-1800 spectrophotometer and CD spectra were collected with a Jasco J-1500 spectropolarimeter using a 1-cm cuvette.

Cuvettes were sealed prior to being transferred from the glovebox to prevent Fe-oxidation. The reaction volume used was 1.1mL to accommodate the size of the cuvette. For quantifying FeS-flscU formation, the size of the 2Fe-2S characteristic negative CD feature at 560nm was measured every 20 seconds until reactions reached completion. Circular dichroism has several advantages over visible absorption¹⁵⁹ signals, so this technique is currently selected as the preferred method for measuring Fe-S cluster assembly. At completion of assembly, visible absorption and CD spectra were collected between 350nm-700nm. Adverse FeS-mineralization was estimated as the change in light scattering that occurred during the course of the reaction. Light scattering was estimated as the change in absorption at 700nm, a wavelength distinct from the expected 2Fe-2S chromophore measured at ~456nm.

3.3.6 Complementation of Yeast ISC by flscU

For *in vivo* studies, the transit peptide sequence of yeast CoxIV (cytochrome c oxidase subunit IV) was fused to the mature sequence of flscU. The flscU gene lacking the first 25 amino acids was amplified, including the in frame restriction sites XbaI and XhoI from the pET151/D-TOPO vector used for bacterial flscU expression. Primers used were:

XbaI-dlscU-fw 5' ataataTCTAGAtatcatgaaaatgtcgttgag 3'; XhoI-dlscU-rv 5'

tattatCTCGAGggttgccaccttcttctgctg 3'. This fragment was inserted, using the respective restriction sites, into the engineered YCplac22 plasmid-Isu1prom-CoxIVL-XbaI-XhoI-STOP-ISU1 3' UTR¹⁶⁰ thereby targeting the flscU to yeast mitochondria with the CoxIV leader sequence. Strain GAL1-ISU1/ Δ Isu2 with the ISU2 paralog deleted and the ISU1 gene under control of the regulated GAL1 promoter was used for complementation studies. The strain was transformed with the YCplac22 plasmid containing the flscU (see above), an identical plasmid containing the yeast Isu1 or the empty YCplac22 plasmid, selecting for Trp1 prototrophy. The chromosomal GAL1 promoter was switched off by shifting cells from galactose to glucose as the carbon source. For spotting on agar plates, serial 10-fold dilutions of the transformants were spotted onto defined medium agar plates containing CSM-Trp/glucose, thereby maintaining selection for the plasmid and repressing the GAL1 promoter at the same time. The plates were photographed 4 days later.

3.3.7 Cellular Iron-Uptake

Cellular iron uptake was measured as previously described¹⁶¹ with minor modifications. Briefly, cells were grown for 16 hours in CSM (complete supplemented defined glucose medium) at 30°C and diluted back to a density of 4×10^6 cells/ml. Cells were washed in 50mM citrate (pH 6.6) and 5% glucose. An aliquot of 1×10^5 cells was further incubated at 30°C for 90min with $1\mu\text{M } ^{55}\text{Fe}^{2+}$ ascorbate dissolved in 50mM citrate (pH 6.6), 5% glucose. After washing away unincorporated iron and harvesting cells with a PHD cell harvester, cells were incubated with scintillation fluid, and ^{55}Fe radioactivity was measured in a Beckman scintillation counter.

3.4 Results

3.4.1 Molecular Characteristics of Recombinant flscU

The molecular characteristics of both flscU and ylsu1 were compared to gain insight into the possible compatibility of these two orthologs. Alignment of the amino acid sequences indicates flscU and ylsu1 are highly homologous (Figure 3.1), with 71% sequence identity and 82% sequence similarity. As with the yeast ortholog,^{142, 152} flscU expresses in *E. coli* in sufficient abundance (~10mg/L culture), and can be isolated at high enough purity (>95%), to allow for *in vitro* characterizational studies (Figure 3.2A). Size exclusion chromatography indicates flscU elutes with a retention volume (61.0mL) similar to that observed with ylsu1 under the same solution conditions (60.6mL), with both eluting between the 44 kDa (58.2mL) and 17 kDa (73.8mL) molecular control standards (data not shown). The approximated molecular weight of flscU is ~33 kDa and that of ylsu1 is ~35kDa as assessed by gel filtration (versus the size of the monomer resolved on SDS PAGE in Figure 3.2A) consistent with both flscU and ylsu1 existing as molecular dimers, in agreement with the reported characteristics of bacterial IscU.^{135, 162}

```

mlpvitrfarpalmairpvnamgvlrassitkrlyhpkviehythprnvgsldkklpnvg 60
-MSLV----RN----SSRLLRSQVKRVQSVVALYHENVVEHYENPRNVGSLDKKDVTVG 51
: :: * : : *..* : *** :*:*** .***** .**

tglvgapacgdvmrlqikvndstgviedvkfktfgcgsaiasssymtelvqgmtlddaak 120
TGLVGAPACGDVMKLQIKVDE-NGKIVDAKFKTFGCGSAIASSSLATEWVKGKSIDEAGK 110
*****:*****: . * * *.***** ** *: * :*:*. *

iknteiakelslppvklhcsmlaedaikaaikdykskrntptmls 165
LKNTDIAKELRLPPVKLHCSMLAEDAIIKAALADYKVKQQKQVAN- 154
:***:***** *****: *** *::. .

```

Figure 3.1: Sequence alignment of full-length open reading frames (ORFs) between *Isu1* from *Saccharomyces cerevisiae* (*yIsu1*, lower case) and *Drosophila melanogaster* (*flscU*, upper case). *flscU* has 71% sequence identity and 82% sequence similarity to *yIsu1*. Residues colored by the ClustalW coloring convention are as follows: acidic (blue), hydrophobic (red), basic (magenta), and hydroxyl/sulphydryl/amine (green).

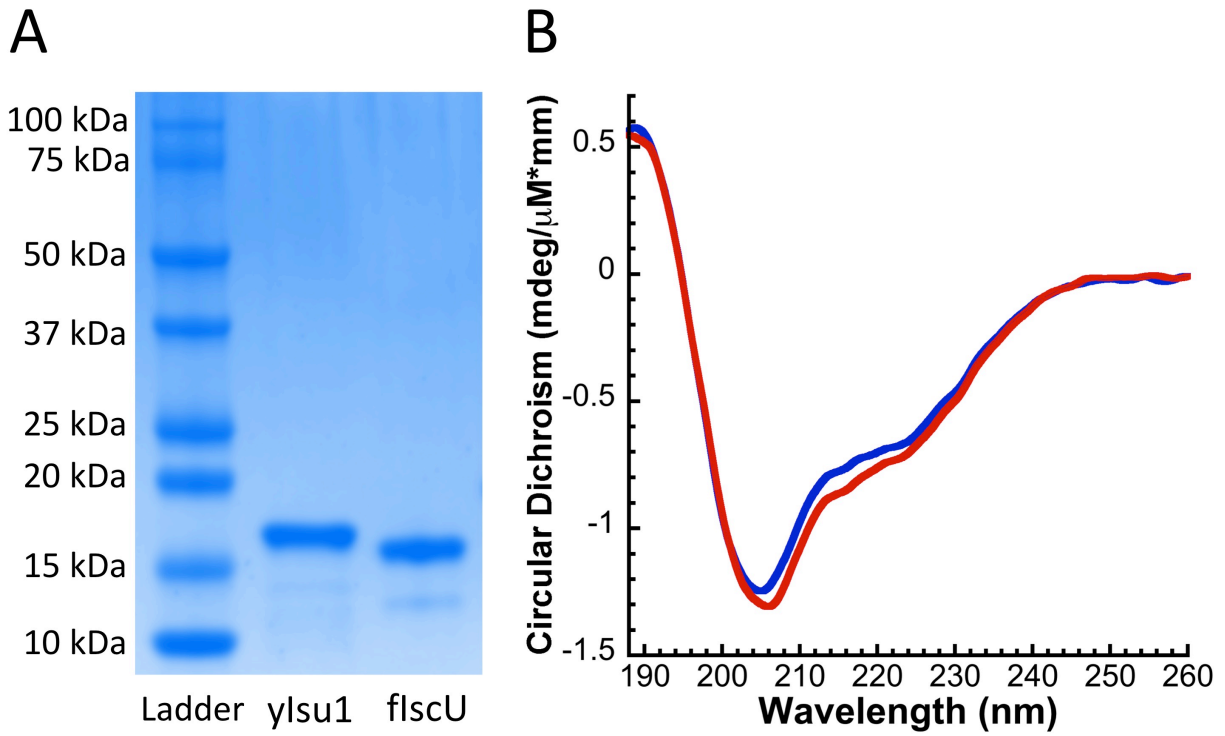


Figure 3.2: A) Representative SDS-PAGE gel comparing recombinant mature *D. melanogaster* IscU (flscU) to *S. cerevisiae* Isu1 (yIsu1). B) Far UV circular dichroism of yIsu1 (blue) and flscU (red) reveals that both proteins share a similar composition of secondary structural features.

3.4.2 Biophysical Characterization of flscU

Secondary Structure and Fe Binding Affinity - Quantitation of the secondary structure content of flscU and ylsu1 was determined by circular dichroism (CD) spectroscopy to provide further insight into the molecular similarities between these orthologs. CD spectra, collected for flscU and ylsu1 under identical solution conditions, show a strong degree of complementary fold (Figure 3.2B). The relative comparison of secondary structural content measured for flscU and ylsu1 provides a picture of the two proteins that is highly similar, and consistent with structurally characterized orthologs. Both flscU and ylsu1 have an α -helical content of 23% and 24%, a β -strand content of 21% and 20%, turn and loop content of 24% and 24%, and an unstructured content of 32% and 32% for flscU and ylsu1, respectively. In comparison, the structural content from the *E. coli* ortholog's crystal structure shows a 28% α -helical content, 12% β -strand content, 25% turn/loop content and a 35% unstructured content.¹⁶³

The Fe binding capacity of flscU was tested to support the role of the protein as the *de novo* Fe-S cluster assembly scaffold. The Fe(II)-binding capacity of flscU was measured using an iron chelation competition assay, developed to match conditions similar to circumstances observed *in vivo* where a variety of biomolecules compete to coordinate the metal. Two Fe-binding ligands, Mag-Fura-2 and Fura-FF, have been shown to be effective Fe-binding chromophores/fluorophores, hence these were used to measure the metal binding affinity of flscU and ylsu1 under our competition conditions. Spectral correlations at progressive [Fe], as well as the subsequent Fe-binding curve with simulation for both ligands in the presence of flscU, are given in Figure 3.3. As controls, dissociation constants for Mag-Fura-2 and Fura-FF Fe(II) binding in the absence of protein were measured as 2.0

$\pm 0.2 \mu\text{M}$ and $0.4 \pm 0.1 \mu\text{M}$, respectively. Best-fit simulation parameters from ligand Fe-binding profiles with flscU are provided in Table 3.1. For both ligands, data indicate two Fe(II) dissociation constants: a tighter binding constant of $695 \pm 242 \text{ nM}$ and $720 \pm 150 \text{ nM}$ for Mag-Fura-2 and Fura-FF, and a weaker binding constant of $5.55 \pm 2.54 \mu\text{M}$ and $2.21 \pm 0.13 \mu\text{M}$ for Mag-Fura-2 and Fura-FF, respectively. Differences in binding constant values between both Fe-binding sites are below the lower limits of detection for these methods and should be considered approximately equivalent.

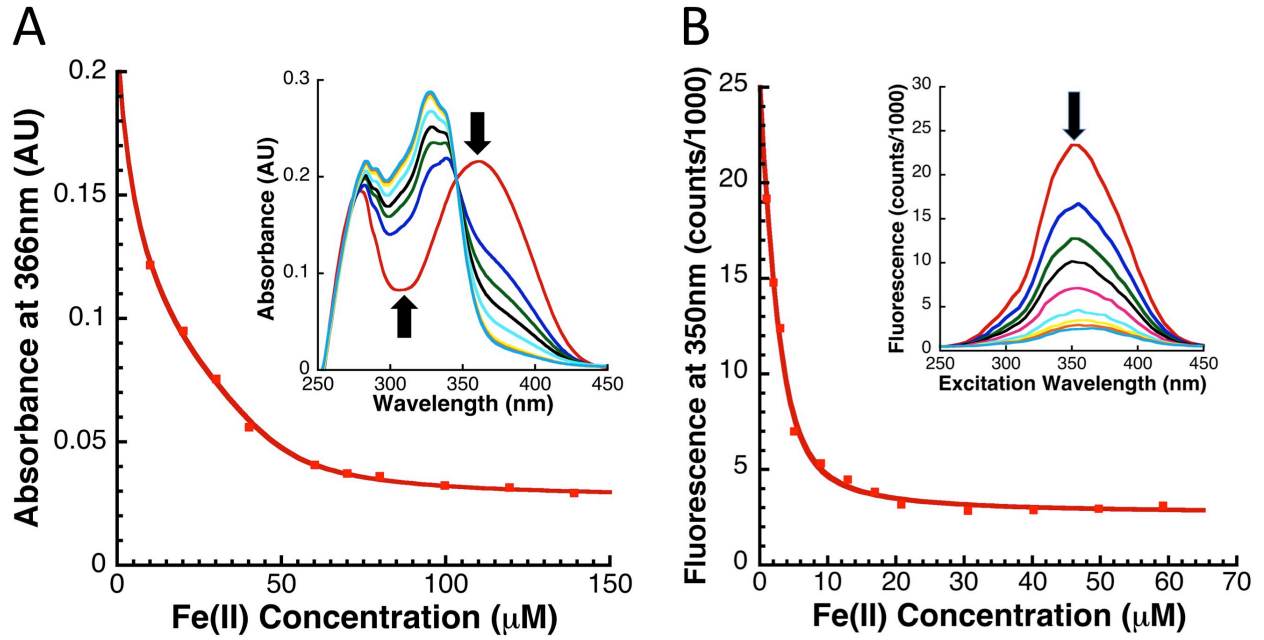


Figure 3.3: Fe-Binding Competition Assay with MagFura (A) and Fura-FF (B) ligands upon titration of Fe(II) in the presence of $8\mu\text{M}$ flscU. Solid line represents best-fit simulation of data. Inset demonstrates disappearance of chromophore observed during Fe(II) titration.

Method	K_{D1}	K_{D2}
Competition with Mag-Fura-2	695 ± 242 nM	5.55 ± 2.54 μ M
Competition with Fura-FF	720 ± 150 nM	2.21 ± 0.13 μ M

Table 3.1: Average simulation results including averaged values for dissociation constants (K_{D1} and K_{D2}).

X-ray Absorption Spectroscopy (XAS) - XAS was used to characterize the metal-site structure for Fe bound to flscU unaccompanied or in the presence of sulfur. X-ray absorption near edge spectroscopy (XANES) analyses for Fe-flscU and FeS-flscU indicate iron is coordinated in a reduced (Fe(II) only) or semi-reduced state (Fe(II)/Fe(III) mixture), respectively (Figure 3.4), when compared to authentic Fe-O/N and Fe-S model compounds. The 1st inflection point energy values for Fe-flscU and FeS-flscU are 7123.4 and 7123.3 eV, similar to the values obtained for the Fe(II) sulfate (7123.2 eV) and Fe(II) chloride (7119.5 eV) standards. A distinct pre-edge feature, attributed to a 1s-3d electronic transition, is observed in all samples at ~7,112 eV. This feature is small (<0.05 NFU*eV) in Fe-flscU (Figure 3.4, inset), consistent with 6-coordinate Fe-O/N symmetric model compounds.¹⁶⁴ In the FeS-flscU sample, this feature is over 4-times larger (0.22 NFU*eV), similar to 1s-3d features observed for 4-coordinate Fe constrained within Fe-S clusters.¹⁴² The large 1s-3d transition in the FeS-flscU spectrum suggests the 4-coordinate geometry in this sample is more tetrahedral than planar, consistent with other Fe-S clusters.¹⁶⁵⁻¹⁶⁶ There are no apparent 1s-4p features in either sample, making pyramidal geometries highly unlikely.¹⁶⁷ Comparison of the FeS-flscU edge with that from as isolated Yah1, an authentic Fe-S cluster containing protein, shows distinct similarities in edge features and in 1s-3d electronic transition height. Subtle pre-edge max and edge 1st inflection point energies between these two samples may suggest Fe in Yah1 is slightly more reduced, or more likely indicate the Fe-S₄ first ligand coordination sphere in Yah1 does not completely match the Fe environment found in FeS-flscU.

Analysis of the extended x-ray absorption fine structure (EXAFS) region of the XAS data was used to provide extremely high-resolution bond lengths, as well as ligand identity

and coordination numbers, for iron bound in both Fe-flscU and FeS-flscU. EXAFS from Fe-flscU and FeS-flscU reveal a pattern consistent with the structural pictures suggested from the XANES above. Figure 3.5 compares the raw EXAFS data and best-fit simulations for each flscU sample, as well as their subsequent Fourier transforms of the EXAFS data; best-fit simulation parameters for both samples are provided in Table 3.2. For Fe-flscU, scattering in the nearest-neighbor ligand environment is strictly constructed from two independent environments of oxygen/nitrogen ligands at 1.99 Å and 2.15 Å. For FeS-flscU, however, in addition to Fe-O/N scattering at 2.03 Å, there is significant Fe-S scattering in the nearest neighbor environment at 2.28 Å, and Fe-Fe scattering features at 2.72 Å. Finally, there is long range Fe•••C scattering observed at $R > 3.0$ Å in both flscU samples. The EXAFS and FT data for Yah1 is compared to that of FeS-flscU as an authentic Fe-S cluster containing molecule. The Fe-S and Fe•••Fe bond lengths for Yah1 are consistent with the values seen for FeS-flscU. There are however subtle differences in the iron nearest neighbor environment's between these two samples, specifically FeS-flscU has an additional Fe-O/N nearest neighbor ligand environment and smaller coordination numbers for both the Fe-S and Fe•••Fe environments, suggesting subtle differences in cluster coordination between the two samples.

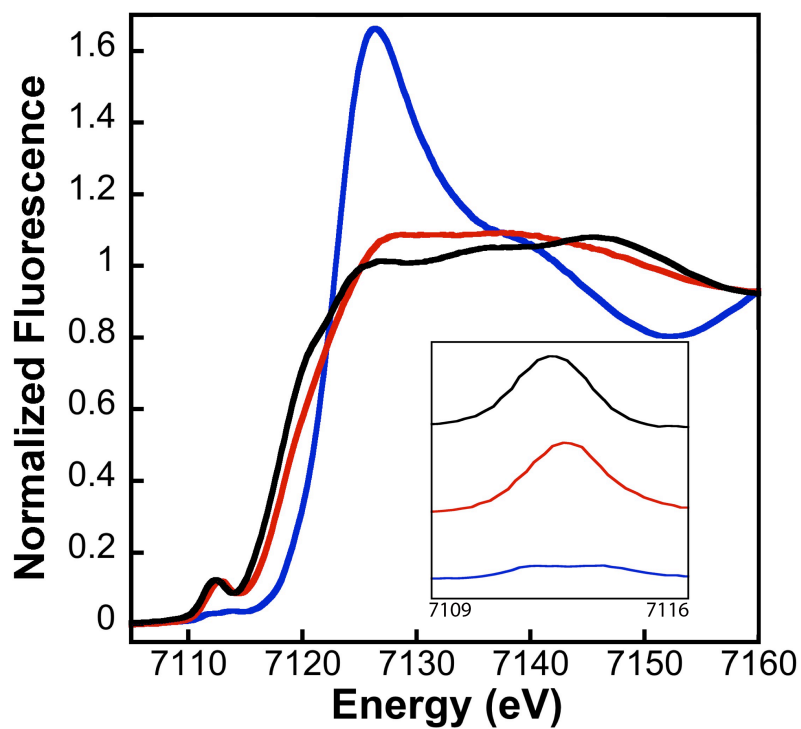


Figure 3.4: X-ray Absorption Near-Edge Spectra (XANES) for Fe-flscU (blue), FeS-flscU (red), and FeS-Yah1 (black). Pre-edge region (inset) demonstrates increased 1s-3d feature in FeS-flscU, similar to that observed with FeS-Yah1.

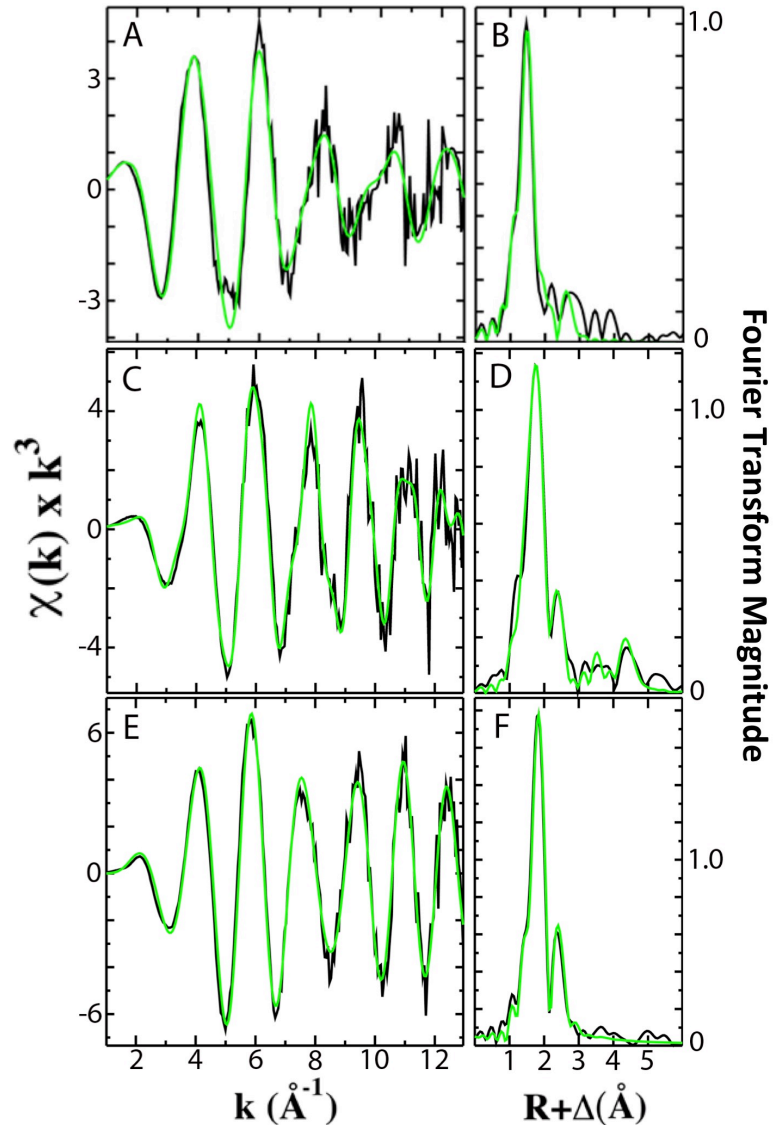


Figure 3.5: Extended X-ray Absorption Fine Structure (EXAFS) and Fourier transforms (FT) of flscU and Yah1. EXAFS spectra are provided in panels A, C, and E and FTs are provided in panels B, D, and F. Data (black) is compared to best fit simulations (green) of Fe-flscU (A,B), FeS-flscU (C,D), and FeS-Yah1 (E, F).

Sample	Fe-Nearest Neighbor Ligands ^a				Fe•••Long Range Ligands ^a				F' f
	Atom ^b	R(Å) ^c	C.N. ^d	σ^2 ^e	Atom ^b	R(Å) ^c	C.N. ^d	σ^2 ^e	
Fe – flscU	O/N	1.99	3.0	3.78	C	3.13	1.5	3.01	0.32
	O/N	2.15	2.0	2.94					
FeS-flscU	O/N	2.03	1.5	4.37	C	4.07	2.0	2.37	0.46
	S	2.28	2.0	5.03	C	4.83	4.0	0.76	
	Fe	2.72	0.5	3.84					
FeS-Yah1	S	2.29	4.0	5.58					0.40
	Fe	2.71	0.75	2.36					

^a Independent metal-ligand scattering environment

^b Scattering atoms: O (Oxygen), N (Nitrogen), C (Carbon), S (Sulfur) and Fe (Iron)

^c Metal-ligand bond length

^d Metal-ligand coordination number

^e Debye-Waller factor given in Å² x 10³

^f Number of degrees of freedom weighted mean square deviation between data and fit

Table 3.2: Best-fit simulation Fe XAS parameters for Fe-flscU, FeS-flscU and Yah1. Difference in parameters suggests the Fe-binding site in Fe-flscU is distinct from an authentic Fe-S cluster coordination site.

3.4.3 Transformation of *apo-flscU* to FeS-flscU *in vitro*

Validation of Fe-S Cluster Formation Assay - As purified, wild-type flscU is in the *apo*-state, as evident by spectrophotometric analysis of the sample and the absence of a CD signal at 560nm, a region phenotypic of Fe-S clusters. Upon addition of reduced Fe and S to *apo*-Isu, *de novo* Fe-S cluster formation can be observed.¹³⁵ Recently, concerns have been raised regarding the traditional spectroscopic methodology used for monitoring Fe-S cluster formation on Isu.^{135, 168} Notably, the use of DTT as a reducing agent was associated with the formation of a secondary iron containing high-molecular weight species (HMWS).³⁴ HMWS is likely an insoluble FeS-mineral not bound to protein and distinct from a Fe-S cluster in its character. In order to address these concerns, we optimized our method for monitoring conversion of *apo*- to the Fe-S cluster loaded flscU species in optimal yield and with minimal formation of this secondary FeS-mineral species.

The preliminary hypothesis was that FeS-mineral formation would not affect FeS-flscU formation, as measured by CD, because unlike with visible absorption spectroscopy, CD spectroscopy is not sensitive to the HMWS. Therefore, to assess potential formation of FeS-mineral, we monitored various FeS-Isu reaction conditions via visible absorption spectroscopy for a non-specific increase in light scattering (Figure 3.6). To quantify the amount of light scattering, we measured visible absorbance at 700nm, a wavelength sufficiently distinct from the 456nm chromophore of a Fe-S cluster. FeS-mineral formation is increased when Isu is excluded (Figure 3.6, solid black) and decreased when the iron-chelator EDTA is added (Figure 3.6, dashed black), suggesting that FeS-mineral formation is related to the presence of free Fe²⁺ in the reaction. In support of this hypothesis, addition of excess Fe²⁺ unexpectedly inhibits FeS-flscU formation (Figure 3.8A). Keeping in mind that

under these conditions (described in section 3.3.5), production of reduced sulfur is the rate-limiting step of FeS-Isu formation, we hypothesize that free Fe²⁺ can bind reduced sulfur from Nfs1-Isd11 to produce FeS-mineral. This inhibitory effect from excess Fe has been previously observed but not clarified in extensive detail.¹⁶⁸ Under these conditions, there is little (<0.05 AU) increase in light scattering at this wavelength, suggesting FeS-mineralization is minimal. Interestingly, when Fe is present in excess under these conditions, the same yield of FeS-flscU is achieved, suggesting free Fe inhibits but does not abolish Fe-S cluster formation on flscU.

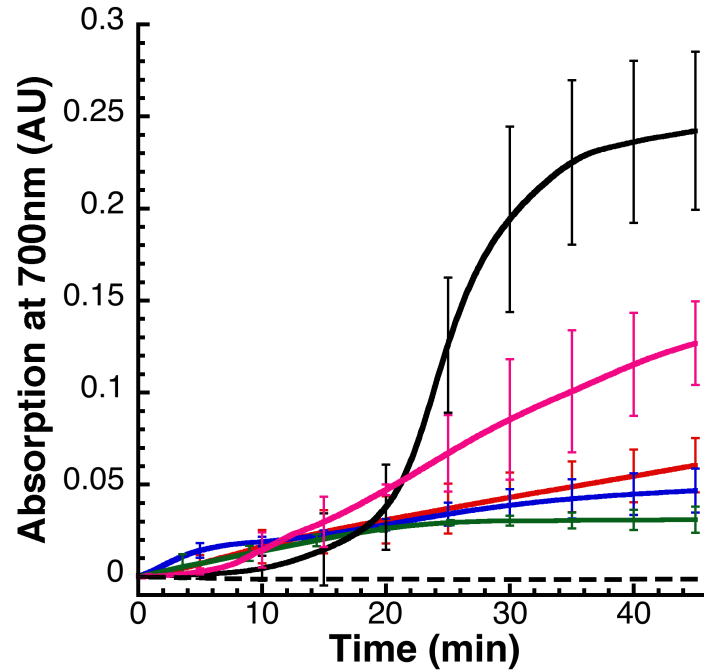


Figure 3.6: Increase in light scattering observed during FeS-Isu formation reaction, as estimated by the increase in absorbance at 700nm under various reaction conditions: ylsu1 (red), flscU (blue), flscU with Yfh1 (green), No Isu (black solid), No Isu with Yfh1 (pink), No Isu with EDTA (black dashed). Note that minimal FeS-mineralization is observed under optimal reaction conditions (red, blue, green).

Characterization of Fe-S cluster formation on flscU - After validation of optimal solution conditions for assembly, the FeS-flscU production pathway was characterized using UV/Vis and CD methodologies in a combined manner (Figure 3.7). The molar extinction coefficient determined for FeS-flscU is 7.5 AU/mM*cm (visible) and 0.6 degrees/mM*cm (CD) at 456nm. The CD spectrum for Yah1 (Figure 3.7, red) was used as a positive control of an Fe-S cluster containing protein (Figure 3.7, green). Similarities in the visible absorption and CD spectra (Figure 3.7) suggest flscU and yIsu1 both form a similar type of Fe-S cluster than found in Yah1. Both flscU and yIsu1 spectra have features similar to those seen in the Yah1 control (negative peaks at 390nm and 560nm, positive peak at 450nm). The larger signal observed for flscU, as compared to yIsu1, is likely representative of a higher specific activity for 2Fe-2S cluster production in the more stable fly ortholog since loading conditions between the proteins is equal.

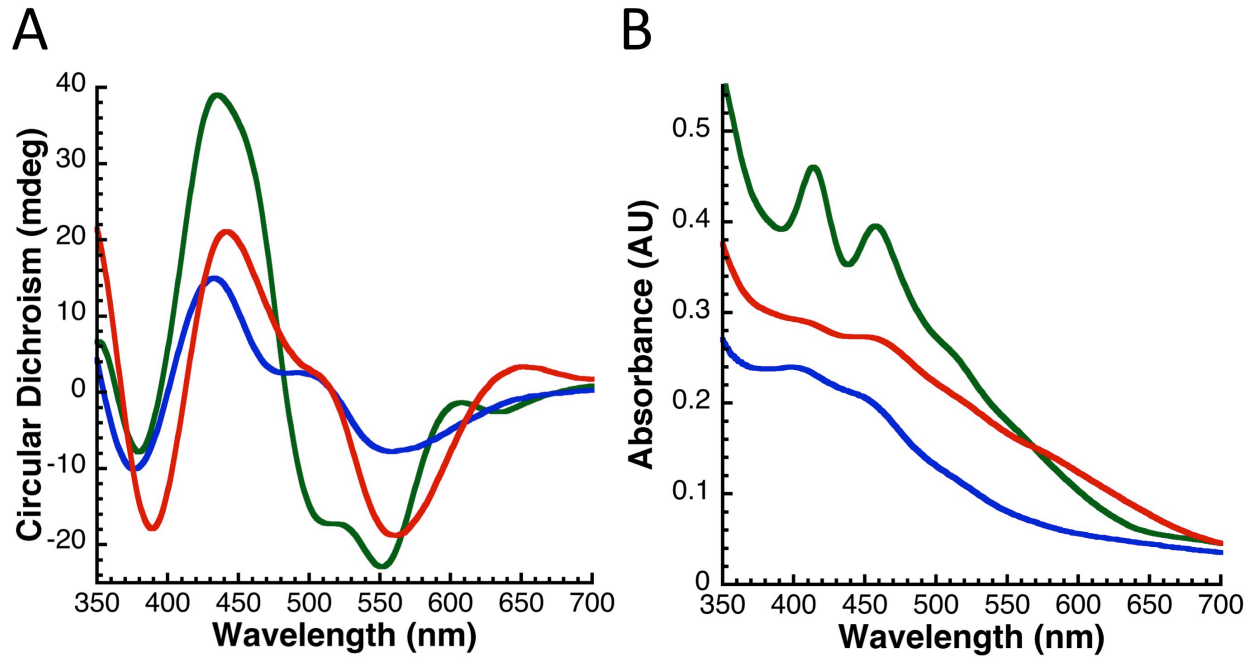


Figure 3.7: Circular dichroism (A) and visible absorption (B) spectra comparing FeS-flscU (green) and FeS-yIsu1 (blue). Both flscU and yIsu1 have similar CD features to an archetypical 2Fe-2S cluster from the yeast ferredoxin, Yah1 (red). All spectra represent 50 μ M protein in a 1-cm path-length cuvette.

3.4.4 Cross-Reactivity of flscU with yeast Nfs1-Isd11 and Yfh1

Our *in vitro* functional assay outlined above and tuned for optimal substrate/protein stoichiometry was used to assess the interaction of flscU with other yeast ISC proteins. As expected, the amount of FeS-flscU formed depends directly on the amount of Fe present (Figure 3.8A). Finally, maximal FeS-flscU formation is demonstrated at 1.5 x Fe equivalents, which is less than the expected saturation at 2 x Fe equivalents for one 2Fe-2S cluster per flscU monomer. Upon addition of Yfh1, significant stimulation (~3-fold) is observed for FeS-flscU formation (Figure 3.8B, green). This stimulation is very similar to what was observed with yIsu1 (Figure 3.8B, blue), suggesting Yfh1 also stimulates cluster assembly in the presence of flscU. Under physiologic salt concentrations (150mM), Yfh1's effect on Fe-S cluster assembly is concentration dependent (Figure S1). Maximum Yfh1-mediated stimulation occurs at a Yfh1 concentration $\sim 1/15^{\text{th}}$ the Fe(II) concentration, but approximately equal to the Nfs1-Isd11 concentration. At higher Yfh1 concentrations, equimolar with flscU under our reaction conditions, frataxin inhibits FeS-flscU formation. This effect has also been observed with the *D. melanogaster* frataxin (unpublished data), however the extent is minimized under high-salt buffer conditions (500mM NaCl). Therefore, in the FeS-flscU formation assay, we used a sub-stoichiometric amount of Yfh1 (10 μM , matching Nfs1-Isd11 concentrations) to reach reaction conditions where frataxin stimulation is maximal. Finally, Fe-S cluster formation can also be observed using yIsu1 (Figure 3.8B, black dashed), however, the yield is significantly lower possibly due to the instability of recombinant yIsu1.

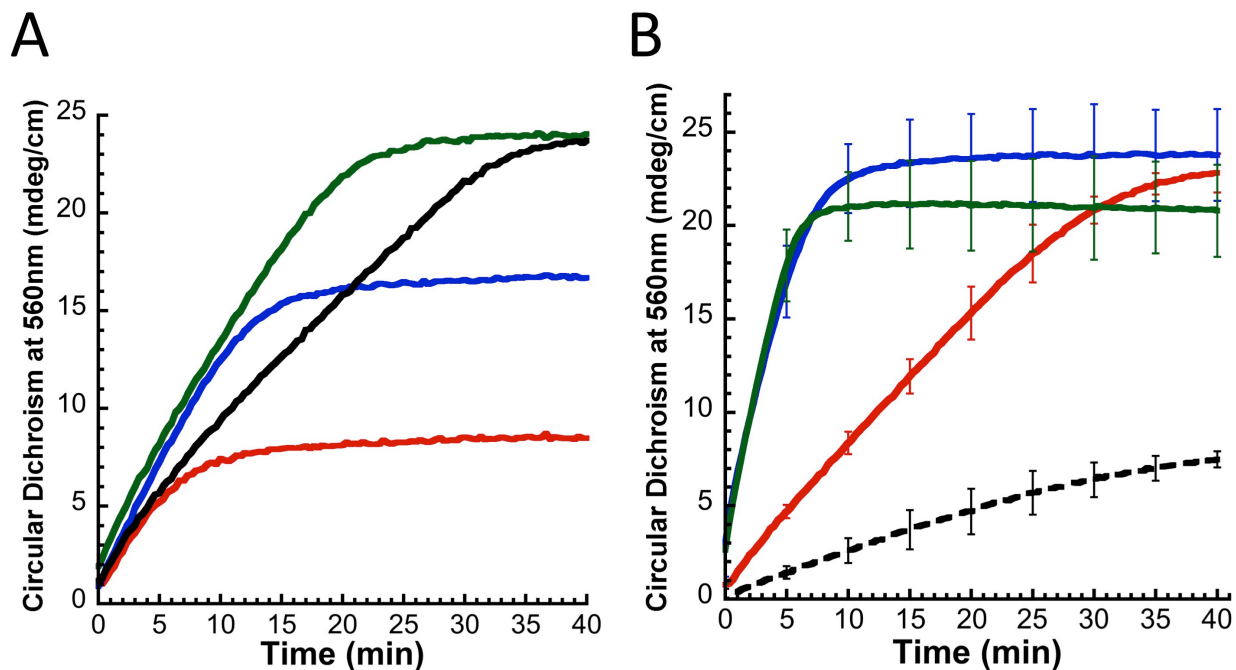


Figure 3.8: A) Change in Circular Dichroism signal at 560nm for 50 μ M flscU monomer and 10 μ M Nfs1-Isd11 monomer under varying Fe(II) concentrations: 25 μ M (red), 50 μ M (blue) 75 μ M (green), 100 μ M (black). Maximal yield at 1.5xFe suggests flscU forms two Fe-S clusters form per dimer. Free Fe²⁺ inhibits FeS-flscU formation by facilitating FeS-mineralization. B) FeS-flscU formation via 50 μ M apo-flscU in the presence of 10 μ M Nfs1-Isd11 (red), 10 μ M Nfs1-Isd11 and 10 μ M Yfh1 (blue), and 10 μ M Nfs1-Isd11, 10 μ M yIsu1, and 10 μ M Yfh1 (green); all proteins overexpressed in *E. coli*. The rate of FeS-flscU formation increases in the presence of Yfh1 (blue) to a similar extent as observed with Yfh1 and yIsu1 (green). Fe-S cluster formation using 50 μ M apo-yIsu1 in place of 50 μ M apo-flscU is included as a comparison (black-dashed).

3.4.5 *In vivo* Replacement of yIsu1 with flscU

To test the physiological consequences of replacing yIsu1 with flscU *in vivo*, we engineered a yeast strain where native yIsu1 and yIsu2 was replaced by flscU. To perform this experiment, the paralogous yeast Isu2 was deleted and the chromosomal yIsu1 was placed under control of the GAL1 promoter. The resulting Gal-Isu1 Δ yIsu2 strain can grow in raffinose/galactose, inducing for Gal-yIsu1 but not in glucose, repressing for Gal-yIsu1. The strain was transformed with empty plasmid YCplac22, with flscU targeted to mitochondria or with yIsu1, and expression of Gal-yIsu1 was shut down upon shifting to glucose as the carbon source. As shown in Figure 3.9A, flscU conferred normal growth similar to yIsu1, whereas empty plasmid conferred minimal growth consistent with the essentiality of Isu. Iron uptake at the cellular level correlates strongly with mitochondrial Fe-S cluster assembly activity,¹⁶⁹ and therefore we analyzed the high affinity cellular iron uptake of both strains using ⁵⁵Fe (Figure 3.9B). A nfs1-14 mutant with a missense NFS1 allele (I191S)¹⁷⁰ showed increased iron uptake activity, and the Δ aft1 deletion strain was a control for low iron uptake activity. These data show that the flscU and yIsu1 complemented strains had equivalent cellular iron uptake activities, suggesting that flscU can completely replace the yeast homologs and support *in vivo* Fe-S cluster assembly.

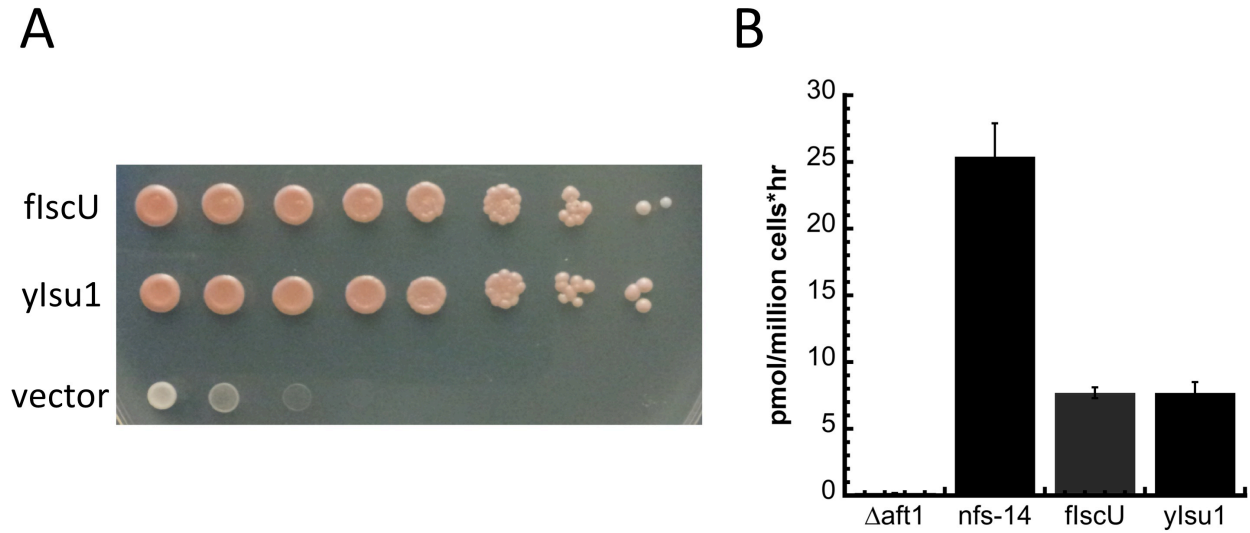


Figure 3.9: In vivo rescue of strain lacking *ylsu1* by expression of *flscU*. A) Growth of GAL-*Isu1*/ Δ *isu2* strain transformed with either the empty YCplac22 plasmid or YCplac22 carrying the mitochondrial targeted *flscU* gene or the yeast *Isu1* gene. Transformants were compared by spotting serial 10-fold dilutions of 10^6 cells on CSM-TRP/Glucose plates and photographing four days later. *ylsu1* and *flscU* show equivalent complementing activity. B) Cellular iron uptake for *flscU* and *ylsu1* complemented GAL-*Isu1*/ Δ *isu2* strain. The strain with the empty plasmid did not grow and so iron uptake could not be assessed. Iron uptake was measured for 1 hour in sodium citrate buffer. Other mutants served as controls for high uptake activity (*nfs1-14*) and low uptake activity (Δ *aft1*).

3.5 Discussion

It is not surprising that the yeast and fly scaffold proteins are so similar in their molecular details. The transition from an anaerobic to aerobic environment 3 billion years ago necessitated evolution of molecules within pathways that would continue to remain functional, while at the same time protect the solubility and redox activity of iron to continue to promote assembly of Fe-S clusters; at this point in the evolutionary scale Fe-S clusters were already ancient and highly utilized in life. Given the close similarity between fly and yeast Isu orthologs, based on their sequence homology, similar structure, and activity towards Fe-S cluster assembly, what is surprising is the difference in stability between the actual flscU and yIsu1 proteins. The high stability of flscU makes this protein an excellent candidate for utilization when studying molecular details of the ISC pathway.

Metal binding properties of flscU, as compared to yIsu1, are consistent with the presumed role of both proteins as the scaffold for *de novo* 2Fe-2S cluster synthesis. Consistent results from two independent Fe-binding methods provide confidence that the binding interaction between Fe(II) and flscU is within the micromolar to nanomolar range. Fe-binding parameters for flscU, obtained from our chelation assay, match very closely to the value we reported with our chelation assay for yIsu1.¹⁵² Binding constants from the competition assay are close but slightly tighter to values obtained from our initial isothermal titration calorimetric values published previously,¹⁴² indicating that competition provides a better evaluation for how these proteins likely bind metal in vivo. Interestingly, the structural characterization of iron bound to flscU by XAS confirmed that the fly protein binds Fe(II) initially at a site devoid of sulfur ligation; a similar initial iron binding site was observed for the yIsu1¹⁵² as well as the human and bacterial orthologs

(manuscript in preparation). These data indicate IscU orthologs bind iron initially at a site independent of the protein's cysteine rich active site. Identification of which specific residues are at that site is currently under investigation. However, once both iron and sulfur are provided to the scaffold, as is the case for FeS-flscU, these data are consistent with iron coordinated in a Fe-S cluster.^{24,25} This suggests a model where Fe translocates from the Fe-binding site to the Fe-S cluster coordination site after accepting the persulfide from Nfs1. The pattern of Fe-N, Fe-S, and Fe-Fe scattering in the FeS-flscU sample agrees with the expected Fe-S cluster coordination at the active site of flscU, which contains three cysteines and one histidine, as compared to the 4 cysteine site observed in the ferredoxin Yah1.¹⁷¹ However, iron-ligand bond lengths we observe are similar to those reported for Fe(II)-binding proteins from other biological systems¹⁷²⁻¹⁷³ and to bond lengths we previously reported for ylsu1.¹⁴²

With regards to Fe-S cluster biosynthesis, our data show maximal FeS-flscU formation is observed at 1.5 x Fe equivalents per Isu molecule, a value less than the expected saturation value of 2 x Fe equivalents for a single 2Fe-2S cluster per flscU monomer. Incomplete homogeneity of our isolated recombinant flscU is likely the cause of nonstoichiometric assembly. Considering our SDS-PAGE gel characteristics (Figure 3.2A), flscU is likely ~95% pure, and from our activity measurements ~80% active as isolated which, taken together, would likely account for FeS-flscU saturation at 1.5 x Fe equivalents. Strategies to increase the fraction of active protein in flscU >80% have been unsuccessful. Considering the incomplete activity of recombinant flscU, Figure 3.8A suggests that a single 2Fe-2S cluster forms per flscU monomer, in agreement with findings for the bacterial and human Isu1 orthologs.^{135, 158} Under Fe-limiting conditions, there is only a slight (<0.05 AU)

increase in non-specific light scattering, suggesting that adverse FeS chemistry was minimal in our activity assay (Figure 3.6).

As noted by several labs, clarification of Fe-S cluster assembly kinetics and the molecular involvement of proteins within the ISC pathway have been hindered by heterogeneity in the FeS-Isu product formation, which has been shown to vary under different reaction conditions. Specifically with regards to substrate concentrations, production of a high molecular weight species consisting of both iron and sulfur can divert substrate from intended product.^{34,35} Our results confirm that limiting the amount of free Fe(II) available in solution dramatically reduces the extent of FeS-mineralization. Regarding the stoichiometry of the ISC protein partners, our results indicate that limiting Yfh1 levels to be stoichiometric with Nfs1-Isd11 causes the maximal frataxin induced stimulation in Fe-S cluster assembly activity. Under elevated stoichiometric abundance, excess frataxin has a negative impact on cluster assembly. These data are consistent with observations that show overexpression of Yfh1 *in vivo* causes a reduction in Fe-S cluster synthesis.¹⁷⁴ Finally, using excess Isu and limiting Nfs1-Isd11 are important for driving FeS-Isu formation, indicating Isu in complex with Nfs1/Isd11 likely can transfer cluster to the excess unbound Isu under *in vitro* assembly conditions, as previously suggested.¹⁵⁸

Combined, our results suggest a model where optimal *in vitro* FeS-Isu formation conditions (i.e., low Nfs1-Isd11 concentrations, high concentration of Isu, limiting concentrations of Fe) enable a high yield of FeS-Isu formation with minimal side reactions (Figure 3.10). In this model, free Fe is able to bind reduced sulfur, preventing sulfur transfer to Fe-Isu, and thus inhibiting FeS-Isu formation. This model agrees with the presumed *in vivo* environment, where substrate concentration must be tightly regulated to

help control cluster assembly, as both Fe and S substrates are toxic in excess. In addition, the stability of the formed cluster is likely enhanced by the distribution of cluster chaperone proteins that accept and deliver the synthesized Fe-S clusters to recipient proteins downstream to assembly. Further regulation within the ISC pathway is provided by control at the genetic level where expression of the ISC genes occurs at levels that optimize activity. Establishing these optimal relative stoichiometries *in vitro* therefore provides direct insight into conditions of maximal efficiency that likely exist *in vivo*.

Finally, the physiological consequence of using flscU in combination with/in replacement of the yeast proteins *in vitro* has been tested *in vivo* for validation that there are no species-specific effects that would dissuade using fly IscU in combination with the yeast proteins within our yeast activity assay. *In vivo* studies show flscU completely complements yeast lacking Isu1 and Isu2. *In vitro*, the behavior of flscU is superior to yIsu1, likely as a result of the high stability of the fly protein. Our biophysical characterization studies showed the similarity in many physical properties between the yeast and flscU proteins, however the stability and functional activity of the fly ortholog are superior to those for the yeast protein. Given our finding that excess Isu is necessary to drive multiple Nfs1 turnovers within the yeast reaction system and since flscU can easily function as recipients for clusters, flscU appears to be a better recipient of the cluster to help characterize the molecular interactions with the pathway. The *in vitro* data coupled with our *in vivo* findings therefore validates the use of the fly protein to help us elucidate the molecular details of the ISC pathway in yeast.

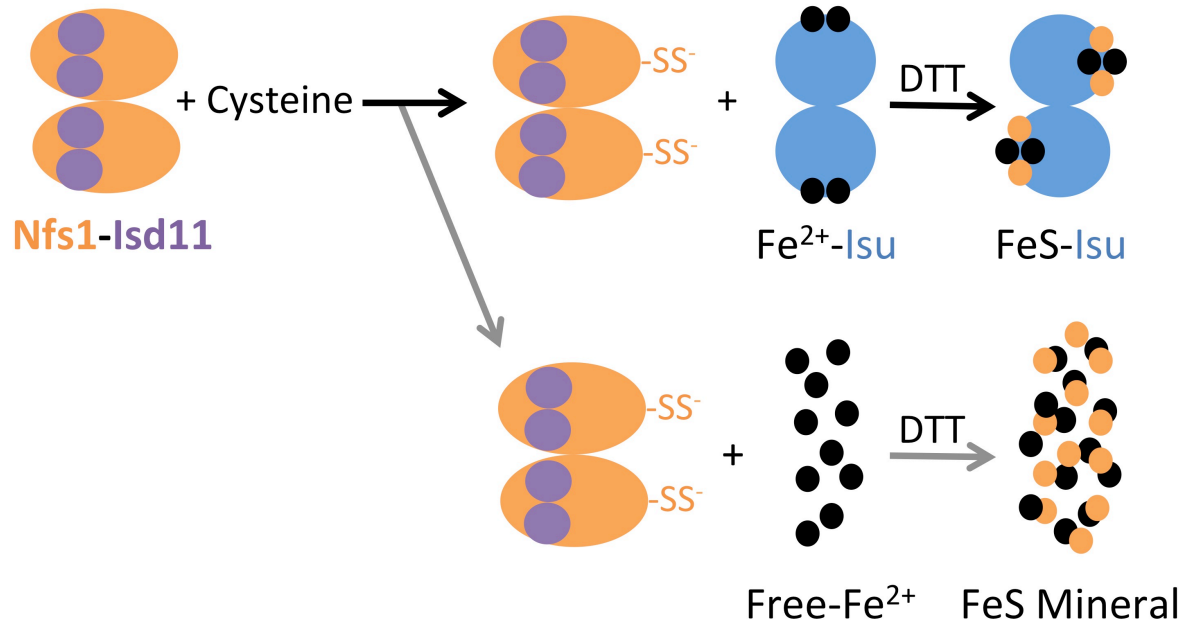


Figure 3.10: Model for competing FeS-Isu (black arrows) and FeS mineralization (gray arrows) pathways. The persulfide from Nfs1-Isd11 does not have a strong preference for Fe²⁺-Isu over free Free Fe²⁺, resulting in competition between these two reactions when free Fe²⁺ is present.

3.6 Acknowledgements

This work was supported by funds for S.P.D. from the American Heart Association and the Friedreich's Ataxia Research Alliance (14PRE18830036), and funds from the National Institutes of Health for S.P.D (F30 DK101230-01), D.P. (GM107542), A.D. (DK53953) and T.L.S. (DK068139). Portions of this research were carried out at the Stanford Synchrotron Radiation Lightsource (SSRL). SSRL is a national user facility operated by Stanford University on behalf of the U.S. Department of Energy, Office of Basic Energy Sciences. The SSRL Structural Molecular Biology Program is supported by the Department of Energy, Office of Biological and Environmental Research, and by the NIH, National Center for Research Resources, Biomedical Technology Program.

CHAPTER 4: ISU1'S INTERACTION WITH NFS1 INHIBITS FES-ISU1 FORMATION *IN VITRO*

4.0 Prelude

The following chapter investigates the interaction between the Nfs1, Isd11, Isu1, and Yfh1 proteins during FeS-cluster bioassembly. This was done by isolating and characterizing the complexes that form between these proteins under overexpression conditions in bacteria. This work correlates with aim 2 from my original prospectus. I need to thank Dulmini Barupala and Andria Rodrigues for allowing me to analyze their data on the melting behavior of the Nfs1-Isd11 and Isu1. I also need to thank Dr. Andrew Dancis and his laboratory members for providing the plasmid constructs for the protein expression. I did the writing and experiments in this section and this chapter is being converted for publication.

4.1 Abstract

FeS-clusters are essential cofactors found in all organisms. In eukaryotes, a single highly conserved pathway, called the FeS-cluster pathway or "ISC", is essential for the formation of most cellular FeS-clusters. Eukaryotic ISC has been best characterized in *Saccharomyces cerevisiae* where it localizes to the mitochondria. In yeast, reduced sulfur is provided as a persulfide from cysteine by the cysteine desulfurase enzyme "Nfs1", with its essential protein cofactor "Isd11". The primary scaffold, "Isu1", assembles the Fe²⁺ and S²⁻ atoms into a stable FeS-cluster. Frataxin, "Yfh1", is an allosteric regulator of Nfs1 and plays a role in iron delivery to Isu1. *In vivo* FeS-cluster assembly occurs via a coordinated interaction of these ISC proteins, however the mechanism of how these proteins interact to accomplish cluster biosynthesis remains unclear.

This study isolates complexes formed between recombinant Nfs1-Isd11, Nfs1-Isd11-Isu1, and Nfs1-Isd11-Isu1-Yfh1, and characterizes their activity related to

substrate binding and cluster assembly. The individual complexes are abbreviated “SD”, “SDU”, and “SDUF”, for their respective Nfs1 (S), Isd11 (D), Isu1 (U), and Yfh1 (F) components. Isu1 and Yfh1 have a weak association to SD that requires low salt (~50mM) conditions for stable binding, in comparison to SD association that is highly stable under multiple solution conditions. Our isolation studies show these complexes exist as dimeric Nfs1 species in the S_2D_4 , $S_2D_4U_2$, and $S_2D_4U_2F_2$ arrangements. SDUF, as isolated under the stoichiometric conditions outlined above, is unable to perform *de novo* FeS-cluster biogenesis without the addition of exogenous *apo*-Isu1. With exogenous *apo*-Isu1, however, SD, SDU, and SDUF are all able to produce FeS-Isu1. The SDUF complex alone retains iron-binding capacity but is unable to functionally utilize iron to complete FeS-cluster formation at a detectable level. This work demonstrates that eukaryotic Isu1’s binding to Nfs1 inhibits its ability to conduct *de novo* FeS-cluster biogenesis. A model is proposed where a conformational change of Isu1 is required for FeS-cluster formation and this change can only occur on exogenous Isu1. While similar findings have been made for the bacterial Isu1 ortholog, IscU,¹⁷⁵⁻¹⁷⁷ the existence of multiple conformers for eukaryotic Isu1 has never been reported.

4.2 Introduction

FeS-clusters are ubiquitous in biology and have been identified in all forms of life.¹⁷⁸ Over the past 20 years, FeS-cluster metabolism has been the subject of intense research as dysfunctional FeS-cluster biogenesis has been directly implicated in a variety of human diseases, including the autosomal recessive genetic disease Friedreich’s ataxia.¹⁷⁹ Proteins that bind FeS-clusters (i.e., “FeS-proteins”) are found in a variety of biochemical pathways including the citric acid cycle,¹⁸⁰ DNA replication,¹⁸¹ and the electron transport chain.¹⁸² FeS-proteins are synthesized in their *apo*-form and receive their FeS-cluster post translation. Considering the wide variety of FeS-proteins,

it is remarkable that in eukaryotes there are a limited number of pathways that provide FeS-clusters to their *apo*-protein partners, the primary assembly pathway of which occurs within the mitochondria.¹⁸³⁻¹⁸⁵ This primary pathway, called the iron-sulfur cluster “ISC” pathway, among eukaryotic systems has been best characterized in the *Saccharomyces cerevisiae* model. In yeast, reduced sulfur is provided from cysteine by the cysteine desulfurase enzyme “Nfs1”,¹⁸⁶ an enzyme that works in union with its essential protein partner “Isd11”.¹⁸⁷ The primary scaffold protein “Isu1” accepts reduced sulfur from Nfs1 via a persulfide intermediate and utilizes this sulfur source to perform *de novo* FeS-cluster formation.¹⁸⁸ The protein frataxin, “Yfh1” in yeast, has been identified as both an allosteric regulator of Nfs1¹⁸⁹⁻¹⁹⁰ and as the iron donor to Isu1.¹⁹¹ A ferredoxin “Yah1” provides reducing equivalents for persulfide transfer¹⁹² and possibly reductive coupling of 2Fe2S-clusters.¹⁸⁸

Efficient *de novo* FeS-cluster biogenesis requires the coordinated interaction of the Nfs1, Isd11, Isu1, and Yfh1 proteins. However, the mechanism by which these proteins interact to complete FeS-cluster assembly remains unclear. These proteins can assemble under appropriate conditions forming Nfs1-Isd11, Nfs1-Isd11-Isu1, and Nfs1-Isd11-Isu1-Yfh1 complexes. These respective complexes are abbreviated “SD”, “SDU”, and “SDUF” for their Nfs1 (S), Isd11 (D), Isu1 (U), and Yfh1 (F) components. Complexes of Isu1-Yfh1 have also been reported, however these were not identified in this study.¹⁹³⁻¹⁹⁴

Research characterizing the interaction between ISC proteins *in vitro* will provide a more detailed understanding of how the ISC proteins potentially function *in vivo*. Few mechanistic details regarding how the eukaryotic ISC pathway proteins function are known, however recent NMR studies of the bacterial orthologs have provided valuable insight into their activity.^{175-177, 195-196} The bacterial ortholog of Isu1,

“IscU”, has a particularly interesting behavior, as it exists in two states, ‘structured’ and ‘disordered’. Only the structured state is able to bind to the bacterial Nfs1 ortholog, IscS.¹⁷⁵ Transitioning between these states is important for IscU function, as IscU mutations that favor the structured state inhibit FeS-cluster production.¹⁷⁷ Similar behavior has also been reported for the alternative scaffold, IscA.¹⁹⁶ For eukaryotic systems, recent reports from murine and human ISC describe the successful isolation and characterization of complexes formed between Nfs1-Isd11,¹⁹⁷⁻¹⁹⁸ Nfs1-Isd11-Isu1, and Nfs1-Isd11-Isu1-Yfh1.¹⁹⁹

In this chapter, we describe similar characterizational studies performed with the yeast ISC multiprotein complexes. Since published work on SDU and SDUF are limited, and the molecular mechanism for *de novo* FeS-cluster biogenesis by Isu1 is unknown, these studies will provide a molecular understanding of how these complexes function. Isu1 within the SDU and SDUF complexes demonstrates inhibited FeS-cluster formation. Upon addition of exogenous Isu1 to SDU or SDUF, however, a 2Fe2S-cluster signal immediately develops as assessed by circular dichroism spectroscopy. Utilizing the Isu1 ortholog from *Drosophila melanogaster*, flscU, is a unique approach to circumvent effects related to Isu1-complexation because flscU can fully complement yeast ISC (see Chapter 3) but does not complex with yeast proteins to form a stable SD-flscU or SD-flscU-F complex *in vitro*. In the presence of excess *apo*-flscU, SDUF demonstrates rapid FeS-flscU formation compared to SD and SDU. This stimulated FeS-flscU formation is possibly due to the high cysteine desulfurase activity observed with SDUF.

4.3 Materials and Methods

4.3.1 Expression and Purification of SD, SDU, and SDUF Complexes

To explore the molecular details of the coordinated activity of yeast Isu1 during

FeS-cluster assembly, we developed a strategy to express and isolate complexed Isu1 within SDU and SDUF. This strategy of working with multiprotein complexes has been highly effective when studying the human and murine systems.²⁰⁰⁻²⁰¹ Development of our yeast SDU and SDUF complex purification strategy followed closely the recent method employed to characterize SDUF in the murine system.²⁰⁰ Details regarding the expression and purification of *Saccharomyces cerevisiae* Nfs1-Isd11 (SD), frataxin (Yfh1), and the *D. melanogaster* Isu1 (flscU) have been reported elsewhere (see Chapter 3).

Expression of SDU and SDUF was done using the Nfs1-Isd11-Isu1 (SDU) genes placed in a pST39 vector and the Yfh1 gene placed in a pCOLAduet vector that contains a C-terminal His-tag. Nfs1-Isd11-Isu1-Yfh1 (SDUF) expression was performed by simultaneous expression of the untagged SDU plasmid with the Yfh1-His6 plasmid. By utilizing different selection markers, ampicillin for SDU and kanamycin for Yfh1, both plasmids could be selected for simultaneously. Transformation of SDU and SDUF constructs was done using competent BL21-RIL cells at 42°C for 30 seconds. All cells were grown in LB media with 50 µg/mL of ampicillin, 25µg/mL of chloramphenicol, and 25µg/mL of kanamycin (when applicable). SDU and SDUF were induced with 0.8mM IPTG and 10µM PLP at an OD ~0.8 for 3 hours at 37°C. After harvesting, cells were lysed using an AVESTIN Emulsiflex-C3 cell homogenizer. Lysis buffer for SDU/SDUF was 20mM imidazole, 20mM HEPES, 150mM NaCl, and 5mM BME. All buffers were adjusted to pH=7.5. Lysate was centrifuged at 21,000 rpm for 45 minutes and the soluble fraction was moved through a 0.2µm filter before being placed onto a Ni-column. The Ni-column was washed with 5 column volumes of lysis buffer, followed by 5 column volumes of 50mM imidazole lysis buffer. Elution of protein was done with 5 column volumes of 200mM imidazole lysis buffer. The eluted fraction was treated with 5mM EDTA to

remove adventitious metal.

After EDTA treatment, the eluted fraction was concentrated to ~2mL via a 10kDa cutoff Amicon centricon and placed on a S200 gel filtration column. Proteins were switched into the experimental buffer during the gel filtration. The experimental buffer for SDU and SDUF was 20mM HEPES, 50mM NaCl, 5mM BME. Fractions containing the desired protein were pooled and concentrated to ~10mg/mL. Protein concentrations were measured using a millipore Direct Detect IR spectrometer and protein purity was estimated by SDS-PAGE as >95%. Typical yields were 3 mg of SDU or SDUF per L of bacterial culture. Proteins were flash frozen in liquid N₂ and stored at -80°C.

4.3.2 Characterization of SDUF Complex Stability

The stability of complex formation between the Nfs1, Isd11, Isu1, and Yfh1 components of SDUF was estimated by applying a gradual imidazole gradient to SDUF bound to a Ni-column. Frataxin-His6 binds to the Ni-column and the Nfs1, Isd11, Isu1 proteins bind to the column indirectly via their interaction with bound frataxin. The column was equilibrated with 20mM imidazole, 50mM NaPi, 300mM NaCl, 5mM BME buffer at pH=7.5. Bacterial lysate from SDUF-expressing BL21-RIL cells was placed on a 5mL Ni-column. The column was washed with 15mL of 50mM NaPi, 300mM NaCl, 5mM BME buffer at pH=7.5 with a progressively increasing imidazole gradient from 20-100mM imidazole. Fractions were collected every 5mL and analyzed via SDS-PAGE to identify the imidazole concentration at which the Nfs1-Isd11, Isu1, and Yfh1 proteins elute from the column.

4.3.3 Identification of SD, SDU, SDUF Complex Protein Stoichiometries

Band densitometry was used to identify the respective Nfs1, Isd11, Isu1, and Yfh1 stoichiometries from the isolated SD, SDU, and SDUF complexes. The amount of respective protein is taken as the density for each band on the SDS-PAGE gel, calculated

as pixel number times the average pixel intensity. Gels were configured to facilitate optimal band volume measurements with the same sample being run across multiple lanes to provide statistical relevance along with a measure of uncertainty. Protein amounts per lane were varied between 0.5-5 μ g. After de-staining, gels were imaged and analyzed by the Bio-Rad Image Lab software package to quantify band volumes. These band volumes were divided by the expected molecular weights of each respective protein to calculate a ‘molar band volume’. Molar band volumes were then divided by the molar band volume of Nfs1 to provide a ‘molar band ratio’ on a per Nfs1 basis.

Identification of the S_aD_bU_cF_d arrangement allowed the estimation of an appropriate molecular weight for the SD, SDU, and SDUF complexes. This molecular weight (MW) was calculated using the following formula:

$$MW_{Complex} = \mathbf{a}(MW_{Nfs1}) + \mathbf{b}(MW_{Isd11}) + \mathbf{c}(MW_{Isu1}) + \mathbf{d}(MW_{Yfh1})$$

It should be noted that the molar band ratio was identified based on the Nfs1 concentration, which through normalization makes **a** always equal to 1. Thus, the molecular weights used in subsequent experimentations were on a ‘per Nfs1’ basis. Note this molecular weight is distinct from the true complex molecular weight, which likely exists as a dimeric species.

4.3.4 Determination of SDUF Fold Stability

Differential Scanning Calorimetry (DSC) was performed to assess any potential changes in fold-stability of SDUF in comparison to its respective individual Nfs1, Isd11, Isu1, and Yfh1 components. DSC was performed using a TA Instruments Nano-DSC calorimeter, located in an anaerobic chamber for protein and reduced metal stability. The SDUF protein solution was diluted to 4 mg/mL with experimental buffer. A ~0.4 mL SDUF solution was injected into the sample cell to accommodate the total cell volume of 0.3 mL. The reference cell was loaded with H₂O. Protein solutions were heated from 10°

to 90°C at a rate of 1°C/min. The heat capacity for the sample was measured at each respective temperature interval. Melting curves for SDUF were compared to curves measured for the respective individual SD, Isu1, and Yfh1 proteins. This process was done on multiple protein preparations to ensure data reproducibility. Best-fit modeling parameters were identified by simulation with the TA instruments NanoAnalyze software package. Three separate two-state scaled models were applied to accommodate the 3 distinct features of the SDUF melt curve. Best-fit values were identified by NanoAnalyze via iteration of the melting parameters: melting temperature (T_m), heat of melting (ΔH), and scaling factor (A_w).

4.3.5 FeS-Isu1 Formation Reaction Assay with Complexed and Exogenous Isu1

FeS-cluster formation on Isu1 was tested under a variety of conditions and with different Isu1 species to give insight into the mechanism for FeS-Isu1 formation. FeS-Isu1 formation was assessed using complexed Isu1 within SDU and SDUF, exogenous Isu1, and exogenous flscU with each Isu1 species providing unique information about FeS-cluster assembly. flscU was utilized in addition to yeast Isu1 because it can fully complement yeast ISC *in vivo* and *in vitro* (see Chapter 3) but does not form a stable complex with yeast Nfs1. Therefore, flscU can be used with yeast SD, SDU, and SDUF proteins as a strategy to minimize effects related to Isu1 complexation to Nfs1 on the FeS-Isu1 formation process.

The protocol for cluster assembly is outlined in detail elsewhere (see Chapter 3), however this procedure is slightly modified for the desired application, as described below. All solutions were prepared anaerobically and mixed within an aqueous anaerobic glovebox (Coy). FeS-cluster formation was performed using yeast *apo*-Isu1 and fly *apo*-IscU (flscU) from purified *apo*-Isu1/flscU stocks. FeS-Isu1 formation on complexed Isu1, within SDU and SDUF, was measured using 50 μ M SDU or SDUF

complexes as the source of complexed Isu1. FeS-Isu1 formation on exogenous Isu1/flscU was performed by adding SD, SDU, and SDUF complexes in a lesser amount (10 μ M) than the exogenous Isu1 or flscU (50 μ M). For flscU experiments under stoichiometric conditions, the concentrations of Nfs1-Isd11 and Yfh1 were increased to 50 μ M, matching that of flscU. A limiting amount of Fe(II) ammonium sulfate solution (75 μ M) was added to all reactions to prevent adverse FeS mineralization during this assay.²⁰² L-cysteine was added in 5-fold excess to a concentration of 500 μ M, making a final reaction volume of 1.1mL. The reaction buffer contained 20mM HEPES (pH = 7.5), 500mM NaCl, 5mM BME, and 5mM dithiothreitol (DTT). Reaction mixtures were sealed prior to removal from the glovebox to prevent oxidation of Fe²⁺.

FeS-Isu1 formation was monitored using circular dichroism (CD) spectroscopy. CD spectra were collected using a Jasco J-1500 spectropolarimeter using 1-cm quartz cuvette. Circular dichroism has several advantages over visible absorption signals (see Chapter 2), so this technique was selected as the preferred method for measuring FeS-cluster assembly. FeS-clusters have a characteristic CD pattern in the visible spectral region which can be used to quantify cluster formation.²⁰³ For quantifying FeS-flscU formation, the size of the 2Fe2S-cluster CD spectral feature at 560 nm was measured every 20 seconds until reactions reached completion. The CD signal at 560nm was selected for quantitation of FeS-cluster formation, as it is sufficiently far from the PLP-feature present ~420nm. This process was done in triplicate to measure uncertainty.

4.3.6 Probing Complex Formation Between Yeast Nfs1-Isd11, flscU, and Yfh1

Gel filtration chromatography was used to assess whether flscU would form a stable complex with the yeast proteins Nfs1-Isd11 and Yfh1 by screening for either SD-flscU or SD-flscU-F complex formation. The gel filtration conditions selected for this study are identical to those used for SDUF purification: 20mM HEPES, 50mM NaCl, 5mM

BME at pH=7.5. Solutions at a total volume of 0.6mL were prepared with 200 μ M flscU, 200 μ M Yfh1, and 100 μ M SD and were incubated overnight under anaerobic conditions. A 0.5mL volume of the SD-flscU-Yfh1 mixture was placed onto a S200 gel filtration column and eluted fractions containing protein were analyzed by SDS-PAGE to screen for potential Nfs1-Isd11-flscU-Yfh1 complex formation. This process was repeated in triplicate to measure data reproducibility.

4.3.7 Measurement of Acid-Labile Sulfide Content

In addition to FeS-Isu1 formation, quantitation of acid-labile sulfide (S^{2-}) is another valuable measure of ISC function by specifically measuring cysteine desulfurase activity. Nfs1 provides reduced sulfur to Isu1 for cluster assembly via the initial formation of a stable persulfide intermediate. The method used to measure S^{2-} concentrations were based on an original protocol first outlined for measuring sulfide in biological applications.²⁰⁴⁻²⁰⁵ In order to provide a valid comparison to results from FeS-flscU formation, reaction conditions in the cysteine desulfurase assay used were similar to those outlined for FeS-flscU formation described above. Reaction conditions employed in this report were 10 μ M SD/SDU/SDUF, 50 μ M flscU, 75 μ M Fe(II)_{aq}, 5mM DTT, and 500 μ M L-cysteine. In addition, buffer conditions were 0.1M HEPES (pH=7.5) with 10 μ M pyridoxal-5'-phosphate (PLP) added to the final reaction solution at a total volume of 100 μ L. All proteins, chemicals, and buffers were allowed to equilibrate to anaerobic conditions by incubation in a glove box. A 0.02M N,N-diethyl-p-phenylenediamine sulfate (DPD) solution was prepared in 7.2N HCl and a 11.5mM FeCl₃ solution was prepared in 1.2N HCl. Upon addition of cysteine, reactions were sealed and incubated for 10 minutes at room temperature. After 10 minutes, 700 μ L of H₂O, 100 μ L of 0.02M (DPD) and 100 μ L of 11.5mM FeCl₃ were added and the reaction mixture was

vortexed for 5 seconds. The mixtures were then incubated at 30°C for 30 minutes. Aggregated protein material was removed via centrifugation at 12krpm for 2 minutes. Decanted solutions were transferred to 1mL cuvettes. The intensity of blue color, measured at 750 nm by visible absorption spectroscopy, was used to quantitate the amount of acid-labile sulfide produced. This process was done in triplicate to measure uncertainty.

4.3.8 Estimation of Fe-Binding via Quantitation of FeS-Mineralization

As outlined previously, adverse FeS-mineralization can be estimated as the change in light scattering that develops during the course of the FeS-Isu1 formation reaction (see Chapter 3). Light scattering was measured as the change in absorption at 700nm, a wavelength distinct from the expected 2Fe2S-cluster chromophore measured at ~456nm. A 1mL solution of 50 μ M SDUF, 5mM DTT, 75 μ M Fe²⁺_{aq} was prepared anaerobically in a sealed 1cm path-length cuvette. Reactions were initiated with addition of cysteine to a final concentration of 500 μ M. Note that the SDU and SDUF-only samples deviate from the ideal FeS-Isu1 conditions identified previously in that 50 μ M SDUF corresponds to 5 times more Nfs1, Isd11, and Yfh1. Reactions were prepared anaerobically and monitored by measuring every 20 seconds for 40 minutes using a Shimadzu UV-1800 UV-Visible absorption spectrophotometer housed within the anaerobic chamber. All experiments were done in triplicate to measure uncertainty.

4.3.9 Visible Absorption Spectroscopy

Visible absorption spectroscopy was performed to study the absorption signal at ~420nm, a feature attributed to the pyridoxal 5'-phosphate (PLP) cofactor of Nfs1.²⁰⁶ Purified SD, SDU, and SDUF proteins samples were diluted to 10 μ M in their respective experimental buffer and placed in a 1cm cuvette. Absorption was measured between 300-700nm with a 1nm bandwidth on a Shimadzu UV-1500 spectrometer using 10 μ M

SD, SDU, and SDUF diluted in experimental buffer. Spectra used for analysis were the average of scans taken from 3 independent protein preparations and provide a valuable comparison of the PLP-feature between these different complexes.

4.4 Results and Discussion

4.4.1 Successful Isolation of SDU, SDUF Complexes

We were able to successfully isolate the SD, SDU, and SDUF complexes in sufficient yield and purity (>95%) for *in vitro* experimentation by following the isolation protocol described in section 4.3.1. The binding of Isu1 and Yfh1 to SD, however, is weak and required the ionic strength of the SDU and SDUF purification buffer to be reduced to 150mM NaCl and of the experimental buffer to 50mM NaCl. In order to estimate the binding strength of SDUF components, a gradual imidazole gradient was applied to SDUF-bound to a Ni-column. Under 300mM NaCl buffer conditions, 50mM imidazole is sufficient to observe dissociation of the SD and Isu1 components from Ni-column bound Yfh1-His6 (Figure 4.1). Gel filtration must proceed rapidly (<2 hours) after Ni-column purification in order to keep the SDU and SDUF complexes intact for the S200 gel filtration chromatography.

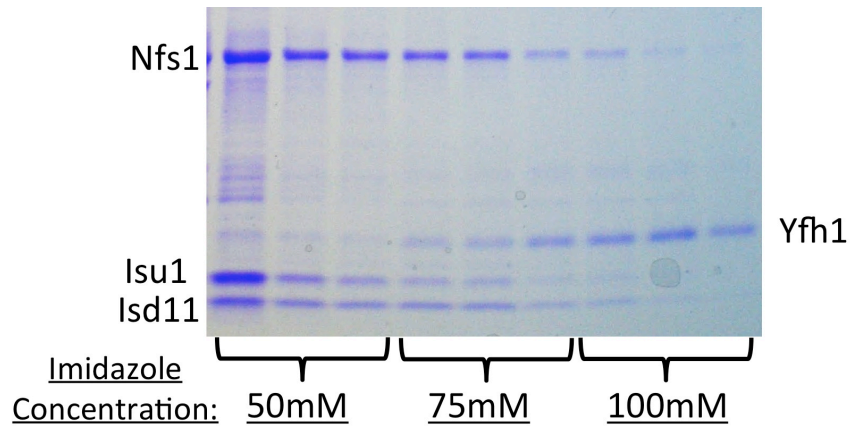


Figure 4.1: Separation of SDUF into SD, U, and F components using standard Ni-column purification method. Consecutive column volumes are ordered from left to right at corresponding imidazole concentrations.

4.4.2 Physical Characteristics of Recombinant SDU and SDUF Complexes

Binding of Isu1 and Yfh1 to SD does not dramatically affect the molecular weight or stoichiometric configuration of the dimeric SD complex. The size of the SD, SDU, and SDUF complexes, as determined via gel filtration, is close enough to be indistinguishable on a S200 column (Figure 4.2A). This suggests that Isu1 and Yfh1 binding to SD do not alter the protein's general configuration. The retention volume near 40mL corresponds with ~150kDa as measured from control molecular standards, suggesting a dimeric species for SD, SDU, and SDUF. The resulting SD, SDU, and SDUF complexes look similar using SDS-PAGE (Figure 4.2B). Even the impurities are similar between these complexes, suggesting that impurities bind to SD. Band densitometry for these complexes reveals a stoichiometric pattern of S_1D_2 , $S_1D_2U_1$, and $S_1D_2U_1F_1$ (Figure 4.2C). Taking this pattern into account with the gel filtration retention volume ~150kDa suggests a S_2D_4 , $S_2D_4U_2$, and $S_2D_4U_2F_2$ arrangement for our SD, SDU and SDUF complexes. This results in estimated monomeric molecular weights of 73.3 kDa for SD, 87.7 kDa for SDU, and 102.4 kDa for SDUF. In the dimeric form, this corresponds with 146.6 kDa for SD, 175.4 kDa for SDU, and 204.8 kDa for SDUF. This agrees with reports from the human and murine systems.²⁰⁷⁻²⁰⁸

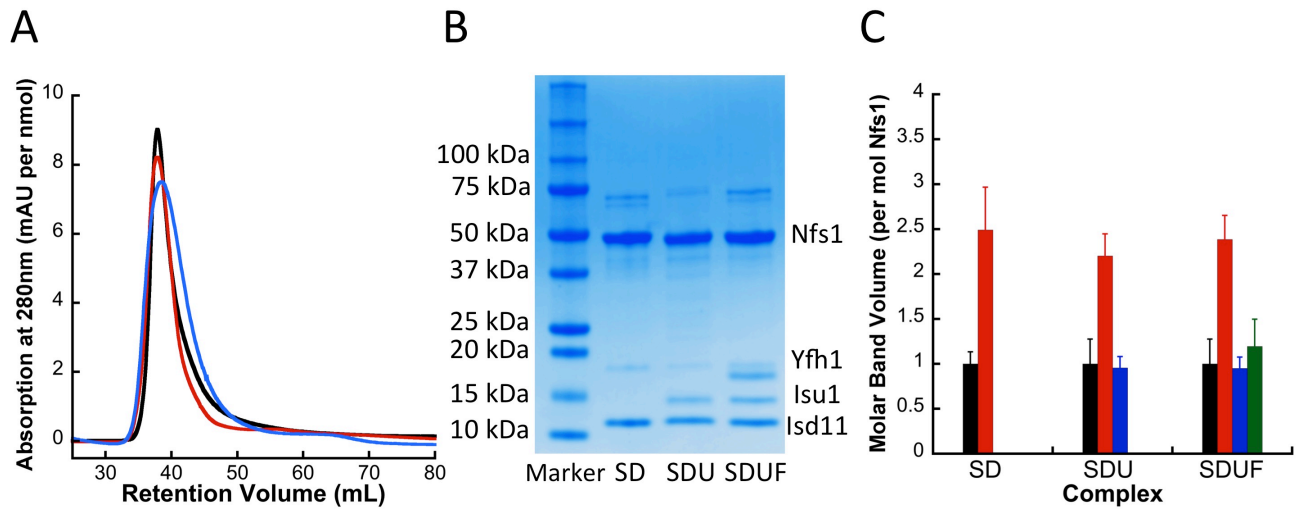


Figure 4.2: Comparison of recombinant SD, SDU, and SDUF complexes as isolated. (A) Gel-filtration chromatograms of SD (black), SDU (red), and SDUF (blue). (B) SDS-PAGE of SD, SDU, and SDUF. (C) SDS-PAGE band densitometry of Nfs1 (black), Isd11 (red), Isu1 (blue), and Yfh1 (green) demonstrating complexes are in S_2D_4 , $S_2D_4U_2$, and $S_2D_4U_2F_2$ arrangements.

4.4.3 Nfs1-Isd11, Isu1, and Yfh1 Complexation Does Not Significantly Effect Protein Fold Stability

Melting of SDUF complex was assessed using differential scanning calorimetry (DSC) to identify any significant change in fold stability when Nfs1, Isd11, Isu1, and Yfh1 proteins were complexed together. Figure 4.3 contains raw data (black) and best-fit models (red, blue, green) for the melting data while Table 4.1 contains the best-fit model parameters for a representative SDUF melting curve. The two higher temperature model features (at 51°C and 60°C) are also observed with the SD complex only. The lower temperature (~43°C) model is very similar to the melting behavior of Yfh1. No melting peak is present for Isu1, but this is consistent with observations that pure yeast Isu1 gives very small melting peaks that would be undetectable on this scale. Therefore, the SDUF melting profile resembles a simple summation of its individual Nfs1, Isd11, Isu1, and Yfh1 components. This agrees with prior observations suggesting that the SDUF complex association does not dramatically alter the individual protein conformations.

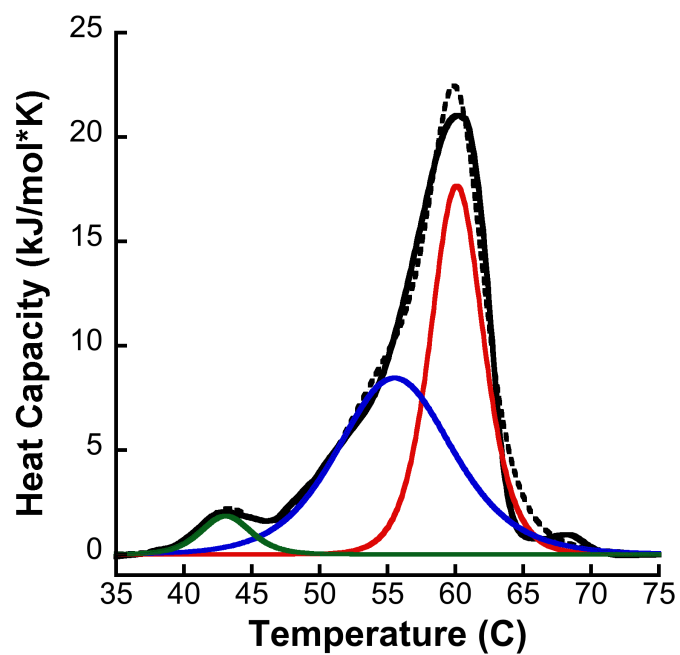


Figure 4.3: Differential Scanning Calorimetric melt profile for SDUF. Raw data (black), model (black-dashed), and individual fit features 1 (red), 2 (blue), and 3 (green).

	Fit 1	Fit 2	Fit 3
A_w	0.13±0.01	0.30±0.03	0.0133±0.003
T_m (°C)	60.1±0.1	55.6±0.3	43.1±0.26
ΔH (kJ/mol*K)	710±20	320±15	680±90

Table 4.1: Best-fit model parameters for fits 1, 2, and 3 of SDUF melt profile including melting temperature (T_m), heat of melting (ΔH), and scaling factor (A_w).

4.4.4 Exogenous Isu1 Required for Formation of FeS-Isu1

Through our FeS-Isu1 formation assay, we have identified no detectable FeS-Isu1 using complexed Isu1 within the SDU or SDUF complexes. This was determined by attempting FeS-Isu1 formation using only complexed Isu1 within the isolated SDU and SDUF complexes. FeS-Isu1 formation was probed via circular dichroism (CD) spectroscopy, as 2Fe2S-clusters produce a characteristic CD spectrum between 300-700nm.^{202, 209-210} Applying findings from bacterial ISC, where conformational changes are essential for FeS-Isu1 formation,^{175, 177} we hypothesized that complexed Isu1 within SDU and SDUF would be constrained and have inhibited FeS-Isu1 formation ability. Supporting this hypothesis, SDU and SDUF alone produced no detectable 2Fe2S-cluster signal (Figure 4.4A, blue-dashed and red-dashed) under assembly conditions. Addition of exogenous Isu1, however, results in successful FeS-Isu1 formation (Figure 4.4A, blue-solid and red-solid). This finding agrees with reports from the human system,²⁰² where stoichiometric amounts of the Nfs1-Isd11, Isu1, Yfh1 human orthologs results in no detectable FeS-Isu1 formation. This behavior also explains why reported protocols for generating FeS-Isu1 have all involved the use of a smaller, catalytic amount of Nfs1 with an excess of Isu1.^{190, 208, 211}

4.4.5 FeS-cluster Formation Using flscU with yeast Nfs1-Isd11 and Yfh1

Using the Isu1 ortholog from *Drosophila melanogaster* (flscU) is a unique approach to circumvent Isu1-complexation effects related to FeS-Isu1 formation and provides valuable insights into SD, SDU, and SDUF function. Attempting FeS-Isu1 formation using SDU and SDUF presents a challenge as all reported methods for converting *apo*-Isu1 to FeS-Isu1 have required using small amounts of Nfs1 and excess Isu1. FeS-Isu1 formation using only SDUF, however, requires stoichiometric amounts of protein that deviates from optimal FeS-Isu1 conditions (see Chapter 2). Therefore, the

lack of FeS-Isu1 within SDUF may be a result of using sub-optimal conditions for assembly that prevent FeS-Isu1 formation in a manner unrelated to Isu1 complexation to SD. To address this concern, yeast Isu1 was replaced with flscU. As shown in Chapter 3, flscU can will complement yeast Isu1 *in vitro* and *in vivo* but does not form a SD-flscU-F complex under conditions that facilitate yeast SDUF association (Figure 4.4B). Testing stoichiometric mixtures of yeast SD, flscU, and Yfh1 results in successful FeS-flscU formation (Figure 4.4C, red) with a yield comparable to that used obtained using excess exogenous flscU (Figure 4.4C, blue). This suggests that stoichiometric SD and Isu1 conditions do not prevent FeS-Isu1 formation if Isu1 remains uncomplexed.

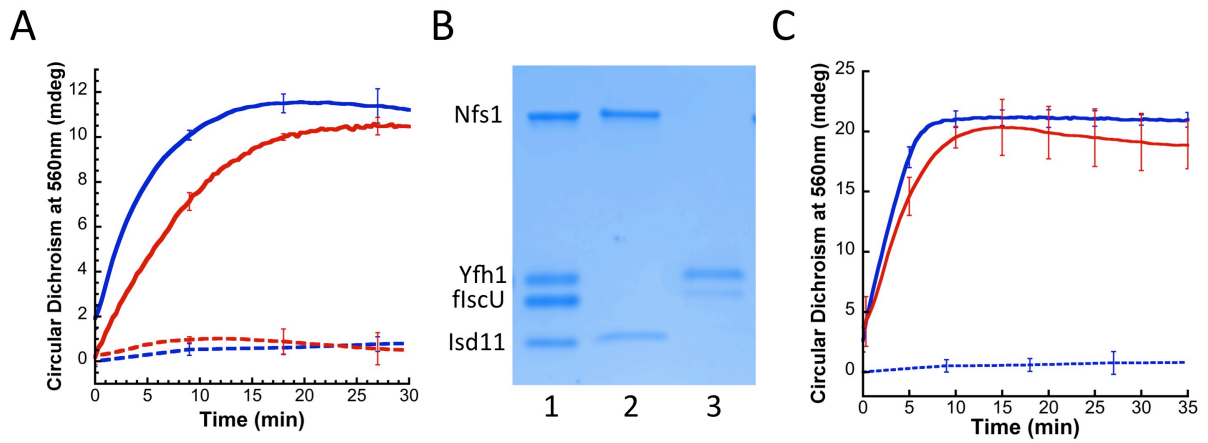


Figure 4.4: Functional studies of SD, SDU, and SDUF. (A) FeS-Isu1 formation using yeast Isu1 assessed via circular dichroism at 560nm. 5-fold complexed Isu1 within SDU (red-dashed) and SDUF (blue-dashed) produces no signal while addition of 5-fold exogenous *apo*-Isu1 produces FeS-Isu1 signal using either SDU (red-solid) or SDUF (blue-solid). (B) SDS-PAGE gel illustrating separation of Nfs1-Isd11, Yfh1, and flscU components during S200 gel filtration. Lane 1: Mixture of Nfs1, Isd11, flscU, and Yfh1 loaded onto column. Lane 2: Isolated SD complex lacking flscU or Yfh1. Lane 3: Unbound flscU and Yfh1 species. (C) Successful FeS-flscU reconstitution using stoichiometric (50 μ M) amounts of SD, Yfh1, and flscU (red), producing similar reaction as observed under optimal FeS-Isu1 conditions: 10 μ M yeast SDUF with 50 μ M exogenous flscU (blue). 50 μ M yeast SDUF without exogenous Isu1 (blue-dashed) provided as comparison.

We then tested the ability of the SD, SDU, and SDUF complexes to generate FeS-clusters on excess exogenous flscU. Compared to yeast Isu1, a greater yield of FeS-cluster formation is observed with flscU, possibly due to instability and insolubility issues reported for yeast Isu1.²¹² FeS-flscU formation is rapidly stimulated by SDUF (Figure 4.5A, blue) compared to SD (black) and SDU (red). Comparing the slopes of the reaction profiles, the rate of FeS-flscU formation is 3-fold higher for SDUF (Figure 4.5B). As SD and SDU produced similar rates of FeS-flscU formation, we hypothesized that frataxin was acting as an allosteric activator of Nfs1^{189-190, 208} and this was the source of the stimulated FeS-flscU formation.

4.4.6 High Cysteine Desulfurase Activity Identified in SDUF

Results from our cysteine desulfurase activity assay indicate that SDUF has a high cysteine desulfurase activity compared to SD and SDU. This assay specifically measures the cysteine desulfurase activity of Nfs1 by measuring the methylene blue acid-labile sulfide content. Addition of methylene blue precursors in a strong acidic environment to SD, SDU, and SDUF reaction mixtures results in the formation of a blue color, demonstrating all complexes were able to reduce sulfur from cysteine to some extent. Figure 4.5C compares the amount of sulfide produced by SD, SDU, SDUF, and SDF under conditions that match those used for optimal FeS-Isu1 formation. SDUF demonstrates a dramatic (~6-fold) increase in sulfide production compared to SD and SDU. This agrees with reports that frataxin acts as an allosteric activator of Nfs1.^{189-190, 201} This stimulation is possibly the source of the accelerated FeS-flscU formation observed in Figure 4.5B. SD and SDU have similar sulfide production rates, consistent with the pattern observed for FeS-flscU formation.

A possible alternative explanation for the lack of 2Fe2S-cluster formation from SDUF alone is that the active site of complexed Isu1 is not solvent exposed. If the Isu1

FeS-cluster coordination site, while complexed within SDU, is buried in the Nfs1 active site, Isu1 may be unable to interact with persulfide or Fe^{2+} due to limited solvent accessibility. Considering the high cysteine desulfurase activity in SDUF, however, the active site of Nfs1 is likely accessible to solvent. Structures published of the SDU bacterial ortholog²¹³ (“IscU” for Isu1 and “IscS” for Nfs1) demonstrate that the IscU FeS-cluster coordination site and IscS active cysteine have a direct interaction. This interaction is expected to be conserved within eukaryotic systems, as Isu1 must interact with Nfs1 via their active sites for persulfide transfer during *de novo* FeS-cluster formation.^{199, 214-215} This implies that the FeS-cluster coordination site of Isu1 is likely solvent exposed, although the binding site of Isd11 onto Nfs1 may alter the binding capacity of Isu1.

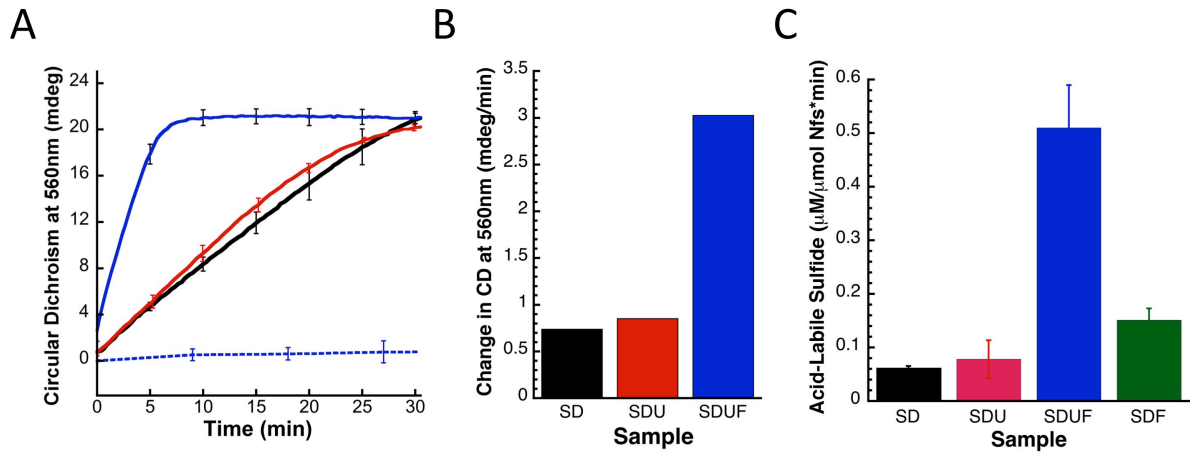


Figure 4.5: FeS-flscU formation with excess flscU. (A) FeS-IscU formation using 5-fold *apo*-flscU with SD (black), SDU (red), and SDUF (blue). (B) Rate of *apo*-flscU to FeS-flscU conversion for SD (black), SDU (red), and SDUF (blue). (C) Acid-labile sulfide content assessed via formation of methylene blue for SD (black), SDU (red), SDUF (blue), and SDF (green).

4.4.7 SDU and SDUF Complexes Retain Ability to Bind Mononuclear Fe²⁺

Although complexed Isu1 does not produce a detectable FeS-cluster, the SDU and SDUF complexes retain some ability to bind mononuclear Fe²⁺. A recent article demonstrated that the iron-accepting site of Isu1 is distinct from the FeS-cluster coordination site.²¹⁶ In addition to the active site, therefore, we considered that the initial iron-accepting site of Isu1 could also be inaccessible to Fe loading. According to recent reports from the murine system,¹⁹⁹ however, this seemed less likely to explain the lack of observable 2Fe2S-cluster CD signal because murine SDUF is able to bind Fe²⁺ in the presence of cysteine. The need for cysteine presents a challenge for measuring SDUF Fe-binding because cysteine is a substrate for Nfs1. Addition of cysteine along with Fe²⁺, therefore, would result in a simultaneous chemical reaction and possible FeS mineral formation that could interfere with traditional methods for assessing Fe²⁺-binding. In Chapter 2, measuring the amount of light scattering during FeS-Isu1 formation was used to assess FeS mineralization. This work demonstrated that adverse FeS mineralization was linked to the presence of free Fe²⁺. The logical extension of this method is that it could, in some capacity, be used to also detect free Fe²⁺. This study utilized this strategy to estimate the Fe-binding capacity of SDU and SDUF. This method is however experimental in nature and should only be used for a qualitative analysis.

Even though SDU and SDUF cannot produce an appreciable 2Fe2S-cluster CD signal, there is only a minimal increase in light scattering (Figure 4.6, blue) during the attempted FeS-Isu1 formation reaction that is similar to the feature observed under ideal FeS-Isu1 conditions using exogenous yeast Isu1 (Figure 4.6, red). This suggests that Isu1 complexed to Nfs1 is, to some extent, able to bind Fe²⁺. This binding is strong enough to prevent free Fe²⁺ from interacting with persulfide from Nfs1, or from free sulfide in solution. This finding agrees with observations from FeS-flscU formation

studies, where there is a slightly reduced yield of *apo-flscU* with SDUF than with SD + frataxin (not shown) under Fe²⁺-limiting conditions.

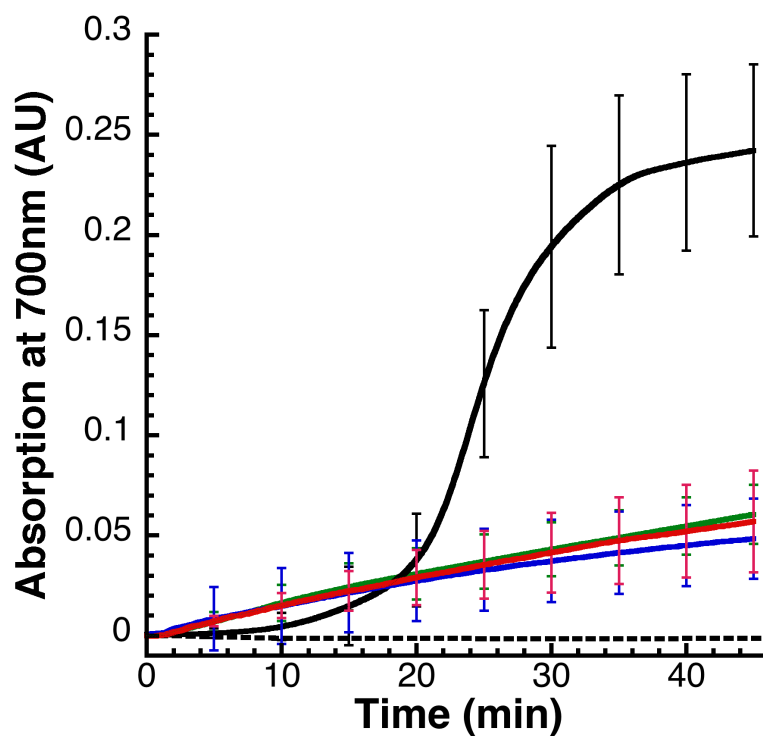


Figure 4.6: FeS mineral production under various FeS-flscU formation conditions: SD with no Isu1 (black), SD with EDTA and no Isu1 (black-dashed), optimal FeS-Isu1 formation conditions with yeast Isu1 (green), SDU alone (red), and SDUF alone (blue). Reduced FeS mineralization observed using only SDU or SDUF demonstrates Fe²⁺ binding of complexed Isu1.

4.4.8 Frataxin Binding Increases PLP-cofactor Binding in SDUF

Frataxin binding to SD increases the pyridoxal 5'-phosphate (PLP)-binding of Nfs1 within as-purified SDUF. SD, SDU, and SDUF complexes as-purified have a yellow color, attributed to the PLP cofactor of Nfs1.²⁰⁶ An early observation, when working with SDUF as purified, was that it was much more "yellow" than the SD or SDU complexes. This observation could be assessed by visible absorption spectroscopy. The absorption spectrum of SDUF demonstrates a 2-fold increase in absorption of the feature attributed to the PLP-cofactor near 420nm (Figure 4.7). The absorption of SDU is intermediate between SD and SDUF, but SDU has a tendency to precipitate and has increased light-scattering that shifts the absorption baseline upward. Centrifugation of precipitated SDU species is able to minimize this effect but not completely eliminate it. By visible inspection, SDU does not have an appreciably different yellow color than SD. These results lead to the conclusion that frataxin affects the PLP-cofactor binding of SD. This agrees with recent reports demonstrating that frataxin-binding to SD exposes the PLP-binding site.¹⁸⁹

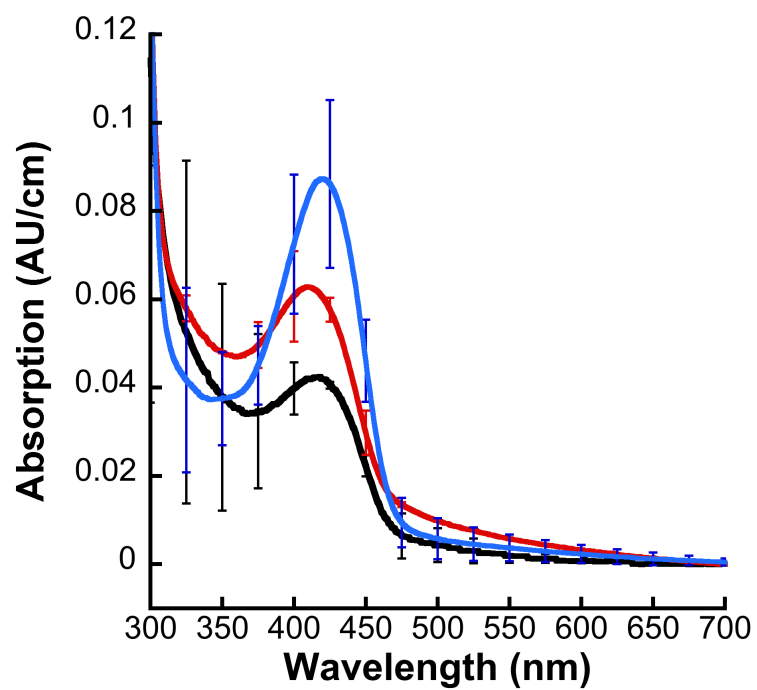


Figure 4.7: Visible absorption spectra of 10 μ M SD (black), SDU (red), and SDUF (blue) complexes demonstrating increased PLP-feature at \sim 420nm for SDUF.

4.4.9 Proposed Model for SDUF Function *in vitro*

Based on the results outlined above, we developed a model for how we believe SDUF functions during *in vitro* FeS-cluster assembly. In this model (Figure 4.8), SDUF functions as a highly active cysteine desulfurase and uncomplexed Isu1 is the site of *de novo* FeS-cluster formation. When you consider the findings from the bacterial ISC system, which is highly conserved with yeast ISC, complexed Isu1 is likely locked in the structured state.¹⁷⁵ In this model, Isu1's transition from the disordered to structured state is essential for *de novo* FeS-cluster biogenesis.¹⁷⁷ However, we speculate that this transition can only occur on uncomplexed Isu1. This model agrees with findings from bacterial ISC where IscU mutants that stabilize the structured IscU state have impaired FeS-cluster formation.¹⁷⁷

Our model however does not coincide with what has recently been proposed in human ISC,²¹⁷ where FeS-cluster formation occurred as an unstable intermediate on SDUF ("FeS-SDUF"). For these results with yeast SDUF, we feel our model is favored for several reasons. First, no evidence has been reported that directly confirms the existence of an FeS-SDUF intermediate. As SDUF-mediated FeS-cluster formation on flscU reaches completion rapidly (~5 minutes), the proposed FeS-SDUF intermediate probably would be present in sufficient quantities to be detectable. Also, the similarity in SD and SDU function suggests that accelerated FeS-cluster formation of SDUF on exogenous flscU is not due to the complexed Isu1, but rather due to frataxin. Furthermore, SD+F produces accelerated FeS-cluster formation similar to SDUF (see Chapter 3). Lastly, there is also no clear explanation for why the FeS-cluster produced by SDUF is unstable when it is stable on exogenous Isu1.

4.4.10 Insights into Mechanism for FeS-Cluster Assembly *in vivo*

This *in vitro* study of SD, SDU, and SDUF complexes may provide novel insights into FeS-cluster formation *in vivo*. ISC-mediated FeS-cluster biogenesis is a tightly regulated process *in vivo* that requires the coordinated interaction between the Nfs1, Isd11, Isu1, and Yfh1 proteins.²¹⁸ Complex formation between these proteins is, therefore, expected to be an integral part of the ISC pathway.²¹⁹ Unexpectedly, flscU can fully complement yeast ISC *in vivo* but does not form an observable complex with yeast Nfs1-Isd11 and Yfh1 *in vitro*. This suggests that SDU and/or SDUF complex formation may not be essential *in vivo*. There remains the possibility that flscU forms a complex *in vivo* that cannot be isolated using the described *in vitro* methods, however.

As complexed Isu1 within SDU and SDUF demonstrates inhibited FeS-cluster formation, this suggests that Isu1 binding to Nfs1 may be transient *in vivo*. Possibly Nfs1-Isu1 binding is required for persulfide transfer but FeS-cluster formation occurs on exogenous Isu1 after Nfs1-Isu1 dissociation. The event that triggers complex dissociation is not present *in vitro*, and thus FeS-cluster formation has not been observed in this work. This event may be Jac1 or Ssq1 binding.^{211, 220}

Lastly, the findings from this work suggest the existence of multiple conformers of eukaryotic Isu1, similar to findings of 'structured' and 'disordered' conformations for bacterial IscU.¹⁷⁵⁻¹⁷⁷ Although the existence of multiple conformations for eukaryotic Isu1 has not been reported, bacterial IscU is highly conserved with yeast Isu1 and is believed to function similarly.^{188, 219} This work further suggests that binding of Isu1 to Nfs1 favors one particular Isu1 conformation and inhibits the conformational change that is required for *de novo* FeS-cluster formation.

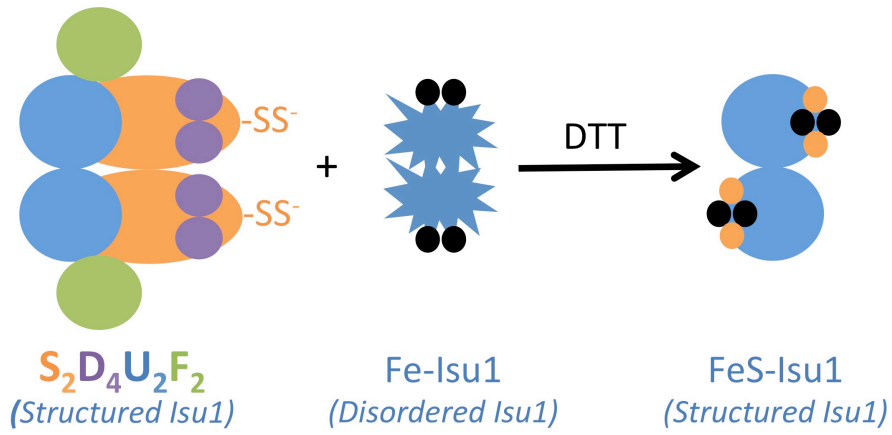


Figure 4.8: Model for SDUF-mediated FeS-Isu1 formation via uncomplexed *apo*-Isu1 in the disordered conformation. Isu1 within SDUF is locked in the structured conformation. Black circles represent Fe^{2+} and orange circles represent S^{2-} .

CHAPTER 5: *IN VITRO* EFFECTS OF FRATAXIN ON *DE NOVO* FE_S-CLUSTER FORMATION

5.0 Prelude

While my major project goals did not specifically involve frataxin, many of my experiments led to interesting observations regarding this protein. As my project focused on the interaction between Nfs1-Isd11, Isu1, and Yfh1, I utilized frataxin regularly in my studies. Most notably, demonstrating stimulation by frataxin was a critical goal for validating the FeS-Isu1 formation method. As I was studying both yeast and fly ISC proteins, I utilized both yeast frataxin, “Yfh1”, and fly frataxin, “Dfh”, in my experiments. But aside from my specific project aims, I was innately curious about this protein and designed separate experiments to test its effects. This led to several interesting observations regarding frataxin’s function *in vitro*. This chapter of my dissertation is a compilation of side experiments related to frataxin that were done while working on my main project. I have organized these results into a concise story and I think this data might be of interest to future lab members. I did all the experiments and writing in this chapter.

5.1 Introduction

The protein frataxin has always been of prime interest to ISC researchers. This is because the genetic disease Friedreich’s ataxia (FRDA), the most obvious clinical correlation for this field, has been linked to a trinucleotide repeat expansion in the frataxin gene.²²¹ To illustrate this point, as of writing this chapter, on pubmed.gov there are ~5 times more articles mentioning “frataxin” than on the scaffold proteins “Isu”/“IscU”/“ISCU”. Despite this increased focus on frataxin, the *in vivo* function of this protein remains unclear. Frataxin has been described as an iron chaperone that delivers iron to Isu1 for *de novo* FeS-

cluster synthesis²²²⁻²²⁶ and to ferrochelatase for the biosynthesis of heme.²²⁷ Structural data in particular has supported the role of frataxin in Fe binding and transport.^{225, 228} But in recent years, there have been a significant amount of reports that frataxin interacts with Nfs1 and acts as an allosteric regulator.²²⁹⁻²³¹ To this effect, reviewing literature on frataxin is challenging because there is such a wide variety of conflicting results that have been published in different systems. This suggests that the role of frataxin is likely more complicated than was initially thought.²³²

The following chapter describes the *in vitro* effects of frataxin related to binding to flscU and to FeS-cluster assembly. Utilizing a reaction system with yeast Nfs1-Isd11 and fly IscU, “flscU”, both yeast frataxin, “Yfh1”, and fly frataxin, “Dfh”, were used in these experiments. These results suggest that frataxin can function as an activator of cysteine desulfurase *in vitro*. Frataxin demonstrates significant stimulation on FeS-flscU formation when present in small amounts (< 10 μ M), consistent with its role as an allosteric regulator. Frataxin’s allosteric effects are possibly related to stimulation of cysteine desulfurase as assessed by measuring acid-labile sulfide production (see Chapter 4). In a reaction system consisting of yeast Nfs1-Isd11 and fly IscU, Yfh1 demonstrates a larger stimulation than Dfh on FeS-flscU formation. Testing Fe-delivery to Isu1 via frataxin *in vitro* was not successful because Fe-transfer steps may occur too quickly to be assessed via the FeS-flscU formation method.

5.2 Methods

5.2.1 Protein Expression and Isolation

Yeast frataxin (Yfh1), *Drosophila* IscU (flscU), and yeast Nfs1-Isd11 were grown and purified as described in Chapter 3. This chapter also utilizes the frataxin ortholog from

Drosophila melanogaster, “Dfh”. Dfh was purified as described in Kondapalli *et al.*²²³ Briefly, the Dfh gene was purchased from the Drosophila Genomics Resource Center (Clone ID: AT09528). The Dfh cDNA was cloned by Kalyan Kondapalli into a pET101/D-TOPO vector. Recombinant expression was done via transformation into BL21(DE3) *E. coli* competent cells.

Dfh growth and purification was done following the same protocol used for untagged Yfh1. Cells expressing Dfh were grown in LB broth and induced with 1mM IPTG at an OD₆₀₀ ~0.6. After induction, cells were induced at 37°C for 4 hours. Cells were isolated from broth *via* centrifugation and resuspended in the purification buffer: 25mM Tris, 10mM EDTA, 5mM BME buffer at pH=8.0. Cells were lysed using an AVESTIN Emulsiflex-C3 homogenizer. Soluble and insoluble cellular materials were separated via centrifugation for 45 minutes at 21,000rpm. The soluble fraction was run through a 0.2µm filter and two steps of ammonium sulfate precipitation were used to isolate Dfh. Salting-in (protein in solution) was done by adding ammonium sulfate to 40% saturation, and salting out (protein in precipitate) was done by increasing the ammonium sulfate to 65% saturation. Salted-out precipitate containing Dfh was dissolved in purification buffer and dialyzed twice into 2L of fresh purification buffer for 3 hours to remove the ammonium sulfate. This protein solution was run through a Q-sepharose column and eluted using an NaCl gradient, increasing from 0 to 1M NaCl. Fractions containing protein were pooled and salt was again removed via two rounds of dialysis into 2L of purification buffer for 3 hours. Next, ammonium sulfate was added to the protein solution to a concentration of 1M and run through a phenyl-sepharose column. Protein was eluted using a decreasing gradient (from 1M down to 0) of ammonium sulfate concentration. Lastly, fractions containing protein

were pooled, concentrated using an Amicon 10kDa cutoff centricon to ~2mL, and run through a S75 size-exclusion column. Frataxin was switched into the final experimental buffer during size-exclusion chromatography: 20mM HEPES, 150mM NaCl, 5mM BME at pH=7.5. Protein quality was estimated via SDS-PAGE and concentration was measured using a Millipore Direct-Detect IR spectrometer.

5.2.2 Effect of Frataxin on FeS-Isu1 Formation

FeS-flscU formation was examined under the “optimal FeS-Isu1 formation” conditions described in Chapter 2 and using *apo*-flscU to test the effect of frataxin on FeS-cluster assembly. In this chapter, conditions used for these studies are identical to those described in Chapter 2 (50μM flscU, 10μM Nfs1-Isd11, 75μM Fe, 500μM cysteine, 5mM DTT) but with the addition of frataxin. Frataxin was utilized in a different manner depending on the particular application. Frataxin concentration dependence studies were performed where the *apo*-frataxin concentration was varied between 0-100μM (as noted) in the following experimental buffer: 20mM HEPES, 5mM BME at pH=7.5 at room temperature with either 150mM or 500mM NaCl (as noted). *holo*-Dfh (with Fe) and *apo*-Dfh (No Fe) were prepared as follows. *holo*-Dfh was produced by incubating stoichiometric amounts of Fe²⁺ and Dfh for 30 minutes. For *holo*-Dfh reactions, the only source of Fe²⁺ was via addition of 75μM *holo*-Dfh. Reactions utilizing *apo*-Dfh involved adding equimolar (75μM) amounts of Fe²⁺ and *apo*-Dfh to the reaction mixture separately, with Fe²⁺ being added to the Isu1 reaction mixture 5 minutes before addition of *apo*-Dfh. The buffer used in *apo* vs. *holo*-Dfh experiments was 20mM HEPES, 150mM NaCl, 5mM BME at pH=7.5 at room temperature. Conditions were, otherwise, identical to the optimal FeS-Isu1 formation conditions described in Chapter 2.

5.2.3 Pull-Down Assay For Measuring Dfh-flscU Binding

A simple pull-down assay was employed to test the effects of Fe on Dfh-flscU complex stability. This pull-down assay was done using Ni-column affinity chromatography with untagged Dfh and N-terminal His6-tagged flscU. All experiments were done in an anaerobic glovebox (Coy), regulated to room temperature. Conditions were selected for pull-down assays were matched as well as possible to conditions used in the Dfh:flscU isothermal titration calorimetry (ITC) studies within Dr. Swati Rawat's dissertation. A Dfh-flscU protein mixture was prepared in 20mM HEPES, 150mM NaCl, 5mM BME buffer at pH=7.5. Concentrated Dfh (~400 μ M) was incubated with 1xFe equivalent for 30 minutes to produce *holo*-Dfh, while *apo*-Dfh was produced adding equal volume of buffer instead of Fe. Either *holo*- or *apo*-Dfh was then mixed with concentrated flscU to create 100 μ M flscU:200 μ M *holo*-Dfh (200 μ M Fe) and 100 μ M flscU:200 μ M *apo*-Dfh mixtures, respectively and samples were prepared at a final volume of 0.3mL. A 0.25mL volume of the flscU:*apo*-Dfh mixture was loaded on to a 5-mL Ni-column as a stable base for testing complex formation, with the His rich attachment site located on the N-terminus of flscU. The column was washed with either 25mL or 50mL of 20mM HEPES, 20mM Imidazole, 150mM NaCl buffer at pH=7.5. Proteins were eluted using 25mL of the same washing buffer with the imidazole concentration increased to 250mM. After elution of the flscU:*apo*-Dfh mixture, the column was re-equilibrated with 50mL of binding buffer and all steps were repeated identically for the flscU:*holo*-Dfh mixture. The eluted fractions were concentrated to 1mL. All fractions were analyzed via SDS-PAGE to estimate the amount of Dfh-binding to flscU.

5.3 Results

5.3.1 Effect of Frataxin is Concentration Dependent Under Physiologic Salt Levels

Under a near-physiologic salt concentration (150mM), frataxin's effect on FeS-flscU formation depends on its concentration. Lower concentrations of frataxin (0-20 μ M) result in stimulation, and higher concentrations (>50 μ M) result in inhibition. Intermediate concentrations (20-50 μ M) have little effect. This pattern was observed for Yfh1 (Figure 5.1 A and B) and Dfh (not shown). This concentration-dependence was minimized when the salt concentration is increased to 500mM for both Yfh1 and Dfh (Figure 5.1C). Under either salt condition, however, frataxin stimulation was profound even when present in small amounts. In fact, concentrations as low as 1 μ M result in 80% of the maximal frataxin stimulation (Figure 5.1C).

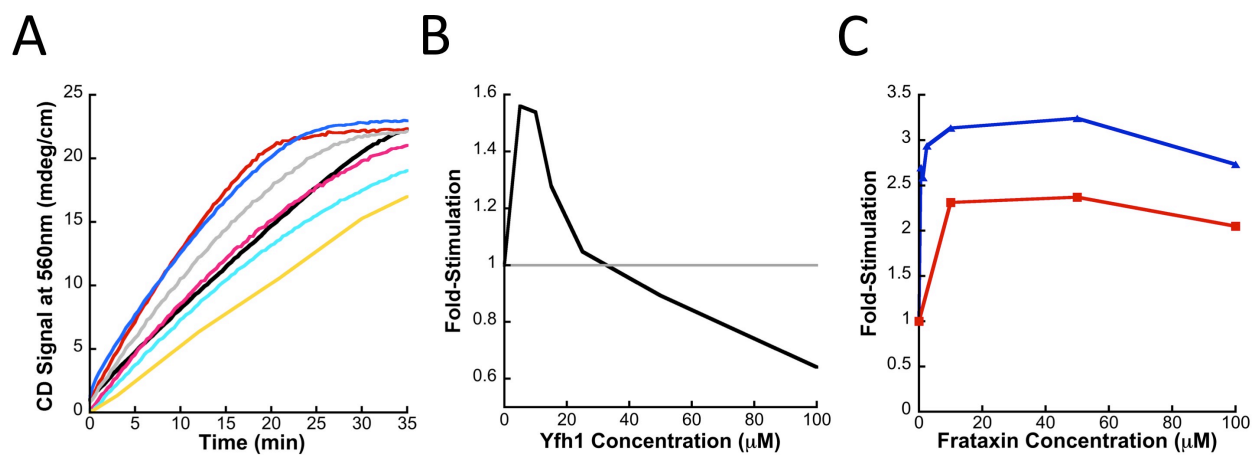


Figure 5.1: (A) FeS-flscU transformation over time under differing Yfh1 concentrations with 150mM NaCl, 50μM flscU, and 75μM Fe: no Yfh1 (black), 5μM Yfh1 (blue), 10μM Yfh1 (red), 15μM (gray), 25μM Yfh1 (pink), 50μM Yfh1 (cyan), 100μM Yfh1 (yellow). (B) Initial rate of FeS-flscU formation under differing Yfh1 concentrations. Gray line indicates transition from stimulation to inhibition. (C) Inhibitory effect from increasing frataxin concentration is dramatically reduced under high salt (500mM NaCl) conditions for both Yfh1 (blue) and Dfh (red).

5.3.2 Testing Dfh as Fe-Donor for FeS-flscU Formation

In order to test the ability of Dfh to function as an Fe-donor during FeS-cluster formation, FeS-flscU formation was assessed by either adding *holo*-Dfh to *apo*-flscU or by adding *apo*-Dfh to Fe-flscU during reaction mixture preparation. Under the conditions described in section 5.2.2, use of *apo*- vs *holo*-Dfh demonstrates no effect on FeS-flscU formation (Figure 5.2). Considering that reaction mixtures are incubated for 5 minutes prior to reaction initiation with cysteine, this suggests that Fe-transfer has reached completion prior to reaction initiation. An assay requiring ~40 minutes may be too slow to provide information about Fe-delivery.

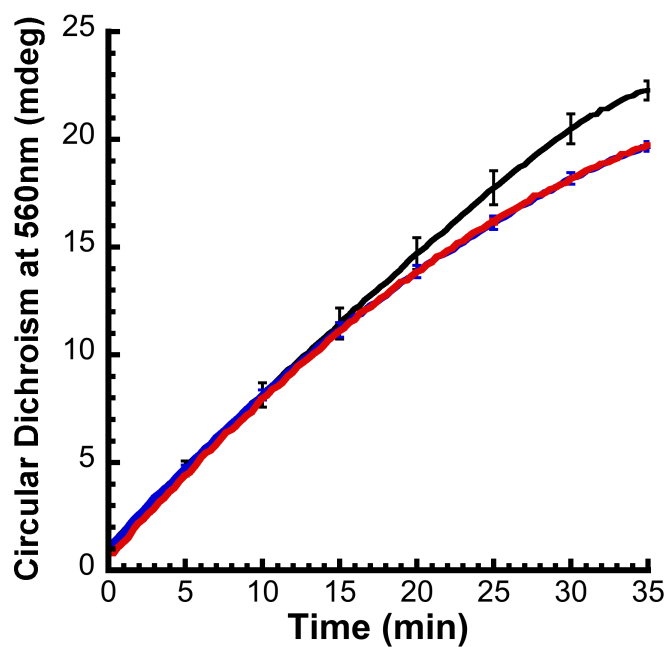


Figure 5.2: Effects of 75 μM *apo*- (blue) vs *holo*- (red) Dfh compared to no frataxin (black) on FeS-flscU formation. Inhibitory effect is observed at 75 μM Dfh under 150mM NaCl buffer conditions. Dfh-mediated effects on FeS-flscU formation do not depend on Fe-binding status (*apo* vs *holo*) of Dfh under the described conditions.

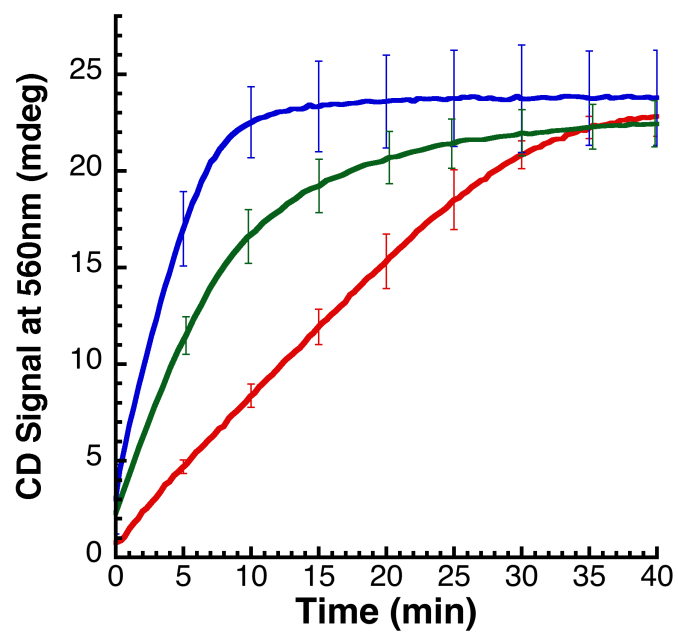


Figure 5.3: FeS-IscU transformation with no frataxin (red), Yfh1 (blue), and Dfh (green). 10 μ M frataxin stimulates FeS-flscU formation using 10 μ M yeast Nfs1-Isd11 and 50 μ M *apo*-flscU in 500mM NaCl solution. Stimulation is ~30% greater using Yfh1 than Dfh.

5.3.3 Both Dfh and Yfh1 Stimulate FeS-flscU Formation Using Yeast Nfs1-Isd11

Using either 10 μ M Yfh1 or Dfh with yeast Nfs1-Isd11 results in stimulated FeS-flscU formation. This agrees with the finding from Chapter 3 that ISC is highly conserved between *S. cerevisiae* and *D. melanogaster* and agrees with previous reports that Dfh can complement yeast ISC (unpublished data). A concentration of 10 μ M frataxin was selected for this study as experimental results show stimulation had reached maximum at this concentration (Figure 5.1C). In 500mM NaCl reaction buffer, Yfh1 demonstrates a significantly greater stimulation (3.0x) than observed for Dfh (2.2x). Assuming that intra-species reactivity is complete, and inter-species reactivity is partial, this data suggests that frataxin stimulation is more associated with Nfs1 than with Isu1. There are potential complications and alternative explanations for this pattern, however. There may be differences in stability or activity of the recombinant Yfh1 and Dfh proteins that affects their stimulatory behavior or there may be incomplete cross-reactivity between the fly IscU and yeast Nfs1-Isd11.

5.3.4 Dfh-flscU Binding Not Significantly Affected by Fe²⁺

Utilizing a Ni-column pull-down assay, binding of Dfh to His6-flscU is not significantly affected by the use of *apo*- or *holo*-Dfh (Figure 5.4A). Repeating this assay with an additional washing step produces a similar pattern (Figure 5.4B). With either *apo*- or *holo*-Dfh, relatively small amounts of Dfh remain bound to flscU. This could possibly have been prevented if non-specific interactions were screened by washing with lysate. This step was not included because of concerns that bacterial lysate was not completely anaerobic, which could introduce potential oxidation of Fe²⁺. Therefore, conclusions regarding the presence or absence of specific Dfh-flscU binding cannot be made, only that

this binding is not significantly affected by the presence of Fe under these binding conditions. This small amount of Dfh:flscU binding, however, is quite similar to similar pull-down studies done on Yfh1:Isu1 binding in mitochondrial lysate.²³³

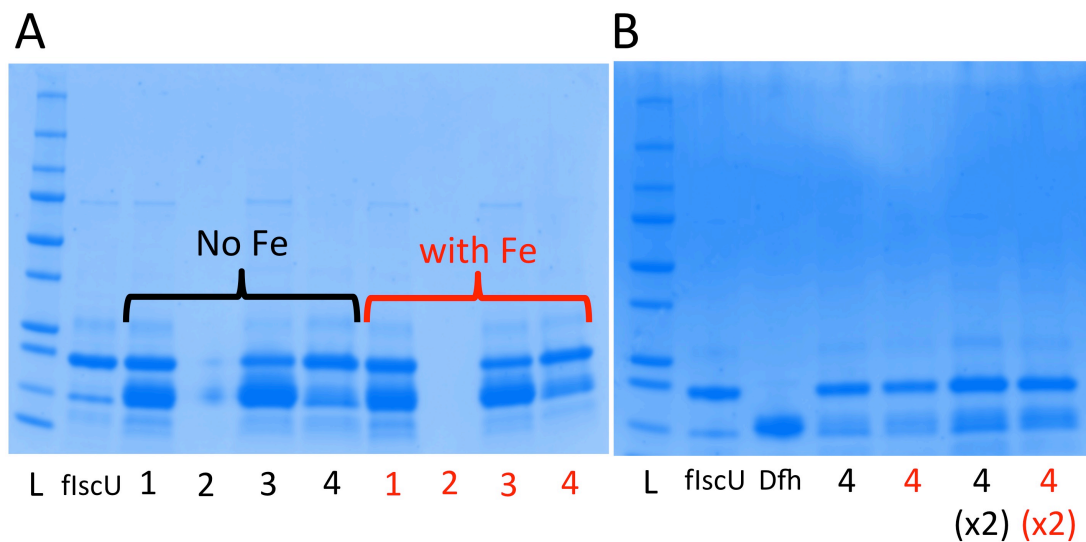


Figure 5.4: SDS-PAGE of various protein mixtures from Ni-column pull down assay measuring His6-flscU binding to untagged Dfh. Dfh-flscU binding is not significantly affected by using *apo*-Dfh (no Fe) in place of *holo*-Dfh (with Fe). Labels in **black** correspond to *apo*-Dfh and in **red** to *holo*-Dfh. Lanes: L (ladder), 1 (2*xapo*/*holo*-Dfh:1*xflscU* mixture), 2 (flow-through), 3 (Wash), and 4 (eluted). After addition of protein mixtures, columns were washed with either 25mL (panel A) or 50mL (panel B) of binding buffer.

5.4 Discussion

5.4.1 Frataxin's Inhibition of FeS-Cluster Formation Related to Protein Instability *in vitro*

The concentration dependent stimulatory vs. inhibitory effect of frataxin on FeS-flscU formation may be an artifact related to protein instability *in vitro*. As described in section 5.3.1, in 150mM NaCl solution, frataxin concentrations 0-20 μ M were stimulatory while frataxin concentrations >50 μ M were inhibitory for FeS-flscU formation. Under higher salt conditions (500mM NaCl), however, frataxin only caused stimulation under all frataxin concentrations tested (0-100 μ M). This dependence on salt concentration suggests that the inhibition caused by frataxin is an artifact related to protein instability. While it has been reported that frataxin orthologs have different effects in different systems,²²⁹ it has never been reported that frataxin stimulation vs. inhibition can be modulated under differing reaction conditions. It is not clear what is creating this frataxin concentration-dependent stimulatory vs. inhibitory effect but one theory is that frataxin is oligomerizing with Fe under lower salt conditions, as there have been several reports noting that frataxin oligomerizes in the presence of Fe.²³⁴⁻²³⁶ This could also explain why in addition to inhibiting FeS-flscU formation, large amounts of frataxin (>50 μ M) also reduce the yield FeS-clusters. As these findings are highly dependent on *in vitro* reaction conditions, this frataxin concentration dependent stimulatory vs. inhibitory effect on FeS-cluster formation may not have physiologic relevance.

5.4.2 Frataxin as an Allosteric Activator of Nfs1

Small amounts (<10 μ M) of either Dfh and Yfh1 demonstrate a profound stimulation on FeS-cluster formation and this supports the role of frataxin as an allosteric activator *in*

vitro. This finding agrees with various reports on the topic.^{229-230, 237-238} Frataxin's allosteric activation may be of the cysteine desulfurase enzyme Nfs1 as frataxin increases acid-labile sulfide production in a pattern consistent with observed FeS-flscU formation (see Chapter 4). Visible absorption spectroscopic analyses of as-purified SD, SDU, and SDUF complexes suggest that frataxin affects the PLP-binding of Nfs1 (see Chapter 4) and this may indicate a possible mechanism for frataxin-mediated stimulation of the cysteine desulfurase activity of Nfs1. An important consideration, however, is that FeS-flscU formation could potentially be complicated by frataxin's combined effects on Fe-delivery and cysteine desulfurase activation. Using sodium sulfide in place of Nfs1-Isd11 and cysteine is a strategy to uniquely consider frataxin's role in Fe-delivery because it circumvents effects related to cysteine desulfurase.

5.4.3 The FeS-Isu1 Formation Method Unable to Assess Fe-Delivery by Dfh to flscU

Studies comparing the effects of *apo*-Dfh with Fe-flscU vs. *holo*-Dfh with *apo*-flscU on FeS-flscU formation suggest that this method is too slow to adequately assess effects related to Fe-transfer. Possibly Fe-delivery to flscU occurs very fast and starts prior to reaction initiation with cysteine. This would agree with previous findings that Fe-transfer from frataxin to Isu1 does not require cysteine.²²² Reaction activation with Fe²⁺ instead of cysteine is a potential approach to study Fe-transfer effects, however this may facilitate FeS-mineralization that could complicate the experiment.

5.4.4 Dfh-flscU Binding is Not Significantly Affected by Iron

The pull-down assay studies (Figure 5.4) using *D. melanogaster* proteins suggest that Dfh-flscU binding is not affected by the presence of Fe. This disagrees with previous findings from both *S. cerevesiae* and *D. melanogaster*. It is unclear, however, if ITC curves

from *Cook et al.*²²² (yeast) and Dr. Swati Rawat's dissertation (fly) were measuring Fe-transfer from frataxin to Isu1 or a direct protein-protein interaction. To support that the ITC curves were actually measuring Fe-transfer, however, binding parameters for *holo*-Yfh1 to Isu1 are similar to the parameters of free Fe²⁺ into Isu1.²²² Also, the binding parameters for *holo*-Dfh into flscU are comparable to free Fe²⁺ into flscU (see Dr. Swati Rawat's dissertation). The described pull-down studies using *apo/holo*-Dfh were an attempt to estimate protein-protein binding specifically in a way that would not be affected by potential Fe-transfer. These pull-down studies have potential complications, however. One possibility to note is that the Ni ions of the Ni-column could functionally bind to *apo*-Dfh, removing any differences from the *holo*-Dfh binding studies. Alternatively, imidazole used in the experimental buffer could interfere with Dfh-flscU binding or could adversely affect the Fe-binding capacity of these proteins. Lastly, the binding interaction between *holo*-Dfh and flscU may interfere with the Ni-column binding of His6-flscU.

5.4.5 Frataxin as Allosteric Activator of Nfs1 *in vivo*

In vitro results suggesting that frataxin is an allosteric activator of cysteine desulfurase may provide insights into frataxin's function *in vivo*. The role of frataxin *in vivo* has a direct clinical significance, as this protein is under-expressed in patients suffering from Friedreich's Ataxia (FRDA).²²¹ This suggests a novel treatment strategy for FRDA, such as a small molecule that functions, like frataxin, to stimulate Nfs1 activity. A structure for a human ISCS-ISD11-ACP1 complex has recently been solved (still unpublished) and hopefully simulated small-molecule design will be possible in the near future.

CHAPTER 6: CONCLUSIONS AND FUTURE DIRECTIONS

6.0 Prelude

This final chapter of my dissertation will summarize results from Chapter 2-5, draw conclusions from them, and propose additional work for future studies. I will also reflect on the strengths and weaknesses of this research and describe its significance to the field of Fe-S cluster biogenesis. I did all the writing in this chapter.

6.1 Introduction

This chapter will summarize the *in vitro* findings outlined previously and attempt to draw *in vivo* conclusions from them. Up to this point, this dissertation has been hesitant to take this step because many of these described results were highly dependent on the *in vitro* conditions selected. This was particularly true for the FeS-Isu1 formation method, where a wide variety of results could be observed by simply manipulating reaction conditions. Unexplored changes to pH, temperature, or salt/protein/buffer concentrations could lead to completely opposite results from what was reported here. Similarly, discrepancies between this work and past findings could be merely a result of using different conditions. Therefore, it seems like a gigantic leap to take these findings, which were made in a dish under very specific conditions, and apply them to a living cell. A logical strategy to combat this problem is to try to use conditions that match those found *in vivo*. While this can be attempted, truly matching *in vivo* conditions may be impossible *in vitro*.²³⁹ *In vivo*, cells utilize a huge number of proteins, nucleic acids, lipids, and other small molecules. Various cellular environments are compartmentalized into micro-environments where conditions are unique and continuously changing.²⁴⁰ Please keep this in mind while considering the *in vivo* conclusions and correlations made in this chapter.

6.2 Summary of Results

The findings discussed in Chapters 2-5 will be summarized in this section. One consistent feature found throughout this dissertation is a heavy reliance on *in vitro* functional studies. In particular, much of this work focused on developing and validating an appropriate method to conduct a functional assay of recombinant Isu1 *in vitro*. Once this method, called the “FeS-Isu1 formation method”, had been validated it was applied to a wide variety of situations in attempt to answer specific questions. While these studies have some utility, the lack of prominent structural techniques in this dissertation, such as X-ray crystallography and Nuclear Magnetic Resonance Spectroscopy, limits our ability to generate structural models and mechanisms.

6.2.1 Optimal Method for Forming FeS-Isu1 *in vitro*

Replicating Isu1’s role *in vivo* can be done *in vitro* via a FeS-Isu1 formation assay. In order to obtain optimal results, however, this assay must be done under a specific set of conditions. These conditions require excess Isu1 and a limiting amount of Nfs1-Isd11 and Fe²⁺. Excess Fe²⁺ leads to an adverse side reaction, termed “FeS-mineralization”, that inhibits Fe-S cluster formation. Circular dichroism is the optimal method for assessing Fe-S cluster formation on Isu1 as it is insensitive to FeS-mineralization. While these optimal conditions may facilitate study of Isu1 *in vitro*, it remains unclear how these conditions relate to ISC function *in vivo*.

6.2.2 Characterization of Isu1 Ortholog from *D. melanogaster*, flscU

The Isu1 ortholog from *D. melanogaster*, “flscU”, is a scaffold for *de novo* Fe-S cluster biogenesis that has similar characteristics as its yeast ortholog. flscU binds 2 mononuclear iron atoms and can assemble these atoms into an Fe-S cluster. This protein is dimeric and

assembles one 2Fe2S-cluster per monomer. flscU can fully complement yeast ISC *in vivo* as flscU can rescue the Isu1/2 deletion phenotype in yeast. Use of flscU is a viable alternative to the unstable yeast Isu1 in the *in vitro* and *in vivo* study of yeast ISC. This strategy may facilitate novel experimentation of the yeast ISC pathway in the future. Challenging experimental techniques such as X-ray crystallography and NMR spectroscopy, for example, may be possible with more stable Isu1 orthologs and this could provide important structural information and identify mechanistic details of ISC.

6.2.3 Isolation and Characterization of Nfs1-Isd11-Isu1-Yfh1 (“SDUF”) Complex

The proteins of upstream *Saccharomyces cerevesiae* ISC (Nfs1, Isd11, Isu1, and Yfh1) form a complex that can be isolated *in vitro*. This complex, sometimes referred to the “Fe-S cluster assembly complex” or “SDUF”, is a result of relatively weak interactions between Nfs1-Isd11 (“SD”), Isu1 (“U”), and Yfh1 (“F”) that requires the use of low-salt conditions (~50mM NaCl) that prevent complex dissociation. Despite being named the “Fe-S cluster assembly complex”, complexed Isu1 within SDU and SDUF demonstrates inhibited Fe-S cluster formation as assessed via circular dichroism spectroscopy. Exogenous *apo*-Isu1, however, is able to produce FeS-Isu1 in the presence of SD, SDU, or SDUF. FeS-flscU formation is accelerated 3-fold by the use of SDUF over SD or SDU. SDUF demonstrates high cysteine desulfurase activity that is possibly the source of its ability to rapidly form FeS-flscU. Despite demonstrating complete complementation with yeast ISC, flscU does not form a stable complex with yeast SD under conditions that allow SDU and SDUF complex isolation. While stoichiometric conditions of Nfs1-Isd11, Isu1, and Yfh1 proteins prevent observable FeS-Isu1 formation, using flscU under these conditions in place of yeast Isu1 results in unhindered Fe-S cluster production.

6.2.4 Frataxin Functions as an Allosteric Activator of Cysteine Desulfurase *in vitro*

Lastly, my activity studies validate that frataxin is an allosteric activator of the cysteine desulfurase enzyme Nfs1-Isd11. Under 500mM NaCl conditions, small amounts of frataxin (<1 μ M) produce a dramatic stimulation (3x) in FeS-Isu1 formation when using 10 μ M Nfs1-Isd11, consistent with frataxin's role as an allosteric regulator. Frataxin affects the PLP-binding of Nfs1 in as-purified SDUF, suggesting a possible mechanism for frataxin-mediated stimulation of ISC. Frataxin's role in Fe-delivery to Isu1 could not be evaluated using the described *in vitro* methods. Using *apo*-frataxin vs. *holo*-frataxin has no effect on FeS-flscU formation, as Fe-S cluster assembly is likely too slow to assess rapid Fe-transfer behavior. Using a simple pull-down assay with *D. melanogaster* proteins, Isu1-frataxin binding is not affected by the use of *apo*- vs *holo*- frataxin. This work suggests that frataxin and Isu1 binding requires the presence of Nfs1-Isd11. These results are consistent with similar pull-down studies from yeast mitochondrial lysate.²⁴¹⁻²⁴²

6.3 Correlations to ISC Function *in vivo*

6.3.1 Regulation of Iron Critical for Efficient Fe-S cluster Formation *in vivo*

In vitro FeS-Isu1 formation studies demonstrate that excess Fe can inhibit FeS-Isu1 formation and we propose that regulation of Fe levels may be important for *in vivo* Fe-S cluster biogenesis. Outside of the ROS-mediated effects of free Fe, it is possible that adverse FeS-mineralization via free Fe could also occur *in vivo*. This insoluble mineral may be difficult for cells to remove and could be a source of toxicity. This agrees with direct *in vivo* evidence that Fe-level control is important for efficient ISC function in yeast.²⁴³⁻²⁴⁴

6.3.2 Nfs1-Isu1 Binding Studies Suggests Model for ISC Function *in vivo*

Studies of SDUF are particularly interesting for describing *in vivo* ISC and suggest a model where the Nfs1-Isu1 interaction is transient *in vivo*. *In vitro* studies of SDUF agree with recent reports that complexed Isu1 is unable to produce an observable Fe-S cluster.²⁴⁵ This suggests that something is ‘missing’ from the complex for it to complete this essential function. While we don’t know precisely what this is, the requirement for exogenous Isu1 provides an interesting clue. Perhaps the missing component is an event (or molecule) that triggers (or modulates) SDUF dissociation (possibly Ssq1 or Jac1 binding)²⁴⁶ and facilitates exogenous Isu1 formation. In this model, complex formation would be important for Fe- or S- transfer but the Fe-S cluster assembly actually occurs after complex dissociation. The SDUF complex association, would therefore, be transient *in vivo* and its dissociation is an essential step for FeS-Isu1 formation. There also could be another required component for SDUF-mediated Fe-S cluster formation that has yet to be identified. Lastly, it is possible that SDUF complexation is not essential *in vivo*. flscU is able to fully complement yeast ISC despite the fact that it has not been observed to form a stable complex with yeast SD and Yfh1 (although there may be an flscU-Nfs1 interaction *in vivo* that cannot be isolated *in vitro*).

6.3.3 Frataxin Can Activate Cysteine Desulfurase Enzyme Nfs1 *in vivo*

In vitro functional studies described in Chapters 4 and 5 suggest that frataxin can stimulate the cysteine desulfurase activity of Nfs1 and we propose that frataxin may demonstrate similar behavior *in vivo*. The role of frataxin has a direct clinical significance, as this protein is under-expressed in patients suffering from Friedreich’s Ataxia (FRDA).²⁴⁷ This suggests a novel treatment strategy for FRDA, such as a small molecule that functions,

like frataxin, to stimulate Nfs1 activity. A structure for a human ISCS-ISD11-ACP1 complex has recently been solved (still unpublished) and hopefully simulated small-molecule design will be possible in the near future.

6.4 Future Directions

Although the time for me to collect data has ended, I continue to think up new experiments that might answer many of the questions raised by this work. I am hopeful that future students, either from Dr. Stemmler's lab or elsewhere, will try to reproduce these findings and/or expand on them. This section will list several ideas to further develop this work. Perhaps if you are struggling with your project and are looking for new ideas you may find these useful.

6.4.1 Structural Characterization of *apo*- vs FeS-Isu1

Structural characterization of eukaryotic Isu1 holds enormous potential that could suggest a mechanism for Isu1-mediated Fe-S cluster formation and Isu1's interaction with Nfs1 and Yfh1. NMR studies of the bacterial Isu1 ortholog, "IscU", have revealed multiple conformations for IscU, "structured" (S) and "disordered" (D).²⁴⁸ IscU inherently exists as a mixture of these conformers, typically in a ~80% S/20% D arrangement.²⁴⁹ The best explanation for SDUF's behavior stems from this work, and possibly eukaryotic Isu1 also demonstrates similar behavior. No structural information for eukaryotic Isu1 is known, however, and there is huge potential in researching this topic. NMR studies comparing *apo*-Isu1 to FeS-Isu1 may be the best choice for probing these conformations.²⁴⁹⁻²⁵⁰ Labs that have expertise in NMR have not reported eukaryotic Isu1 structural information, however, so one could deduce that this would be difficult. Circular dichroism secondary structure estimation may also be useful, but this is a qualitative technique at best and it could be

difficult to identify differences in a species that, at most, makes up 20% of the sample. Using flscU may be a novel approach for structural characterization of Isu1 as it is highly conserved with yeast Isu1 but has increased stability and solubility.

6.4.2 Investigation of Direct Sulfur Transfer from Nfs1 to Isu1

Despite all the FeS-Isu1 studies reported here, very little has been identified regarding how Isu1 gets reduced sulfur. Possible mechanisms include direct persulfide transfer from Nfs1 to Isu1 or, a free hydrogen-sulfide intermediate produced by Nfs1 that interacts with Isu1. Seeing as flscU possibly does not complex with Nfs1 (although there may be a weak transient interaction that cannot be isolated), it is unclear how flscU gets reduced sulfur during the *in vitro* FeS-flscU formation reaction. Persulfide identification using radioactive S₃₅-labeled cysteine could be very useful to answer these questions.²⁵¹⁻²⁵² Dr. Dancis and Dr. Pain have familiarity with this method and could be a tremendous resource. But before persulfide studies of Isu1 can be done, successful persulfide formation on Nfs1 must be demonstrated.

6.4.3 Functional Assays Incorporating Downstream ISC

While Yah1 was utilized as a 2Fe2S-cluster standard in Chapter 3, further experimentation could investigate this protein with respect to its *in vivo* function as a source of electrons for FeS-Isu1 formation. Excess reduced Yah1 could potentially be used in place of DTT for this reaction.²⁵³ This would likely require either an excess of Yah1 (>100 μM for 50 μM Isu), or use of the Yah1 reductase enzyme “Arh1” and excess NADPH. An important note is that this work should utilize a near-limiting amount of cysteine, as excess cysteine can be used in place of DTT for reducing equivalents.

Although little is known regarding the early stages of ISC, perhaps even less is known regarding downstream processes. Grx5 is the *in vivo* acceptor of the Fe-S cluster from Isu1 and this has been demonstrated *in vitro*.²⁵⁴⁻²⁵⁶ Efficient transfer from Isu1 to Grx5, however, requires Ssq1 and Jac1,²⁵⁷ which would increase the number of proteins needed for this reaction to 7. With these additional proteins, stoichiometries could be appropriately adjusted and the FeS-Isu1 formation reaction could be re-designed to incorporate an entire additional step of ISC. Likely this would involve an enzymatic amount of Nfs1-Isd11, *apo*-Isu1, Yfh1, Ssq1, and Jac1 and excess *apo*-Grx5.²⁵⁷

6.4.4 Additional Characterization of SDUF

This dissertation only provides a limited study on SDUF and there is much more that needs to be done to characterize this complex. One challenge posed by this work is that many of the typical methods used for recombinant protein are difficult to perform with SDUF because SDUF is a mixture of proteins that, by mass, is predominantly Nfs1-Isd11.²⁵⁸ The melting behavior of SDUF, for example, is very similar to Nfs1-Isd11. Circular dichroism secondary structure estimation would likely produce a spectrum that looks similar to Nfs1-Isd11. A crystallographic structure for SDUF would be immensely useful, or for any yeast ISC component for that matter, but this may be difficult.

The work described in Chapter 4 did not adequately investigate SDUF's inability to make a CD-active Fe-S cluster. The model described in Chapter 4 suggests that no Fe-S cluster formation is occurring with complexed Isu1, but perhaps complexed Isu1 is producing a non CD-active or transient Fe-S cluster that could be detected by other means. XAS studies were attempted on this topic but these studies were unsuccessful. As attempted FeS-Isu1 formation with SDUF did not produce a significant FeS-mineral signal,

it appears as though complexed Isu1 still binds Fe to some extent. Much more work could be done to estimate SDUF Fe-binding, however. Fluorescence quenching studies via competition with the Fura-FF ligand may be a good choice for this application (see Chapter 3). The reported requirement for cysteine presents a potential complication for these studies, as cysteine is a substrate for the cysteine desulfurase enzyme.

6.4.5 Expanding ISC Studies to Other Organisms

This work utilized ISC proteins from yeast (*Saccharomyces cerevesiae*) and fly (*Drosophila melanogaster*) systems. Mixing and matching these proteins was essential to perform these experiments. For example, flscU is much more stable/soluble/active than yeast Isu1, but I have observed that *Drosophila* Nfs1-Isd11 is less stable/soluble/active than its yeast counterpart. Considering that the last common ancestor of flies and yeast lived ~1 billion years ago,²⁵⁹ there are probably many, many other organisms that demonstrate similar complementation between their ISC proteins and many ISC systems remain unexplored. For the purposes of this work, yeast Nfs1-Isd11, Yfh1, and flscU were sufficient but for more challenging methods such as crystallography, NMR, ITC, etc., there may be highly stable proteins found in other systems that could facilitate these methods.

REFERENCES

1. George, S. J.; Armstrong, F. A.; Hatchikian, E. C.; Thomson, A. J., Electrochemical and spectroscopic characterization of the conversion of the 7Fe into the 8Fe form of ferredoxin III from *Desulfovibrio africanus*. Identification of a [4Fe-4S] cluster with one non-cysteine ligand. *The Biochemical journal*. 1989; 264: 275-284.
2. Bertini, I.; Sigel, A.; Sigel, H., *Handbook on metalloproteins*. Marcel Dekker: New York, 2001; p xxvii, 1182 p.
3. Brown, E. N.; Friemann, R.; Karlsson, A.; Parales, J. V.; Couture, M. M.; Eltis, L. D.; Ramaswamy, S., Determining Rieske cluster reduction potentials. *Journal of biological inorganic chemistry : JBIC : a publication of the Society of Biological Inorganic Chemistry*. 2008; 13: 1301-1313.
4. Bak, D. W.; Elliott, S. J., Alternative FeS cluster ligands: tuning redox potentials and chemistry. *Current opinion in chemical biology*. 2014; 19: 50-58.
5. Jacobson, M. R.; Cash, V. L.; Weiss, M. C.; Laird, N. F.; Newton, W. E.; Dean, D. R., Biochemical and genetic analysis of the nifUSVWZM cluster from *Azotobacter vinelandii*. *Molecular & general genetics : MGG*. 1989; 219: 49-57.
6. Kispal, G.; Csere, P.; Prohl, C.; Lill, R., The mitochondrial proteins Atm1p and Nfs1p are essential for biogenesis of cytosolic Fe/S proteins. *The EMBO journal*. 1999; 18: 3981-3989.

7. Gerber, J.; Neumann, K.; Prohl, C.; Muhlenhoff, U.; Lill, R., The yeast scaffold proteins Isu1p and Isu2p are required inside mitochondria for maturation of cytosolic Fe/S proteins. *Molecular and cellular biology*. 2004; 24: 4848-4857.
8. Agar, J. N.; Krebs, C.; Frazzon, J.; Huynh, B. H.; Dean, D. R.; Johnson, M. K., IscU as a scaffold for iron-sulfur cluster biosynthesis: sequential assembly of [2Fe-2S] and [4Fe-4S] clusters in IscU. *Biochemistry*. 2000; 39: 7856-7862.
9. Urbina, H. D.; Silberg, J. J.; Hoff, K. G.; Vickery, L. E., Transfer of sulfur from IscS to IscU during Fe/S cluster assembly. *The Journal of biological chemistry*. 2001; 276: 44521-44526.
10. Wiedemann, N.; Urzica, E.; Guiard, B.; Muller, H.; Lohaus, C.; Meyer, H. E.; Ryan, M. T.; Meisinger, C.; Muhlenhoff, U.; Lill, R.; Pfanner, N., Essential role of Isd11 in mitochondrial iron-sulfur cluster synthesis on Isu scaffold proteins. *The EMBO journal*. 2006; 25: 184-195.
11. Webert, H.; Freibert, S. A.; Gallo, A.; Heidenreich, T.; Linne, U.; Amlacher, S.; Hurt, E.; Muhlenhoff, U.; Banci, L.; Lill, R., Functional reconstitution of mitochondrial Fe/S cluster synthesis on Isu1 reveals the involvement of ferredoxin. *Nature communications*. 2014; 5: 5013.
12. Yan, R.; Adinolfi, S.; Pastore, A., Ferredoxin, in conjunction with NADPH and ferredoxin-NADP reductase, transfers electrons to the IscS/IscU complex to promote iron-sulfur cluster assembly. *Biochimica et biophysica acta*. 2015.
13. Pandey, A.; Gordon, D. M.; Pain, J.; Stemmler, T. L.; Dancis, A.; Pain, D., Frataxin directly stimulates mitochondrial cysteine desulfurase by exposing substrate-binding sites, and a mutant Fe-S cluster scaffold protein with

- frataxin-bypassing ability acts similarly. *The Journal of biological chemistry*. 2013; 288: 36773-36786.
14. Krebs, C.; Agar, J. N.; Smith, A. D.; Frazzon, J.; Dean, D. R.; Huynh, B. H.; Johnson, M. K., IscA, an alternate scaffold for Fe-S cluster biosynthesis. *Biochemistry*. 2001; 40: 14069-14080.
 15. Tong, W. H.; Jameson, G. N.; Huynh, B. H.; Rouault, T. A., Subcellular compartmentalization of human Nfu, an iron-sulfur cluster scaffold protein, and its ability to assemble a [4Fe-4S] cluster. *Proceedings of the National Academy of Sciences of the United States of America*. 2003; 100: 9762-9767.
 16. Yoon, T.; Cowan, J. A., Iron-sulfur cluster biosynthesis. Characterization of frataxin as an iron donor for assembly of [2Fe-2S] clusters in ISU-type proteins. *Journal of the American Chemical Society*. 2003; 125: 6078-6084.
 17. Bencze, K. Z.; Kondapalli, K. C.; Cook, J. D.; McMahon, S.; Millan-Pacheco, C.; Pastor, N.; Stemmler, T. L., The structure and function of frataxin. *Critical reviews in biochemistry and molecular biology*. 2006; 41: 269-291.
 18. Kim, J. H.; Bothe, J. R.; Frederick, R. O.; Holder, J. C.; Markley, J. L., Role of IscX in iron-sulfur cluster biogenesis in *Escherichia coli*. *J Am Chem Soc*. 2014; 136: 7933-7942.
 19. Ding, H.; Harrison, K.; Lu, J., Thioredoxin reductase system mediates iron binding in IscA and iron delivery for the iron-sulfur cluster assembly in IscU. *The Journal of biological chemistry*. 2005; 280: 30432-30437.

20. Ding, H.; Clark, R. J.; Ding, B., IscA mediates iron delivery for assembly of iron-sulfur clusters in IscU under the limited accessible free iron conditions. *The Journal of biological chemistry*. 2004; 279: 37499-37504.
21. Yang, J.; Bitoun, J. P.; Ding, H., Interplay of IscA and IscU in biogenesis of iron-sulfur clusters. *The Journal of biological chemistry*. 2006; 281: 27956-27963.
22. Qi, W.; Cowan, J. A., Mechanism of glutaredoxin-ISU [2Fe-2S] cluster exchange. *Chemical communications*. 2011; 47: 4989-4991.
23. Muhlenhoff, U.; Gerber, J.; Richhardt, N.; Lill, R., Components involved in assembly and dislocation of iron-sulfur clusters on the scaffold protein Isu1p. *The EMBO journal*. 2003; 22: 4815-4825.
24. Mapolelo, D. T.; Zhang, B.; Randeniya, S.; Albetel, A. N.; Li, H.; Couturier, J.; Outten, C. E.; Rouhier, N.; Johnson, M. K., Monothiol glutaredoxins and A-type proteins: partners in Fe-S cluster trafficking. *Dalton transactions*. 2013; 42: 3107-3115.
25. Uzarska, M. A.; Dutkiewicz, R.; Freibert, S. A.; Lill, R.; Muhlenhoff, U., The mitochondrial Hsp70 chaperone Ssq1 facilitates Fe/S cluster transfer from Isu1 to Grx5 by complex formation. *Molecular biology of the cell*. 2013; 24: 1830-1841.
26. Hoff, K. G.; Silberg, J. J.; Vickery, L. E., Interaction of the iron-sulfur cluster assembly protein IscU with the Hsc66/Hsc20 molecular chaperone system of *Escherichia coli*. *Proceedings of the National Academy of Sciences of the United States of America*. 2000; 97: 7790-7795.

27. Bandyopadhyay, S.; Gama, F.; Molina-Navarro, M. M.; Gualberto, J. M.; Claxton, R.; Naik, S. G.; Huynh, B. H.; Herrero, E.; Jacquot, J. P.; Johnson, M. K.; Rouhier, N., Chloroplast monothiol glutaredoxins as scaffold proteins for the assembly and delivery of [2Fe-2S] clusters. *The EMBO journal*. 2008; 27: 1122-1133.
28. Rodriguez-Manzaneque, M. T.; Tamarit, J.; Belli, G.; Ros, J.; Herrero, E., Grx5 is a mitochondrial glutaredoxin required for the activity of iron/sulfur enzymes. *Molecular biology of the cell*. 2002; 13: 1109-1121.
29. Kim, K. D.; Chung, W. H.; Kim, H. J.; Lee, K. C.; Roe, J. H., Monothiol glutaredoxin Grx5 interacts with Fe-S scaffold proteins Isa1 and Isa2 and supports Fe-S assembly and DNA integrity in mitochondria of fission yeast. *Biochemical and biophysical research communications*. 2010; 392: 467-472.
30. Yeung, N.; Gold, B.; Liu, N. L.; Prathapam, R.; Sterling, H. J.; Willams, E. R.; Butland, G., The E. coli monothiol glutaredoxin GrxD forms homodimeric and heterodimeric FeS cluster containing complexes. *Biochemistry*. 2011; 50: 8957-8969.
31. Brancaccio, D.; Gallo, A.; Mikolajczyk, M.; Zovo, K.; Palumaa, P.; Novellino, E.; Piccioli, M.; Ciofi-Baffoni, S.; Banci, L., Formation of [4Fe-4S] clusters in the mitochondrial iron-sulfur cluster assembly machinery. *J Am Chem Soc*. 2014; 136: 16240-16250.
32. Rouault, T. A., Biogenesis of iron-sulfur clusters in mammalian cells: new insights and relevance to human disease. *Disease models & mechanisms*. 2012; 5: 155-164.

33. Rouault, T. A., Mammalian iron-sulphur proteins: novel insights into biogenesis and function. *Nature reviews. Molecular cell biology*. 2015; 16: 45-55.
34. Biederbick, A.; Stehling, O.; Rosser, R.; Niggemeyer, B.; Nakai, Y.; Elsasser, H. P.; Lill, R., Role of human mitochondrial Nfs1 in cytosolic iron-sulfur protein biogenesis and iron regulation. *Molecular and cellular biology*. 2006; 26: 5675-5687.
35. Sharma, A. K.; Pallesen, L. J.; Spang, R. J.; Walden, W. E., Cytosolic iron-sulfur cluster assembly (CIA) system: factors, mechanism, and relevance to cellular iron regulation. *The Journal of biological chemistry*. 2010; 285: 26745-26751.
36. Paul, V. D.; Lill, R., Biogenesis of cytosolic and nuclear iron-sulfur proteins and their role in genome stability. *Biochimica et biophysica acta*. 2015; 1853: 1528-1539.
37. Cavadini, P.; Biasiotto, G.; Poli, M.; Levi, S.; Verardi, R.; Zanella, I.; Derosas, M.; Ingrassia, R.; Corrado, M.; Arosio, P., RNA silencing of the mitochondrial ABCB7 transporter in HeLa cells causes an iron-deficient phenotype with mitochondrial iron overload. *Blood*. 2007; 109: 3552-3559.
38. Lange, H.; Lisowsky, T.; Gerber, J.; Muhlenhoff, U.; Kispal, G.; Lill, R., An essential function of the mitochondrial sulfhydryl oxidase Erv1p/ALR in the maturation of cytosolic Fe/S proteins. *EMBO reports*. 2001; 2: 715-720.
39. Netz, D. J.; Pierik, A. J.; Stumpfig, M.; Muhlenhoff, U.; Lill, R., The Cfd1-Nbp35 complex acts as a scaffold for iron-sulfur protein assembly in the yeast cytosol. *Nature chemical biology*. 2007; 3: 278-286.

40. Netz, D. J.; Stumpfig, M.; Dore, C.; Muhlenhoff, U.; Pierik, A. J.; Lill, R., Tah18 transfers electrons to Dre2 in cytosolic iron-sulfur protein biogenesis. *Nature chemical biology*. 2010; 6: 758-765.
41. Banci, L.; Bertini, I.; Calderone, V.; Ciofi-Baffoni, S.; Giachetti, A.; Jaiswal, D.; Mikolajczyk, M.; Piccioli, M.; Winkelmann, J., Molecular view of an electron transfer process essential for iron-sulfur protein biogenesis. *Proceedings of the National Academy of Sciences of the United States of America*. 2013; 110: 7136-7141.
42. Song, D.; Lee, F. S., Mouse knock-out of IOP1 protein reveals its essential role in mammalian cytosolic iron-sulfur protein biogenesis. *The Journal of biological chemistry*. 2011; 286: 15797-15805.
43. Song, D.; Lee, F. S., A role for IOP1 in mammalian cytosolic iron-sulfur protein biogenesis. *The Journal of biological chemistry*. 2008; 283: 9231-9238.
44. Stehling, O.; Mascarenhas, J.; Vashisht, A. A.; Sheftel, A. D.; Niggemeyer, B.; Rosser, R.; Pierik, A. J.; Wohlschlegel, J. A.; Lill, R., Human CIA2A-FAM96A and CIA2B-FAM96B integrate iron homeostasis and maturation of different subsets of cytosolic-nuclear iron-sulfur proteins. *Cell metabolism*. 2013; 18: 187-198.
45. Moller, S. G.; Kunkel, T.; Chua, N. H., A plastidic ABC protein involved in intercompartmental communication of light signaling. *Genes & development*. 2001; 15: 90-103.
46. Kumar, B.; Chaubey, S.; Shah, P.; Tanveer, A.; Charan, M.; Siddiqi, M. I.; Habib, S., Interaction between sulphur mobilisation proteins SufB and SufC:

- evidence for an iron-sulphur cluster biogenesis pathway in the apicoplast of *Plasmodium falciparum*. *International journal for parasitology*. 2011; 41: 991-999.
47. Tsaousis, A. D.; Gentekaki, E.; Eme, L.; Gaston, D.; Roger, A. J., Evolution of the cytosolic iron-sulfur cluster assembly machinery in Blastocystis species and other microbial eukaryotes. *Eukaryotic cell*. 2014; 13: 143-153.
 48. Tokumoto, U.; Kitamura, S.; Fukuyama, K.; Takahashi, Y., Interchangeability and distinct properties of bacterial Fe-S cluster assembly systems: functional replacement of the isc and suf operons in *Escherichia coli* with the nifSU-like operon from *Helicobacter pylori*. *Journal of biochemistry*. 2004; 136: 199-209.
 49. Takahashi, Y.; Tokumoto, U., A third bacterial system for the assembly of iron-sulfur clusters with homologs in archaea and plastids. *The Journal of biological chemistry*. 2002; 277: 28380-28383.
 50. Dai, Y.; Outten, F. W., The *E. coli* SufS-SufE sulfur transfer system is more resistant to oxidative stress than IscS-IscU. *FEBS letters*. 2012; 586: 4016-4022.
 51. Chahal, H. K.; Dai, Y.; Saini, A.; Ayala-Castro, C.; Outten, F. W., The SufBCD Fe-S scaffold complex interacts with SufA for Fe-S cluster transfer. *Biochemistry*. 2009; 48: 10644-10653.
 52. Saini, A.; Mapolelo, D. T.; Chahal, H. K.; Johnson, M. K.; Outten, F. W., SufD and SufC ATPase activity are required for iron acquisition during in vivo Fe-S cluster formation on SufB. *Biochemistry*. 2010; 49: 9402-9412.

53. Wollers, S.; Layer, G.; Garcia-Serres, R.; Signor, L.; Clemancey, M.; Latour, J. M.; Fontecave, M.; Ollagnier de Choudens, S., Iron-sulfur (Fe-S) cluster assembly: the SufBCD complex is a new type of Fe-S scaffold with a flavin redox cofactor. *The Journal of biological chemistry*. 2010; 285: 23331-23341.
54. Chahal, H. K.; Outten, F. W., Separate FeS scaffold and carrier functions for SufB(2)C(2) and SufA during in vitro maturation of [2Fe2S] Fdx. *Journal of inorganic biochemistry*. 2012; 116: 126-134.
55. Loiseau, L.; Ollagnier-de-Choudens, S.; Nachin, L.; Fontecave, M.; Barras, F., Biogenesis of Fe-S cluster by the bacterial Suf system: SufS and SufE form a new type of cysteine desulfurase. *The Journal of biological chemistry*. 2003; 278: 38352-38359.
56. Ollagnier-de-Choudens, S.; Lascoux, D.; Loiseau, L.; Barras, F.; Forest, E.; Fontecave, M., Mechanistic studies of the SufS-SufE cysteine desulfurase: evidence for sulfur transfer from SufS to SufE. *FEBS letters*. 2003; 555: 263-267.
57. Lu, J.; Yang, J.; Tan, G.; Ding, H., Complementary roles of SufA and IscA in the biogenesis of iron-sulfur clusters in Escherichia coli. *The Biochemical journal*. 2008; 409: 535-543.
58. Gupta, V.; Sendra, M.; Naik, S. G.; Chahal, H. K.; Huynh, B. H.; Outten, F. W.; Fontecave, M.; Ollagnier de Choudens, S., Native Escherichia coli SufA, coexpressed with SufBCDSE, purifies as a [2Fe-2S] protein and acts as an Fe-S transporter to Fe-S target enzymes. *J Am Chem Soc*. 2009; 131: 6149-6153.

59. Tan, G.; Lu, J.; Bitoun, J. P.; Huang, H.; Ding, H., IscA/SufA paralogues are required for the [4Fe-4S] cluster assembly in enzymes of multiple physiological pathways in *Escherichia coli* under aerobic growth conditions. *The Biochemical journal*. 2009; 420: 463-472.
60. Pinske, C.; Sawers, R. G., A-type carrier protein ErpA is essential for formation of an active formate-nitrate respiratory pathway in *Escherichia coli* K-12. *Journal of bacteriology*. 2012; 194: 346-353.
61. Roche, B.; Aussel, L.; Ezraty, B.; Mandin, P.; Py, B.; Barras, F., Iron/sulfur proteins biogenesis in prokaryotes: formation, regulation and diversity. *Biochimica et biophysica acta*. 2013; 1827: 455-469.
62. Lill, R., Function and biogenesis of iron-sulphur proteins. *Nature*. 2009; 460: 831-838.
63. Blanc, B.; Clemancey, M.; Latour, J. M.; Fontecave, M.; Ollagnier de Choudens, S., Molecular investigation of iron-sulfur cluster assembly scaffolds under stress. *Biochemistry*. 2014; 53: 7867-7869.
64. Fleischhacker, A. S.; Stubna, A.; Hsueh, K. L.; Guo, Y.; Teter, S. J.; Rose, J. C.; Brunold, T. C.; Markley, J. L.; Munck, E.; Kiley, P. J., Characterization of the [2Fe-2S] cluster of *Escherichia coli* transcription factor IscR. *Biochemistry*. 2012; 51: 4453-4462.
65. Rajagopalan, S.; Teter, S. J.; Zwart, P. H.; Brennan, R. G.; Phillips, K. J.; Kiley, P. J., Studies of IscR reveal a unique mechanism for metal-dependent regulation of DNA binding specificity. *Nature structural & molecular biology*. 2013; 20: 740-747.

66. Schwartz, C. J.; Giel, J. L.; Patschkowski, T.; Luther, C.; Ruzicka, F. J.; Beinert, H.; Kiley, P. J., IscR, an Fe-S cluster-containing transcription factor, represses expression of *Escherichia coli* genes encoding Fe-S cluster assembly proteins. *Proceedings of the National Academy of Sciences of the United States of America*. 2001; 98: 14895-14900.
67. Vinella, D.; Loiseau, L.; Ollagnier de Choudens, S.; Fontecave, M.; Barras, F., In vivo [Fe-S] cluster acquisition by IscR and NsrR, two stress regulators in *Escherichia coli*. *Molecular microbiology*. 2013; 87: 493-508.
68. Crack, J. C.; Green, J.; Hutchings, M. I.; Thomson, A. J.; Le Brun, N. E., Bacterial iron-sulfur regulatory proteins as biological sensor-switches. *Antioxidants & redox signaling*. 2012; 17: 1215-1231.
69. Yeo, W. S.; Lee, J. H.; Lee, K. C.; Roe, J. H., IscR acts as an activator in response to oxidative stress for the suf operon encoding Fe-S assembly proteins. *Molecular microbiology*. 2006; 61: 206-218.
70. Lee, K. C.; Yeo, W. S.; Roe, J. H., Oxidant-responsive induction of the suf operon, encoding a Fe-S assembly system, through Fur and IscR in *Escherichia coli*. *Journal of bacteriology*. 2008; 190: 8244-8247.
71. Desnoyers, G.; Morissette, A.; Prevost, K.; Masse, E., Small RNA-induced differential degradation of the polycistronic mRNA iscRSUA. *The EMBO journal*. 2009; 28: 1551-1561.
72. Masse, E.; Vanderpool, C. K.; Gottesman, S., Effect of RyhB small RNA on global iron use in *Escherichia coli*. *Journal of bacteriology*. 2005; 187: 6962-6971.

73. Johnson, D. C.; Dean, D. R.; Smith, A. D.; Johnson, M. K., Structure, function, and formation of biological iron-sulfur clusters. *Annual review of biochemistry*. 2005; 74: 247-281.
74. Carter, C. W., Jr.; Kraut, J.; Freer, S. T.; Alden, R. A.; Sieker, L. C.; Adman, E.; Jensen, L. H., A comparison of Fe₄S₄ clusters in high-potential iron protein and in ferredoxin. *Proceedings of the National Academy of Sciences of the United States of America*. 1972; 69: 3526-3529.
75. Sticht, H.; Rosch, P., The structure of iron-sulfur proteins. *Progress in biophysics and molecular biology*. 1998; 70: 95-136.
76. Lange, H.; Kaut, A.; Kispal, G.; Lill, R., A mitochondrial ferredoxin is essential for biogenesis of cellular iron-sulfur proteins. *Proceedings of the National Academy of Sciences of the United States of America*. 2000; 97: 1050-1055.
77. Vinothkumar, K. R.; Zhu, J.; Hirst, J., Architecture of mammalian respiratory complex I. *Nature*. 2014; 515: 80-84.
78. Janssen, S.; Schafer, G.; Anemuller, S.; Moll, R., A succinate dehydrogenase with novel structure and properties from the hyperthermophilic archaeon *Sulfolobus acidocaldarius*: genetic and biophysical characterization. *Journal of bacteriology*. 1997; 179: 5560-5569.
79. Silman, H. I.; Rieske, J. S.; Lipton, S. H.; Baum, H., A new protein component of complex 3 of the mitochondrial electron transfer chain. *The Journal of biological chemistry*. 1967; 242: 4867-4875.
80. Shergill, J. K.; Joannou, C. L.; Mason, J. R.; Cammack, R., Coordination of the Rieske-type [2Fe-2S] cluster of the terminal iron-sulfur protein of

- Pseudomonas putida* benzene 1,2-dioxygenase, studied by one- and two-dimensional electron spin-echo envelope modulation spectroscopy. *Biochemistry*. 1995; 34: 16533-16542.
81. Switzer, R. L., Non-redox roles for iron-sulfur clusters in enzymes. *BioFactors*. 1989; 2: 77-86.
82. Kuo, C. F.; McRee, D. E.; Fisher, C. L.; O'Handley, S. F.; Cunningham, R. P.; Tainer, J. A., Atomic structure of the DNA repair [4Fe-4S] enzyme endonuclease III. *Science*. 1992; 258: 434-440.
83. Leone, M.; Brignolio, F.; Rosso, M. G.; Curtioni, E. S.; Moroni, A.; Tribolo, A.; Schiffer, D., Friedreich's ataxia: a descriptive epidemiological study in an Italian population. *Clinical genetics*. 1990; 38: 161-169.
84. Lopez-Arlandis, J. M.; Vilchez, J. J.; Palau, F.; Sevilla, T., Friedreich's ataxia: an epidemiological study in Valencia, Spain, based on consanguinity analysis. *Neuroepidemiology*. 1995; 14: 14-19.
85. Lodi, R.; Tonon, C.; Calabrese, V.; Schapira, A. H., Friedreich's ataxia: from disease mechanisms to therapeutic interventions. *Antioxidants & redox signaling*. 2006; 8: 438-443.
86. Campuzano, V.; Montermini, L.; Molto, M. D.; Pianese, L.; Cossee, M.; Cavalcanti, F.; Monros, E.; Rodius, F.; Duclos, F.; Monticelli, A.; Zara, F.; Canizares, J.; Koutnikova, H.; Bidichandani, S. I.; Gellera, C.; Brice, A.; Trouillas, P.; De Michele, G.; Filla, A.; De Frutos, R.; Palau, F.; Patel, P. I.; Di Donato, S.; Mandel, J. L.; Coccozza, S.; Koenig, M.; Pandolfo, M., Friedreich's ataxia:

- autosomal recessive disease caused by an intronic GAA triplet repeat expansion. *Science*. 1996; 271: 1423-1427.
87. Ohshima, K.; Montermini, L.; Wells, R. D.; Pandolfo, M., Inhibitory effects of expanded GAA.TTC triplet repeats from intron I of the Friedreich ataxia gene on transcription and replication in vivo. *The Journal of biological chemistry*. 1998; 273: 14588-14595.
88. Pastore, A.; Puccio, H., Frataxin: a protein in search for a function. *Journal of neurochemistry*. 2013; 126 Suppl 1: 43-52.
89. Stemmler, T. L.; Lesuisse, E.; Pain, D.; Dancis, A., Frataxin and mitochondrial FeS cluster biogenesis. *The Journal of biological chemistry*. 2010; 285: 26737-26743.
90. Whitnall, M.; Suryo Rahmanto, Y.; Huang, M. L.; Saletta, F.; Lok, H. C.; Gutierrez, L.; Lazaro, F. J.; Fleming, A. J.; St Pierre, T. G.; Mikhael, M. R.; Ponka, P.; Richardson, D. R., Identification of nonferritin mitochondrial iron deposits in a mouse model of Friedreich ataxia. *Proceedings of the National Academy of Sciences of the United States of America*. 2012; 109: 20590-20595.
91. Delatycki, M. B.; Corben, L. A., Clinical features of Friedreich ataxia. *Journal of child neurology*. 2012; 27: 1133-1137.
92. Tsou, A. Y.; Paulsen, E. K.; Lagedrost, S. J.; Perlman, S. L.; Mathews, K. D.; Wilmot, G. R.; Ravina, B.; Koeppen, A. H.; Lynch, D. R., Mortality in Friedreich ataxia. *J Neurol Sci*. 2011; 307: 46-49.
93. Crooks, D. R.; Jeong, S. Y.; Tong, W. H.; Ghosh, M. C.; Olivierre, H.; Haller, R. G.; Rouault, T. A., Tissue specificity of a human mitochondrial disease:

- differentiation-enhanced mis-splicing of the Fe-S scaffold gene ISCU renders patient cells more sensitive to oxidative stress in ISCU myopathy. *The Journal of biological chemistry*. 2012; 287: 40119-40130.
94. Mochel, F.; Knight, M. A.; Tong, W. H.; Hernandez, D.; Ayyad, K.; Taivassalo, T.; Andersen, P. M.; Singleton, A.; Rouault, T. A.; Fischbeck, K. H.; Haller, R. G., Splice mutation in the iron-sulfur cluster scaffold protein ISCU causes myopathy with exercise intolerance. *American journal of human genetics*. 2008; 82: 652-660.
95. Kollberg, G.; Melberg, A.; Holme, E.; Oldfors, A., Transient restoration of succinate dehydrogenase activity after rhabdomyolysis in iron-sulphur cluster deficiency myopathy. *Neuromuscular disorders : NMD*. 2011; 21: 115-120.
96. Mochel, F.; Haller, R. G., Myopathy with Deficiency of ISCU. In *GeneReviews(R)*, Pagon, R. A.; Adam, M. P.; Ardinger, H. H.; Wallace, S. E.; Amemiya, A.; Bean, L. J. H.; Bird, T. D.; Dolan, C. R.; Fong, C. T.; Smith, R. J. H.; Stephens, K., Eds. Seattle (WA), 1993.
97. Kollberg, G.; Tulinius, M.; Melberg, A.; Darin, N.; Andersen, O.; Holmgren, D.; Oldfors, A.; Holme, E., Clinical manifestation and a new ISCU mutation in iron-sulphur cluster deficiency myopathy. *Brain : a journal of neurology*. 2009; 132: 2170-2179.
98. Ye, H.; Jeong, S. Y.; Ghosh, M. C.; Kovtunovych, G.; Silvestri, L.; Ortillo, D.; Uchida, N.; Tisdale, J.; Camaschella, C.; Rouault, T. A., Glutaredoxin 5 deficiency causes sideroblastic anemia by specifically impairing heme

- biosynthesis and depleting cytosolic iron in human erythroblasts. *The Journal of clinical investigation*. 2010; 120: 1749-1761.
99. Wingert, R. A.; Galloway, J. L.; Barut, B.; Foott, H.; Fraenkel, P.; Axe, J. L.; Weber, G. J.; Dooley, K.; Davidson, A. J.; Schmid, B.; Paw, B. H.; Shaw, G. C.; Kingsley, P.; Palis, J.; Schubert, H.; Chen, O.; Kaplan, J.; Zon, L. I.; Tübingen Screen, C., Deficiency of glutaredoxin 5 reveals Fe-S clusters are required for vertebrate haem synthesis. *Nature*. 2005; 436: 1035-1039.
100. Wilkinson, N.; Pantopoulos, K., The IRP/IRE system in vivo: insights from mouse models. *Frontiers in pharmacology*. 2014; 5: 176.
101. Benn, D. E.; Robinson, B. G.; Clifton-Bligh, R. J., 15 YEARS OF PARAGANGLIOMA: Clinical manifestations of paraganglioma syndromes types 1-5. *Endocrine-related cancer*. 2015; 22: T91-T103.
102. Na, U.; Yu, W.; Cox, J.; Bricker, D. K.; Brockmann, K.; Rutter, J.; Thummel, C. S.; Winge, D. R., The LYR factors SDHAF1 and SDHAF3 mediate maturation of the iron-sulfur subunit of succinate dehydrogenase. *Cell metabolism*. 2014; 20: 253-266.
103. Ghezzi, D.; Goffrini, P.; Uziel, G.; Horvath, R.; Klopstock, T.; Lochmüller, H.; D'Adamo, P.; Gasparini, P.; Strom, T. M.; Prokisch, H.; Invernizzi, F.; Ferrero, I.; Zeviani, M., SDHAF1, encoding a LYR complex-II specific assembly factor, is mutated in SDH-defective infantile leukoencephalopathy. *Nat Genet*. 2009; 41: 654-656.
104. Cameron, J. M.; Janer, A.; Levandovskiy, V.; Mackay, N.; Rouault, T. A.; Tong, W. H.; Ogilvie, I.; Shoubridge, E. A.; Robinson, B. H., Mutations in iron-sulfur

- cluster scaffold genes NFU1 and BOLA3 cause a fatal deficiency of multiple respiratory chain and 2-oxoacid dehydrogenase enzymes. *American journal of human genetics*. 2011; 89: 486-495.
105. Agar, J. N.; Krebs, C.; Frazzon, J.; Huynh, B. H.; Dean, D. R.; Johnson, M. K., IscU as a scaffold for iron-sulfur cluster biosynthesis: sequential assembly of [2Fe-2S] and [4Fe-4S] clusters in IscU. *Biochemistry*. 2000; 39: 7856-7862.
106. Lill, R., Function and biogenesis of iron-sulphur proteins. *Nature*. 2009; 460: 831-838.
107. Muhlenhoff, U.; Gerber, J.; Richhardt, N.; Lill, R., Components involved in assembly and dislocation of iron-sulfur clusters on the scaffold protein Isu1p. *EMBO J*. 2003; 22: 4815-4825.
108. Muhlenhoff, U.; Balk, J.; Richhardt, N.; Kaiser, J. T.; Sipos, K.; Kispal, G.; Lill, R., Functional characterization of the eukaryotic cysteine desulfurase Nfs1p from *Saccharomyces cerevisiae*. *J Biol Chem*. 2004; 279: 36906-36915.
109. Adam, A. C.; Bornhovd, C.; Prokisch, H.; Neupert, W.; Hell, K., The Nfs1 interacting protein Isd11 has an essential role in Fe/S cluster biogenesis in mitochondria. *EMBO J*. 2006; 25: 174-183.
110. Webert, H.; Freibert, S. A.; Gallo, A.; Heidenreich, T.; Linne, U.; Amlacher, S.; Hurt, E.; Muhlenhoff, U.; Banci, L.; Lill, R., Functional reconstitution of mitochondrial Fe/S cluster synthesis on Isu1 reveals the involvement of ferredoxin. *Nat Commun*. 2014; 5: 5013.

111. Fox, N. G.; Das, D.; Chakrabarti, M.; Lindahl, P. A.; Barondeau, D. P., Frataxin Accelerates [2Fe-2S] Cluster Formation on the Human Fe-S Assembly Complex. *Biochemistry*. 2015; 54: 3880-3889.
112. Bridwell-Rabb, J.; Iannuzzi, C.; Pastore, A.; Barondeau, D. P., Effector role reversal during evolution: the case of frataxin in Fe-S cluster biosynthesis. *Biochemistry*. 2012; 51: 2506-2514.
113. Pandey, A.; Gordon, D. M.; Pain, J.; Stemmler, T. L.; Dancis, A.; Pain, D., Frataxin directly stimulates mitochondrial cysteine desulfurase by exposing substrate-binding sites, and a mutant Fe-S cluster scaffold protein with frataxin-bypassing ability acts similarly. *J Biol Chem*. 2013; 288: 36773-36786.
114. Qi, W.; Cowan, J. A., A structural and functional homolog supports a general role for frataxin in cellular iron chemistry. *Chem Commun (Camb)*. 2010; 46: 719-721.
115. Cook, J. D.; Kondapalli, K. C.; Rawat, S.; Childs, W. C.; Murugesan, Y.; Dancis, A.; Stemmler, T. L., Molecular details of the yeast frataxin-Isu1 interaction during mitochondrial Fe-S cluster assembly. *Biochemistry*. 2010; 49: 8756-8765.
116. Schagerlof, U.; Elmlund, H.; Gakh, O.; Nordlund, G.; Hebert, H.; Lindahl, M.; Isaya, G.; Al-Karadaghi, S., Structural basis of the iron storage function of frataxin from single-particle reconstruction of the iron-loaded oligomer. *Biochemistry*. 2008; 47: 4948-4954.

117. Dutkiewicz, R.; Marszalek, J.; Schilke, B.; Craig, E. A.; Lill, R.; Muhlenhoff, U., The Hsp70 chaperone Ssq1p is dispensable for iron-sulfur cluster formation on the scaffold protein Isu1p. *J Biol Chem.* 2006; 281: 7801-7808.
118. Tsai, C. L.; Barondeau, D. P., Human frataxin is an allosteric switch that activates the Fe-S cluster biosynthetic complex. *Biochemistry.* 2010; 49: 9132-9139.
119. Bridwell-Rabb, J.; Fox, N. G.; Tsai, C. L.; Winn, A. M.; Barondeau, D. P., Human frataxin activates Fe-S cluster biosynthesis by facilitating sulfur transfer chemistry. *Biochemistry.* 2014; 53: 4904-4913.
120. Kondapalli, K. C.; Kok, N. M.; Dancis, A.; Stemmler, T. L., Drosophila frataxin: an iron chaperone during cellular Fe-S cluster bioassembly. *Biochemistry.* 2008; 47: 6917-6927.
121. Stephens, P. J.; Thomson, A. J.; Dunn, J. B.; Keiderling, T. A.; Rawlings, J.; Rao, K. K.; Hall, D. O., Circular dichroism and magnetic circular dichroism of iron-sulfur proteins. *Biochemistry.* 1978; 17: 4770-4778.
122. Qi, W.; Cowan, J. A., Structural, Mechanistic and Coordination Chemistry of Relevance to the Biosynthesis of Iron-Sulfur and Related Iron Cofactors. *Coord Chem Rev.* 2011; 255: 688-699.
123. Sticht, H.; Rosch, P., The structure of iron-sulfur proteins. *Prog Biophys Mol Biol.* 1998; 70: 95-136.
124. Huang, J.; Cowan, J. A., Iron-sulfur cluster biosynthesis: role of a semi-conserved histidine. *Chem Commun (Camb).* 2009: 3071-3073.

125. Fox, N. G.; Chakrabarti, M.; McCormick, S. P.; Lindahl, P. A.; Barondeau, D. P., The Human Iron-Sulfur Assembly Complex Catalyzes the Synthesis of [2Fe-2S] Clusters on ISCU2 That Can Be Transferred to Acceptor Molecules. *Biochemistry*. 2015; 54: 3871-3879.
126. Di Stasio, E.; Bizzarri, P.; Bove, M.; Casato, M.; Giardina, B.; Fiorilli, M.; Galtieri, A.; Pucillo, L. P., Analysis of the dynamics of cryoaggregation by light-scattering spectrometry. *Clin Chem Lab Med*. 2003; 41: 152-158.
127. Uzarska, M. A.; Dutkiewicz, R.; Freibert, S. A.; Lill, R.; Muhlenhoff, U., The mitochondrial Hsp70 chaperone Ssq1 facilitates Fe/S cluster transfer from Isu1 to Grx5 by complex formation. *Mol Biol Cell*. 2013; 24: 1830-1841.
128. Kim, J. H.; Tonelli, M.; Markley, J. L., Disordered form of the scaffold protein IscU is the substrate for iron-sulfur cluster assembly on cysteine desulfurase. *Proc Natl Acad Sci U S A*. 2012; 109: 454-459.
129. Campuzano, V.; Montermini, L.; Molto, M. D.; Pianese, L.; Cossee, M.; Cavalcanti, F.; Monros, E.; Rodius, F.; Duclos, F.; Monticelli, A.; Zara, F.; Canizares, J.; Koutnikova, H.; Bidichandani, S. I.; Gellera, C.; Brice, A.; Trouillas, P.; De Michele, G.; Filla, A.; De Frutos, R.; Palau, F.; Patel, P. I.; Di Donato, S.; Mandel, J. L.; Coccozza, S.; Koenig, M.; Pandolfo, M., Friedreich's ataxia: autosomal recessive disease caused by an intronic GAA triplet repeat expansion. *Science*. 1996; 271: 1423-1427.
130. Lodi, R.; Tonon, C.; Calabrese, V.; Schapira, A. H., Friedreich's ataxia: from disease mechanisms to therapeutic interventions. *Antioxidants & redox signaling*. 2006; 8: 438-443.

131. Mochel, F.; Haller, R. G., Myopathy with Deficiency of ISCU. In *GeneReviews(R)*, Pagon, R. A.; Adam, M. P.; Ardinger, H. H.; Wallace, S. E.; Amemiya, A.; Bean, L. J. H.; Bird, T. D.; Dolan, C. R.; Fong, C. T.; Smith, R. J. H.; Stephens, K., Eds. Seattle (WA), 1993.
132. Mochel, F.; Knight, M. A.; Tong, W. H.; Hernandez, D.; Ayyad, K.; Taivassalo, T.; Andersen, P. M.; Singleton, A.; Rouault, T. A.; Fischbeck, K. H.; Haller, R. G., Splice mutation in the iron-sulfur cluster scaffold protein ISCU causes myopathy with exercise intolerance. *American journal of human genetics*. 2008; 82: 652-660.
133. Lill, R.; Srinivasan, V.; Muhlenhoff, U., The role of mitochondria in cytosolic-nuclear iron-sulfur protein biogenesis and in cellular iron regulation. *Current opinion in microbiology*. 2014; 22: 111-119.
134. Lill, R., Function and biogenesis of iron-sulphur proteins. *Nature*. 2009; 460: 831-838.
135. Agar, J. N.; Krebs, C.; Frazzon, J.; Huynh, B. H.; Dean, D. R.; Johnson, M. K., IscU as a scaffold for iron-sulfur cluster biosynthesis: sequential assembly of [2Fe-2S] and [4Fe-4S] clusters in IscU. *Biochemistry*. 2000; 39: 7856-7862.
136. Gerber, J.; Neumann, K.; Prohl, C.; Muhlenhoff, U.; Lill, R., The yeast scaffold proteins Isu1p and Isu2p are required inside mitochondria for maturation of cytosolic Fe/S proteins. *Molecular and cellular biology*. 2004; 24: 4848-4857.
137. Urbina, H. D.; Silberg, J. J.; Hoff, K. G.; Vickery, L. E., Transfer of sulfur from IscS to IscU during Fe/S cluster assembly. *The Journal of biological chemistry*. 2001; 276: 44521-44526.

138. Wiedemann, N.; Urzica, E.; Guiard, B.; Muller, H.; Lohaus, C.; Meyer, H. E.; Ryan, M. T.; Meisinger, C.; Muhlenhoff, U.; Lill, R.; Pfanner, N., Essential role of Isd11 in mitochondrial iron-sulfur cluster synthesis on Isu scaffold proteins. *The EMBO journal*. 2006; 25: 184-195.
139. Webert, H.; Freibert, S. A.; Gallo, A.; Heidenreich, T.; Linne, U.; Amlacher, S.; Hurt, E.; Muhlenhoff, U.; Banci, L.; Lill, R., Functional reconstitution of mitochondrial Fe/S cluster synthesis on Isu1 reveals the involvement of ferredoxin. *Nature communications*. 2014; 5: 5013.
140. Bridwell-Rabb, J.; Fox, N. G.; Tsai, C. L.; Winn, A. M.; Barondeau, D. P., Human frataxin activates Fe-S cluster biosynthesis by facilitating sulfur transfer chemistry. *Biochemistry*. 2014; 53: 4904-4913.
141. Pandey, A.; Gordon, D. M.; Pain, J.; Stemmler, T. L.; Dancis, A.; Pain, D., Frataxin directly stimulates mitochondrial cysteine desulfurase by exposing substrate-binding sites, and a mutant Fe-S cluster scaffold protein with frataxin-bypassing ability acts similarly. *The Journal of biological chemistry*. 2013; 288: 36773-36786.
142. Cook, J. D.; Kondapalli, K. C.; Rawat, S.; Childs, W. C.; Murugesan, Y.; Dancis, A.; Stemmler, T. L., Molecular details of the yeast frataxin-Isu1 interaction during mitochondrial Fe-S cluster assembly. *Biochemistry*. 2010; 49: 8756-8765.
143. Kondapalli, K. C.; Kok, N. M.; Dancis, A.; Stemmler, T. L., Drosophila frataxin: an iron chaperone during cellular Fe-S cluster bioassembly. *Biochemistry*. 2008; 47: 6917-6927.

144. Bridwell-Rabb, J.; Iannuzzi, C.; Pastore, A.; Barondeau, D. P., Effector role reversal during evolution: the case of frataxin in Fe-S cluster biosynthesis. *Biochemistry*. 2012; 51: 2506-2514.
145. Tan, S., A modular polycistronic expression system for overexpressing protein complexes in *Escherichia coli*. *Protein expression and purification*. 2001; 21: 224-234.
146. Kleber-Janke, T.; Becker, W. M., Use of modified BL21(DE3) *Escherichia coli* cells for high-level expression of recombinant peanut allergens affected by poor codon usage. *Protein expression and purification*. 2000; 19: 419-424.
147. Studier, F. W., Protein production by auto-induction in high density shaking cultures. *Protein expression and purification*. 2005; 41: 207-234.
148. Strug, I.; Utzat, C.; Cappione, A., 3rd; Gutierrez, S.; Amara, R.; Lento, J.; Capito, F.; Skudas, R.; Chernokalskaya, E.; Nadler, T., Development of a univariate membrane-based mid-infrared method for protein quantitation and total lipid content analysis of biological samples. *Journal of analytical methods in chemistry*. 2014; 2014: 657079.
149. Sreerama, N.; Woody, R. W., Estimation of protein secondary structure from circular dichroism spectra: comparison of CONTIN, SELCON, and CDSSTR methods with an expanded reference set. *Analytical biochemistry*. 2000; 287: 252-260.
150. Johnson, W. C., Analyzing protein circular dichroism spectra for accurate secondary structures. *Proteins*. 1999; 35: 307-312.

151. Provencher, S. W.; Glockner, J., Estimation of globular protein secondary structure from circular dichroism. *Biochemistry*. 1981; 20: 33-37.
152. Rodrigues, A. V.; Kandegedara, A.; Rotondo, J. A.; Dancis, A.; Stemmler, T. L., Iron loading site on the Fe-S cluster assembly scaffold protein is distinct from the active site. *Biometals : an international journal on the role of metal ions in biology, biochemistry, and medicine*. 2015; 28: 567-576.
153. Kuzmic, P., DynaFit--a software package for enzymology. *Methods in enzymology*. 2009; 467: 247-280.
154. George, G. N.; George, S. J.; Pickering, I. J. EXAFSPAK, <http://www-ssrl.slac.stanford.edu/~george/exafspak/exafs.htm>: Menlo Park, CA, 2001.
155. Cook, J. D.; Bencze, K. Z.; Jankovic, A. D.; Crater, A. K.; Busch, C. N.; Bradley, P. B.; Stemmler, A. J.; Spaller, M. R.; Stemmler, T. L., Monomeric yeast frataxin is an iron-binding protein. *Biochemistry*. 2006; 45: 7767-7777.
156. George, G. N.; Hedman, B.; Hodgson, K. O., An edge with XAS. *Nature structural biology*. 1998; 5 Suppl: 645-647.
157. Cotelesage, J. J.; Pushie, M. J.; Grochulski, P.; Pickering, I. J.; George, G. N., Metalloprotein active site structure determination: synergy between X-ray absorption spectroscopy and X-ray crystallography. *Journal of inorganic biochemistry*. 2012; 115: 127-137.
158. Fox, N. G.; Chakrabarti, M.; McCormick, S. P.; Lindahl, P. A.; Barondeau, D. P., The Human Iron-Sulfur Assembly Complex Catalyzes the Synthesis of [2Fe-2S] Clusters on ISCU2 That Can Be Transferred to Acceptor Molecules. *Biochemistry*. 2015; 54: 3871-3879.

159. Stephens, P. J.; Thomson, A. J.; Dunn, J. B.; Keiderling, T. A.; Rawlings, J.; Rao, K. K.; Hall, D. O., Circular dichroism and magnetic circular dichroism of iron-sulfur proteins. *Biochemistry*. 1978; 17: 4770-4778.
160. Yoon, H.; Knight, S. A.; Pandey, A.; Pain, J.; Turkarslan, S.; Pain, D.; Dancis, A., Turning *Saccharomyces cerevisiae* into a Frataxin-Independent Organism. *PLoS genetics*. 2015; 11: e1005135.
161. Seguin, A.; Santos, R.; Pain, D.; Dancis, A.; Camadro, J. M.; Lesuisse, E., Co-precipitation of phosphate and iron limits mitochondrial phosphate availability in *Saccharomyces cerevisiae* lacking the yeast frataxin homologue (YFH1). *The Journal of biological chemistry*. 2011; 286: 6071-6079.
162. Shimomura, Y.; Kamikubo, H.; Nishi, Y.; Masako, T.; Kataoka, M.; Kobayashi, Y.; Fukuyama, K.; Takahashi, Y., Characterization and crystallization of an IscU-type scaffold protein with bound [2Fe-2S] cluster from the hyperthermophile, *aquifex aeolicus*. *Journal of biochemistry*. 2007; 142: 577-586.
163. Kim, J. H.; Tonelli, M.; Kim, T.; Markley, J. L., Three-dimensional structure and determinants of stability of the iron-sulfur cluster scaffold protein IscU from *Escherichia coli*. *Biochemistry*. 2012; 51: 5557-5563.
164. Randall, C. R.; Zang, Y.; True, A. E.; Que, L., Jr.; Charnock, J. M.; Garner, C. D.; Fujishima, Y.; Schofield, C. J.; Baldwin, J. E., X-ray absorption studies of the ferrous active site of isopenicillin N synthase and related model complexes. *Biochemistry*. 1993; 32: 6664-6673.

165. Chen, C. J.; Lin, Y. H.; Huang, Y. C.; Liu, M. Y., Crystal structure of rubredoxin from *Desulfovibrio gigas* to ultra-high 0.68 Å resolution. *Biochemical and biophysical research communications*. 2006; 349: 79-90.
166. Mena, N. P.; Bulteau, A. L.; Salazar, J.; Hirsch, E. C.; Nunez, M. T., Effect of mitochondrial complex I inhibition on Fe-S cluster protein activity. *Biochemical and biophysical research communications*. 2011; 409: 241-246.
167. Colpas, G. J.; Maroney, M. J.; Bagyinka, C.; Kumar, M.; Willis, W. S.; Suib, S. L.; Baidya, N.; Mascharak, P. K., X-ray Spectroscopic Studies of Nickel Complexes, with Application to the Structure of Nickel Sites in Hydrogenases. *Inorganic chemistry*. 1991; 30: 920-928.
168. Dutkiewicz, R.; Marszalek, J.; Schilke, B.; Craig, E. A.; Lill, R.; Muhlenhoff, U., The Hsp70 chaperone Ssq1p is dispensable for iron-sulfur cluster formation on the scaffold protein Isu1p. *The Journal of biological chemistry*. 2006; 281: 7801-7808.
169. Muhlenhoff, U.; Hoffmann, B.; Richter, N.; Rietzschel, N.; Spantgar, F.; Stehling, O.; Uzarska, M. A.; Lill, R., Compartmentalization of iron between mitochondria and the cytosol and its regulation. *European journal of cell biology*. 2015; 94: 292-308.
170. Li, J.; Kogan, M.; Knight, S. A.; Pain, D.; Dancis, A., Yeast mitochondrial protein, Nfs1p, coordinately regulates iron-sulfur cluster proteins, cellular iron uptake, and iron distribution. *The Journal of biological chemistry*. 1999; 274: 33025-33034.

171. Qi, W.; Cowan, J. A., Structural, Mechanistic and Coordination Chemistry of Relevance to the Biosynthesis of Iron-Sulfur and Related Iron Cofactors. *Coordination chemistry reviews*. 2011; 255: 688-699.
172. Sazinsky, M. H.; LeMoine, B.; Orofino, M.; Davydov, R.; Bencze, K. Z.; Stemmler, T. L.; Hoffman, B. M.; Arguello, J. M.; Rosenzweig, A. C., Characterization and structure of a Zn²⁺ and [2Fe-2S]-containing copper chaperone from *Archaeoglobus fulgidus*. *The Journal of biological chemistry*. 2007; 282: 25950-25959.
173. Traverso, M. E.; Subramanian, P.; Davydov, R.; Hoffman, B. M.; Stemmler, T. L.; Rosenzweig, A. C., Identification of a hemerythrin-like domain in a P1B-type transport ATPase. *Biochemistry*. 2010; 49: 7060-7068.
174. Seguin, A.; Bayot, A.; Dancis, A.; Rogowska-Wrzesinska, A.; Auchere, F.; Camadro, J. M.; Bulteau, A. L.; Lesuisse, E., Overexpression of the yeast frataxin homolog (Yfh1): contrasting effects on iron-sulfur cluster assembly, heme synthesis and resistance to oxidative stress. *Mitochondrion*. 2009; 9: 130-138.
175. Yan, R.; Kelly, G.; Pastore, A., The scaffold protein IscU retains a structured conformation in the Fe-S cluster assembly complex. *ChemBiochem*. 2014; 15: 1682-1686.
176. Kim, J. H.; Tonelli, M.; Kim, T.; Markley, J. L., Three-dimensional structure and determinants of stability of the iron-sulfur cluster scaffold protein IscU from *Escherichia coli*. *Biochemistry*. 2012; 51: 5557-5563.

177. Kim, J. H.; Tonelli, M.; Markley, J. L., Disordered form of the scaffold protein IscU is the substrate for iron-sulfur cluster assembly on cysteine desulfurase. *Proc Natl Acad Sci U S A.* 2012; 109: 454-459.
178. Sticht, H.; Rosch, P., The structure of iron-sulfur proteins. *Prog Biophys Mol Biol.* 1998; 70: 95-136.
179. Campuzano, V.; Montermini, L.; Molto, M. D.; Pianese, L.; Cossee, M.; Cavalcanti, F.; Monros, E.; Rodius, F.; Duclos, F.; Monticelli, A.; Zara, F.; Canizares, J.; Koutnikova, H.; Bidichandani, S. I.; Gellera, C.; Brice, A.; Trouillas, P.; De Michele, G.; Filla, A.; De Frutos, R.; Palau, F.; Patel, P. I.; Di Donato, S.; Mandel, J. L.; Coccozza, S.; Koenig, M.; Pandolfo, M., Friedreich's ataxia: autosomal recessive disease caused by an intronic GAA triplet repeat expansion. *Science.* 1996; 271: 1423-1427.
180. Beinert, H.; Kennedy, M. C., Aconitase, a two-faced protein: enzyme and iron regulatory factor. *FASEB J.* 1993; 7: 1442-1449.
181. Netz, D. J.; Stith, C. M.; Stumpfig, M.; Kopf, G.; Vogel, D.; Genau, H. M.; Stodola, J. L.; Lill, R.; Burgers, P. M.; Pierik, A. J., Eukaryotic DNA polymerases require an iron-sulfur cluster for the formation of active complexes. *Nat Chem Biol.* 2012; 8: 125-132.
182. Vinothkumar, K. R.; Zhu, J.; Hirst, J., Architecture of mammalian respiratory complex I. *Nature.* 2014; 515: 80-84.
183. Rouault, T. A., Mammalian iron-sulphur proteins: novel insights into biogenesis and function. *Nat Rev Mol Cell Biol.* 2015; 16: 45-55.

184. Biederbick, A.; Stehling, O.; Rosser, R.; Niggemeyer, B.; Nakai, Y.; Elsasser, H. P.; Lill, R., Role of human mitochondrial Nfs1 in cytosolic iron-sulfur protein biogenesis and iron regulation. *Mol Cell Biol.* 2006; 26: 5675-5687.
185. Kispal, G.; Csere, P.; Prohl, C.; Lill, R., The mitochondrial proteins Atm1p and Nfs1p are essential for biogenesis of cytosolic Fe/S proteins. *EMBO J.* 1999; 18: 3981-3989.
186. Muhlenhoff, U.; Balk, J.; Richhardt, N.; Kaiser, J. T.; Sipos, K.; Kispal, G.; Lill, R., Functional characterization of the eukaryotic cysteine desulfurase Nfs1p from *Saccharomyces cerevisiae*. *J Biol Chem.* 2004; 279: 36906-36915.
187. Adam, A. C.; Bornhovd, C.; Prokisch, H.; Neupert, W.; Hell, K., The Nfs1 interacting protein Isd11 has an essential role in Fe/S cluster biogenesis in mitochondria. *EMBO J.* 2006; 25: 174-183.
188. Agar, J. N.; Krebs, C.; Frazzon, J.; Huynh, B. H.; Dean, D. R.; Johnson, M. K., IscU as a scaffold for iron-sulfur cluster biosynthesis: sequential assembly of [2Fe-2S] and [4Fe-4S] clusters in IscU. *Biochemistry.* 2000; 39: 7856-7862.
189. Pandey, A.; Gordon, D. M.; Pain, J.; Stemmler, T. L.; Dancis, A.; Pain, D., Frataxin directly stimulates mitochondrial cysteine desulfurase by exposing substrate-binding sites, and a mutant Fe-S cluster scaffold protein with frataxin-bypassing ability acts similarly. *J Biol Chem.* 2013; 288: 36773-36786.
190. Bridwell-Rabb, J.; Fox, N. G.; Tsai, C. L.; Winn, A. M.; Barondeau, D. P., Human frataxin activates Fe-S cluster biosynthesis by facilitating sulfur transfer chemistry. *Biochemistry.* 2014; 53: 4904-4913.

191. Cook, J. D.; Kondapalli, K. C.; Rawat, S.; Childs, W. C.; Murugesan, Y.; Dancis, A.; Stemmler, T. L., Molecular details of the yeast frataxin-Isu1 interaction during mitochondrial Fe-S cluster assembly. *Biochemistry*. 2010; 49: 8756-8765.
192. Lange, H.; Kaut, A.; Kispal, G.; Lill, R., A mitochondrial ferredoxin is essential for biogenesis of cellular iron-sulfur proteins. *Proc Natl Acad Sci U S A*. 2000; 97: 1050-1055.
193. Ranatunga, W.; Gakh, O.; Galeano, B. K.; Smith, D. Y. t.; Soderberg, C. A.; Al-Karadaghi, S.; Thompson, J. R.; Isaya, G., Architecture of the Yeast Mitochondrial Iron-Sulfur Cluster Assembly Machinery: The Sub-Complex Formed by the Iron Donor, Yfh1, and the Scaffold, Isu1. *J Biol Chem*. 2016.
194. Voisine, C.; Schilke, B.; Ohlson, M.; Beinert, H.; Marszalek, J.; Craig, E. A., Role of the mitochondrial Hsp70s, Ssc1 and Ssq1, in the maturation of Yfh1. *Mol Cell Biol*. 2000; 20: 3677-3684.
195. Kim, J. H.; Fuzery, A. K.; Tonelli, M.; Ta, D. T.; Westler, W. M.; Vickery, L. E.; Markley, J. L., Structure and dynamics of the iron-sulfur cluster assembly scaffold protein IscU and its interaction with the cochaperone HscB. *Biochemistry*. 2009; 48: 6062-6071.
196. Popovic, M.; Pastore, A., Chemical shift assignment of the alternative scaffold protein IscA. *Biomol NMR Assign*. 2016; 10: 227-231.
197. Terali, K.; Bevil, R. L.; Pickersgill, R. W.; van der Giezen, M., The effect of the adaptor protein Isd11 on the quaternary structure of the eukaryotic cysteine desulphurase Nfs1. *Biochem Biophys Res Commun*. 2013; 440: 235-240.

198. Pandey, A.; Golla, R.; Yoon, H.; Dancis, A.; Pain, D., Persulfide formation on mitochondrial cysteine desulfurase: enzyme activation by a eukaryote-specific interacting protein and Fe-S cluster synthesis. *Biochem J.* 2012; 448: 171-187.
199. Colin, F.; Martelli, A.; Clemancey, M.; Latour, J. M.; Gambarelli, S.; Zeppieri, L.; Birck, C.; Page, A.; Puccio, H.; Ollagnier de Choudens, S., Mammalian frataxin controls sulfur production and iron entry during de novo Fe₄S₄ cluster assembly. *J Am Chem Soc.* 2013; 135: 733-740.
200. Schmucker, S.; Martelli, A.; Colin, F.; Page, A.; Wattenhofer-Donze, M.; Reutenauer, L.; Puccio, H., Mammalian frataxin: an essential function for cellular viability through an interaction with a preformed ISCU/NFS1/ISD11 iron-sulfur assembly complex. *PLoS One.* 2011; 6: e16199.
201. Bridwell-Rabb, J.; Iannuzzi, C.; Pastore, A.; Barondeau, D. P., Effector role reversal during evolution: the case of frataxin in Fe-S cluster biosynthesis. *Biochemistry.* 2012; 51: 2506-2514.
202. Fox, N. G.; Chakrabarti, M.; McCormick, S. P.; Lindahl, P. A.; Barondeau, D. P., The Human Iron-Sulfur Assembly Complex Catalyzes the Synthesis of [2Fe-2S] Clusters on ISCU2 That Can Be Transferred to Acceptor Molecules. *Biochemistry.* 2015; 54: 3871-3879.
203. Stephens, P. J.; Thomson, A. J.; Dunn, J. B.; Keiderling, T. A.; Rawlings, J.; Rao, K. K.; Hall, D. O., Circular dichroism and magnetic circular dichroism of iron-sulfur proteins. *Biochemistry.* 1978; 17: 4770-4778.

204. Fogo, J., Popowsky, M., Spectrophotometric Determination of Hydrogen Sulfide. *Anal Chem.* 1949; 21: 732-734.
205. Siegel, L. M., A Direct Microdetermination for Sulfide. *Anal Biochem.* 1965; 11: 126-132.
206. Urbina, H. D.; Cupp-Vickery, J. R.; Vickery, L. E., Preliminary crystallographic analysis of the cysteine desulfurase IscS from *Escherichia coli*. *Acta Crystallogr D Biol Crystallogr.* 2002; 58: 1224-1225.
207. Blanc, B.; Clemancey, M.; Latour, J. M.; Fontecave, M.; Ollagnier de Choudens, S., Molecular investigation of iron-sulfur cluster assembly scaffolds under stress. *Biochemistry.* 2014; 53: 7867-7869.
208. Tsai, C. L.; Barondeau, D. P., Human frataxin is an allosteric switch that activates the Fe-S cluster biosynthetic complex. *Biochemistry.* 2010; 49: 9132-9139.
209. Mapolelo, D. T.; Zhang, B.; Naik, S. G.; Huynh, B. H.; Johnson, M. K., Spectroscopic and functional characterization of iron-sulfur cluster-bound forms of *Azotobacter vinelandii* (Nif)IscA. *Biochemistry.* 2012; 51: 8071-8084.
210. Shakamuri, P.; Zhang, B.; Johnson, M. K., Monothiol glutaredoxins function in storing and transporting [Fe₂S₂] clusters assembled on IscU scaffold proteins. *J Am Chem Soc.* 2012; 134: 15213-15216.
211. Dutkiewicz, R.; Marszalek, J.; Schilke, B.; Craig, E. A.; Lill, R.; Muhlenhoff, U., The Hsp70 chaperone Ssq1p is dispensable for iron-sulfur cluster formation on the scaffold protein Isu1p. *J Biol Chem.* 2006; 281: 7801-7808.

212. Webert, H.; Freibert, S. A.; Gallo, A.; Heidenreich, T.; Linne, U.; Amlacher, S.; Hurt, E.; Muhlenhoff, U.; Banci, L.; Lill, R., Functional reconstitution of mitochondrial Fe/S cluster synthesis on Isu1 reveals the involvement of ferredoxin. *Nat Commun.* 2014; 5: 5013.
213. Shi, R.; Proteau, A.; Villarroja, M.; Moukadiri, I.; Zhang, L.; Trempe, J. F.; Matte, A.; Armengod, M. E.; Cygler, M., Structural basis for Fe-S cluster assembly and tRNA thiolation mediated by IscS protein-protein interactions. *PLoS Biol.* 2010; 8: e1000354.
214. Nuth, M.; Cowan, J. A., Iron-sulfur cluster biosynthesis: characterization of IscU-IscS complex formation and a structural model for sulfide delivery to the [2Fe-2S] assembly site. *J Biol Inorg Chem.* 2009; 14: 829-839.
215. Urbina, H. D.; Silberg, J. J.; Hoff, K. G.; Vickery, L. E., Transfer of sulfur from IscS to IscU during Fe/S cluster assembly. *J Biol Chem.* 2001; 276: 44521-44526.
216. Rodrigues, A. V.; Kandegedara, A.; Rotondo, J. A.; Dancis, A.; Stemmler, T. L., Iron loading site on the Fe-S cluster assembly scaffold protein is distinct from the active site. *Biomaterials.* 2015; 28: 567-576.
217. Fox, N. G.; Das, D.; Chakrabarti, M.; Lindahl, P. A.; Barondeau, D. P., Frataxin Accelerates [2Fe-2S] Cluster Formation on the Human Fe-S Assembly Complex. *Biochemistry.* 2015; 54: 3880-3889.
218. Barupala, D. P.; Dzul, S. P.; Riggs-Gelasco, P. J.; Stemmler, T. L., Synthesis, delivery and regulation of eukaryotic heme and Fe-S cluster cofactors. *Arch Biochem Biophys.* 2016; 592: 60-75.

219. Muhlenhoff, U.; Gerber, J.; Richhardt, N.; Lill, R., Components involved in assembly and dislocation of iron-sulfur clusters on the scaffold protein Isu1p. *EMBO J.* 2003; 22: 4815-4825.
220. Uzarska, M. A.; Dutkiewicz, R.; Freibert, S. A.; Lill, R.; Muhlenhoff, U., The mitochondrial Hsp70 chaperone Ssq1 facilitates Fe/S cluster transfer from Isu1 to Grx5 by complex formation. *Mol Biol Cell.* 2013; 24: 1830-1841.
221. Campuzano, V.; Montermini, L.; Molto, M. D.; Pianese, L.; Cossee, M.; Cavalcanti, F.; Monros, E.; Rodius, F.; Duclos, F.; Monticelli, A.; Zara, F.; Canizares, J.; Koutnikova, H.; Bidichandani, S. I.; Gellera, C.; Brice, A.; Trouillas, P.; De Michele, G.; Filla, A.; De Frutos, R.; Palau, F.; Patel, P. I.; Di Donato, S.; Mandel, J. L.; Coccozza, S.; Koenig, M.; Pandolfo, M., Friedreich's ataxia: autosomal recessive disease caused by an intronic GAA triplet repeat expansion. *Science.* 1996; 271: 1423-1427.
222. Cook, J. D.; Kondapalli, K. C.; Rawat, S.; Childs, W. C.; Murugesan, Y.; Dancis, A.; Stemmler, T. L., Molecular details of the yeast frataxin-Isu1 interaction during mitochondrial Fe-S cluster assembly. *Biochemistry.* 2010; 49: 8756-8765.
223. Kondapalli, K. C.; Kok, N. M.; Dancis, A.; Stemmler, T. L., Drosophila frataxin: an iron chaperone during cellular Fe-S cluster bioassembly. *Biochemistry.* 2008; 47: 6917-6927.
224. Cook, J. D.; Bencze, K. Z.; Jankovic, A. D.; Crater, A. K.; Busch, C. N.; Bradley, P. B.; Stemmler, A. J.; Spaller, M. R.; Stemmler, T. L., Monomeric yeast frataxin is an iron-binding protein. *Biochemistry.* 2006; 45: 7767-7777.

225. Ranatunga, W.; Gakh, O.; Galeano, B. K.; Smith, D. Y. t.; Soderberg, C. A.; Al-Karadaghi, S.; Thompson, J. R.; Isaya, G., Architecture of the Yeast Mitochondrial Iron-Sulfur Cluster Assembly Machinery: The Sub-Complex Formed by the Iron Donor, Yfh1, and the Scaffold, Isu1. *J Biol Chem*. 2016.
226. Zaidi, A.; Singh, K. P.; Anwar, S.; Suman, S. S.; Equbal, A.; Singh, K.; Dikhit, M. R.; Bimal, S.; Pandey, K.; Das, P.; Ali, V., Interaction of frataxin, an iron binding protein, with IscU of Fe-S clusters biogenesis pathway and its upregulation in AmpB resistant *Leishmania donovani*. *Biochimie*. 2015; 115: 120-135.
227. Bencze, K. Z.; Yoon, T.; Millan-Pacheco, C.; Bradley, P. B.; Pastor, N.; Cowan, J. A.; Stemmler, T. L., Human frataxin: iron and ferrochelatase binding surface. *Chem Commun (Camb)*. 2007: 1798-1800.
228. Soderberg, C. G.; Gillam, M. E.; Ahlgren, E. C.; Hunter, G. A.; Gakh, O.; Isaya, G.; Ferreira, G. C.; Al-Karadaghi, S., The Structure of the Complex Between Yeast Frataxin and Ferrochelatase: Characterization and pre-Steady State Reaction of Ferrous Iron Delivery and Heme Synthesis. *J Biol Chem*. 2016.
229. Bridwell-Rabb, J.; Iannuzzi, C.; Pastore, A.; Barondeau, D. P., Effector role reversal during evolution: the case of frataxin in Fe-S cluster biosynthesis. *Biochemistry*. 2012; 51: 2506-2514.
230. Bridwell-Rabb, J.; Fox, N. G.; Tsai, C. L.; Winn, A. M.; Barondeau, D. P., Human frataxin activates Fe-S cluster biosynthesis by facilitating sulfur transfer chemistry. *Biochemistry*. 2014; 53: 4904-4913.
231. Colin, F.; Martelli, A.; Clemancey, M.; Latour, J. M.; Gambarelli, S.; Zeppieri, L.; Birck, C.; Page, A.; Puccio, H.; Ollagnier de Choudens, S., Mammalian frataxin

- controls sulfur production and iron entry during de novo Fe₄S₄ cluster assembly. *J Am Chem Soc.* 2013; 135: 733-740.
232. Pastore, A.; Puccio, H., Frataxin: a protein in search for a function. *J Neurochem.* 2013; 126 Suppl 1: 43-52.
233. Wang, T.; Craig, E. A., Binding of yeast frataxin to the scaffold for Fe-S cluster biogenesis, *Isu. J Biol Chem.* 2008; 283: 12674-12679.
234. Soderberg, C. A.; Rajan, S.; Shkumatov, A. V.; Gakh, O.; Schaefer, S.; Ahlgren, E. C.; Svergun, D. I.; Isaya, G.; Al-Karadaghi, S., The molecular basis of iron-induced oligomerization of frataxin and the role of the ferroxidation reaction in oligomerization. *J Biol Chem.* 2013; 288: 8156-8167.
235. Schagerlof, U.; Elmlund, H.; Gakh, O.; Nordlund, G.; Hebert, H.; Lindahl, M.; Isaya, G.; Al-Karadaghi, S., Structural basis of the iron storage function of frataxin from single-particle reconstruction of the iron-loaded oligomer. *Biochemistry.* 2008; 47: 4948-4954.
236. Karlberg, T.; Schagerlof, U.; Gakh, O.; Park, S.; Ryde, U.; Lindahl, M.; Leath, K.; Garman, E.; Isaya, G.; Al-Karadaghi, S., The structures of frataxin oligomers reveal the mechanism for the delivery and detoxification of iron. *Structure.* 2006; 14: 1535-1546.
237. Tsai, C. L.; Barondeau, D. P., Human frataxin is an allosteric switch that activates the Fe-S cluster biosynthetic complex. *Biochemistry.* 2010; 49: 9132-9139.
238. Pandey, A.; Gordon, D. M.; Pain, J.; Stemmler, T. L.; Dancis, A.; Pain, D., Frataxin directly stimulates mitochondrial cysteine desulfurase by exposing

- substrate-binding sites, and a mutant Fe-S cluster scaffold protein with frataxin-bypassing ability acts similarly. *J Biol Chem.* 2013; 288: 36773-36786.
239. Hunt, C. A.; Ropella, G. E.; Lam, T. N.; Tang, J.; Kim, S. H.; Engelberg, J. A.; Sheikh-Bahaei, S., At the biological modeling and simulation frontier. *Pharm Res.* 2009; 26: 2369-2400.
240. Garcia-Contreras, R.; Vos, P.; Westerhoff, H. V.; Boogerd, F. C., Why in vivo may not equal in vitro - new effectors revealed by measurement of enzymatic activities under the same in vivo-like assay conditions. *FEBS J.* 2012; 279: 4145-4159.
241. Manicki, M.; Majewska, J.; Ciesielski, S.; Schilke, B.; Blenska, A.; Kominek, J.; Marszalek, J.; Craig, E. A.; Dutkiewicz, R., Overlapping binding sites of the frataxin homologue assembly factor and the heat shock protein 70 transfer factor on the Isu iron-sulfur cluster scaffold protein. *J Biol Chem.* 2014; 289: 30268-30278.
242. Wang, T.; Craig, E. A., Binding of yeast frataxin to the scaffold for Fe-S cluster biogenesis, Isu. *J Biol Chem.* 2008; 283: 12674-12679.
243. Wofford, J. D.; Lindahl, P. A., Mitochondrial Iron-Sulfur Cluster Activity and Cytosolic Iron Regulate Iron Traffic in *Saccharomyces cerevisiae*. *J Biol Chem.* 2015; 290: 26968-26977.
244. Miao, R.; Martinho, M.; Morales, J. G.; Kim, H.; Ellis, E. A.; Lill, R.; Hendrich, M. P.; Munck, E.; Lindahl, P. A., EPR and Mossbauer spectroscopy of intact

- mitochondria isolated from Yah1p-depleted *Saccharomyces cerevisiae*.
Biochemistry. 2008; 47: 9888-9899.
245. Fox, N. G.; Chakrabarti, M.; McCormick, S. P.; Lindahl, P. A.; Barondeau, D. P.,
The Human Iron-Sulfur Assembly Complex Catalyzes the Synthesis of [2Fe-
2S] Clusters on ISCU2 That Can Be Transferred to Acceptor Molecules.
Biochemistry. 2015; 54: 3871-3879.
246. Dutkiewicz, R.; Marszalek, J.; Schilke, B.; Craig, E. A.; Lill, R.; Muhlenhoff, U.,
The Hsp70 chaperone Ssq1p is dispensable for iron-sulfur cluster formation
on the scaffold protein Isu1p. *J Biol Chem*. 2006; 281: 7801-7808.
247. Campuzano, V.; Montermini, L.; Molto, M. D.; Pianese, L.; Cossee, M.;
Cavalcanti, F.; Monros, E.; Rodius, F.; Duclos, F.; Monticelli, A.; Zara, F.;
Canizares, J.; Koutnikova, H.; Bidichandani, S. I.; Gellera, C.; Brice, A.;
Trouillas, P.; De Michele, G.; Filla, A.; De Frutos, R.; Palau, F.; Patel, P. I.; Di
Donato, S.; Mandel, J. L.; Coccozza, S.; Koenig, M.; Pandolfo, M., Friedreich's
ataxia: autosomal recessive disease caused by an intronic GAA triplet repeat
expansion. *Science*. 1996; 271: 1423-1427.
248. Kim, J. H.; Tonelli, M.; Kim, T.; Markley, J. L., Three-dimensional structure and
determinants of stability of the iron-sulfur cluster scaffold protein IscU from
Escherichia coli. *Biochemistry*. 2012; 51: 5557-5563.
249. Kim, J. H.; Tonelli, M.; Markley, J. L., Disordered form of the scaffold protein
IscU is the substrate for iron-sulfur cluster assembly on cysteine desulfurase.
Proc Natl Acad Sci U S A. 2012; 109: 454-459.

250. Yan, R.; Kelly, G.; Pastore, A., The scaffold protein IscU retains a structured conformation in the Fe-S cluster assembly complex. *Chembiochem*. 2014; 15: 1682-1686.
251. Yoon, H.; Golla, R.; Lesuisse, E.; Pain, J.; Donald, J. E.; Lyver, E. R.; Pain, D.; Dancis, A., Mutation in the Fe-S scaffold protein Isu bypasses frataxin deletion. *Biochem J*. 2012; 441: 473-480.
252. Pandey, A.; Gordon, D. M.; Pain, J.; Stemmler, T. L.; Dancis, A.; Pain, D., Frataxin directly stimulates mitochondrial cysteine desulfurase by exposing substrate-binding sites, and a mutant Fe-S cluster scaffold protein with frataxin-bypassing ability acts similarly. *J Biol Chem*. 2013; 288: 36773-36786.
253. Weber, H.; Freibert, S. A.; Gallo, A.; Heidenreich, T.; Linne, U.; Amlacher, S.; Hurt, E.; Muhlenhoff, U.; Banci, L.; Lill, R., Functional reconstitution of mitochondrial Fe/S cluster synthesis on Isu1 reveals the involvement of ferredoxin. *Nat Commun*. 2014; 5: 5013.
254. Brancaccio, D.; Gallo, A.; Mikolajczyk, M.; Zovo, K.; Palumaa, P.; Novellino, E.; Piccioli, M.; Ciofi-Baffoni, S.; Banci, L., Formation of [4Fe-4S] clusters in the mitochondrial iron-sulfur cluster assembly machinery. *J Am Chem Soc*. 2014; 136: 16240-16250.
255. Shakamuri, P.; Zhang, B.; Johnson, M. K., Monothiol glutaredoxins function in storing and transporting [Fe₂S₂] clusters assembled on IscU scaffold proteins. *J Am Chem Soc*. 2012; 134: 15213-15216.

256. Kim, K. D.; Chung, W. H.; Kim, H. J.; Lee, K. C.; Roe, J. H., Monothiol glutaredoxin Grx5 interacts with Fe-S scaffold proteins Isa1 and Isa2 and supports Fe-S assembly and DNA integrity in mitochondria of fission yeast. *Biochem Biophys Res Commun.* 2010; 392: 467-472.
257. Uzarska, M. A.; Dutkiewicz, R.; Freibert, S. A.; Lill, R.; Muhlenhoff, U., The mitochondrial Hsp70 chaperone Ssq1 facilitates Fe/S cluster transfer from Isu1 to Grx5 by complex formation. *Mol Biol Cell.* 2013; 24: 1830-1841.
258. Colin, F.; Martelli, A.; Clemancey, M.; Latour, J. M.; Gambarelli, S.; Zeppieri, L.; Birck, C.; Page, A.; Puccio, H.; Ollagnier de Choudens, S., Mammalian frataxin controls sulfur production and iron entry during de novo Fe₄S₄ cluster assembly. *J Am Chem Soc.* 2013; 135: 733-740.
259. van der Linde, K.; Houle, D.; Spicer, G. S.; Steppan, S. J., A supermatrix-based molecular phylogeny of the family Drosophilidae. *Genet Res (Camb).* 2010; 92: 25-38.

ABSTRACT**INSIGHTS INTO *DE NOVO* FES-CLUSTER BIOGENESIS VIA THE
EUKARYOTIC FES-CLUSTER PATHWAY (ISC) *IN VITRO***

by

STEPHEN DZUL**August 2016****Advisors:** Dr. Timothy Stemmler and Dr. David Evans**Major:** Biochemistry and Molecular Biology**Degree:** Doctor of Philosophy

FeS-clusters are iron-containing cofactors utilized by numerous proteins within several biological pathways essential to life. In eukaryotes, the primary pathway for FeS-cluster production is the iron-sulfur cluster (ISC) pathway. The eukaryotic ISC pathway, localized primarily within the mitochondria, has been best characterized within *Saccharomyces cerevisiae*. In yeast, *de novo* FeS-cluster formation is accomplished through coordinated assembly of the substrates iron and sulfur on the primary scaffold assembly protein "Isu1". The sulfur used for cluster assembly is provided by the cysteine desulfurase "Nfs1", a protein that works in union with its accessory protein "Isd11". Frataxin "Yfh1" helps direct cluster assembly by serving as a modulator of Nfs1 activity, by assisting in the delivery of Fe(II) to Isu1, or through a combination of roles.

This work describes and optimizes an *in vitro* method for generating an FeS-cluster on the scaffold Isu1. Further *in vitro* studies on the yeast ISC system have been limited, however, due to the inherent instability of recombinant Isu1, a molecule prone to

degradation and aggregation. To circumvent Isu1 stability issues, this research demonstrates successful cross-reactivity between the fly Isu1 ortholog, “flscU”, and yeast ISC *in vitro* and *in vivo*. This strategy could facilitate novel experimentation of the yeast ISC pathway in the future. This work also isolates complexes formed between recombinant yeast Nfs1-Isd11, Nfs1-Isd11-Isu1, and Nfs1-Isd11-Isu1-Yfh1, and characterizes their activity related to substrate binding and cluster assembly. Complexed Isu1, as isolated within Nfs1-Isd11-Isu1 and Nfs1-Isd11-Isu1-Yfh1 complexes, demonstrates inhibited FeS-cluster biogenesis without the addition of exogenous *apo*-Isu1. This suggests a mechanism for *de novo* FeS-cluster formation on Isu1 that is similar to recent observations from bacterial ISC. Lastly, evidence is provided that suggests that frataxin can function as an allosteric activator of Nfs1 *in vitro*.

AUTOBIOGRAPHICAL STATEMENT

Stephen Paul Dzul was born in Detroit, Michigan on April 15th, 1988 and was raised in the Detroit suburb of Grosse Pointe. He attended the University of Michigan and received his Bachelor's degree in chemical engineering in 2010. While at the University of Michigan, Stephen became involved in a variety of medical research topics where he developed an interest in basic science research and clinical medicine. These combined interests directed him to pursue MD and PhD degrees at Wayne State University in Detroit, Michigan. Stephen joined Dr. Timothy Stemmler's research lab in Biochemistry and Molecular Biology in October 2012.

Education:

B.S.E **Chemical Engineering** (2006-2010) University of Michigan, Ann Arbor, MI

Publications:

1. **Dzul, S. P.**; Barupala, D. P.; Riggs-Gelasco, P. J.; Stemmler, T. L., Synthesis, delivery and regulation of eukaryotic heme and Fe-S cluster cofactors. *Arch Biochem Biophys.* 2016; 592: 60-75.
2. **Dzul, S.P.**; Stemmler, T.L.; Penner-Hahn, J.E. "Manganese Proteins with Mono- and Dinuclear Metal Sites" in *Encyclopedia of Inorganic and Bioinorganic Chemistry*, Robert A. Scott Eds., Chichester, UK: John Wiley & Sons, Ltd., 2015
3. Bafaro, E. M.; Antala, S.; Nguyen, T. V.; **Dzul, S. P.**; Doyon, B.; Stemmler, T. L.; Dempski, R. E., The large intracellular loop of hZIP4 is an intrinsically disordered zinc binding domain. *Metallomics.* 2015; 7: 1319-1330.
4. Plegaria, J. S.; **Dzul, S. P.**; Zuiderweg, E. R.; Stemmler, T. L.; Pecoraro, V. L., Apoprotein Structure and Metal Binding Characterization of a de Novo Designed Peptide, alpha3DIV, that Sequesters Toxic Heavy Metals. *Biochemistry.* 2015; 54: 2858-2873.
5. Byrne, E.; **Dzul, S.**; Solomon, M.; Younger, J.; Bortz, D. M., Postfragmentation density function for bacterial aggregates in laminar flow. *Phys Rev E Stat Nonlin Soft Matter Phys.* 2011; 83: 041911.
6. **Dzul, S. P.**; Thornton, M. M.; Hohne, D. N.; Stewart, E. J.; Shah, A. A.; Bortz, D. M.; Solomon, M. J.; Younger, J. G., Contribution of the *Klebsiella pneumoniae* capsule to bacterial aggregate and biofilm microstructures. *Appl Environ Microbiol.* 2011; 77: 1777-1782.

Fellowships:

AHA: 13PRE16490009	Dzul (PI)	1/1/2014-12/1/2014
<i>Characterizing Isu Scaffolding Protein and ISC Multiprotein Complex Structure and Function In Vitro</i>		
NIH: 1F30DK101230-01A1	Dzul (PI)	12/1/2014-7/1/2018
<i>Characterizing Isu Scaffolding Protein and ISC Multiprotein Complex Structure and Function In Vitro</i>		

Honors and Awards:

Magna Cum Laude. Biochemistry Department 3-Minute Talk Competition 2015
First Place Oral Presentation. Wayne State University MD/PhD Research Day 2016